# Neuronal and glial responses to dopaminergic denervation

Li, Chang

2024

*Document Version:*
Publisher's PDF, also known as Version of record

# Neuronal and glial responses to dopaminergic denervation

CHANG LI
EXPERIMENTAL MEDICAL SCIENCE | FACULTY OF MEDICINE | LUND UNIVERSITY

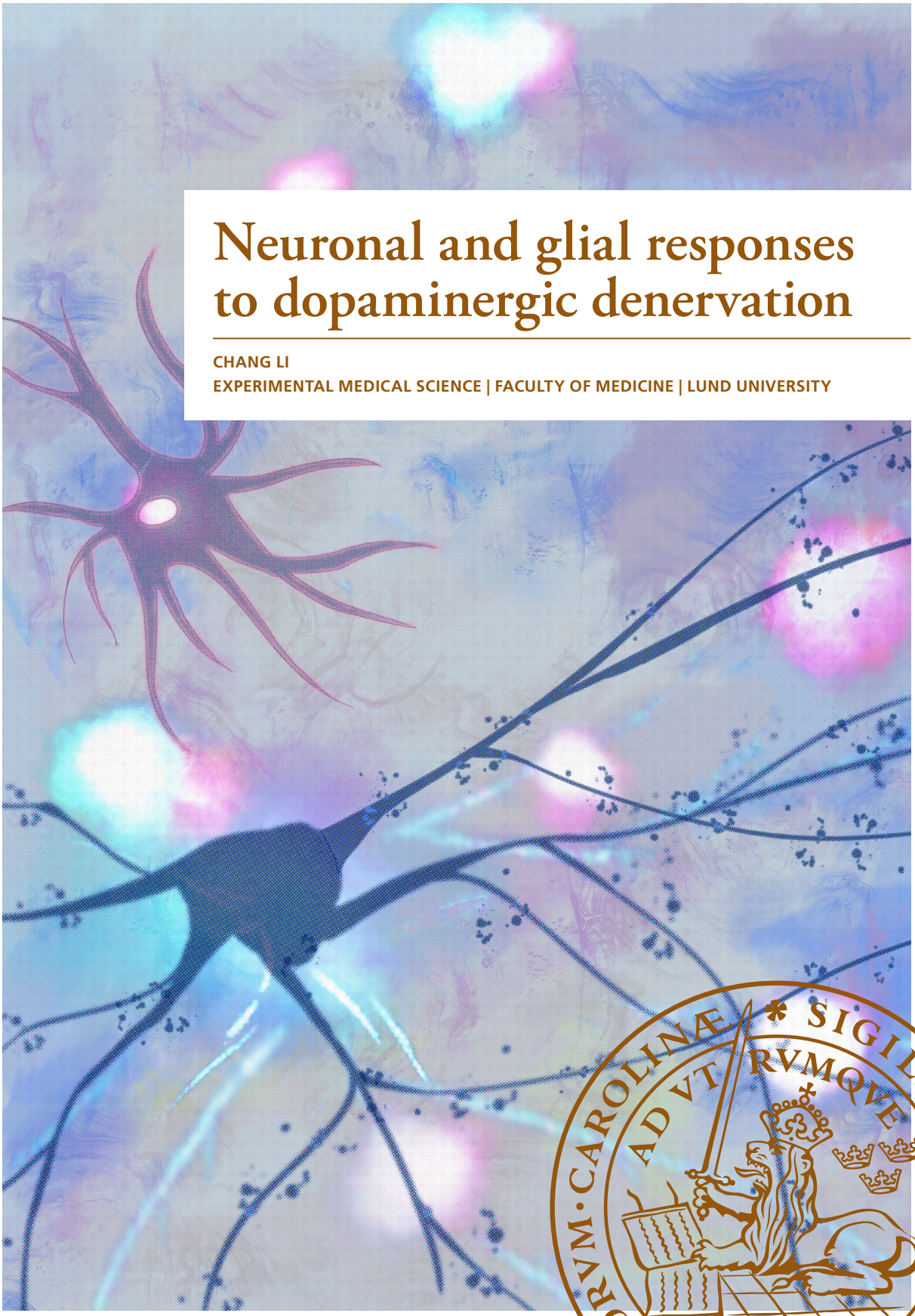

Printed by Media-Tryck, Lund 2024 NORDIC SWAN ECOLABEL 3041 0903

LUND UNIVERSITY

FACULTY OF MEDICINE

Department of Experimental Medical Science

Lund University, Faculty of Medicine
Doctoral Dissertation Series 2024:93
ISBN 978-91-8021-588-6
ISSN 1652-8220

Neuronal and glial responses to dopaminergic denervation

# Neuronal and glial responses to dopaminergic denervation

Chang Li


LUND
UNIVERSITY

DOCTORAL DISSERTATION

Doctoral dissertation for the degree of Doctor of Philosophy (PhD) at the Faculty of Medicine at Lund University to be publicly defended on 24th of September 2024 at 13:00 in Segerfalksalen, Department of Experimental Medical Science, Lund

*Faculty opponent*
Prof. Marcela Pekna

Göteborgs Universitet, Institutionen för neurovetenskap och fysiologi

**Organization:** LUND UNIVERSITY
**Document name:** Doctoral Dissertation **Date of issue:** 24th September 2024
**Author(s):** Chang Li **Sponsoring organization:**

**Title and subtitle:** Neuronal and glial responses to dopaminergic denervation

**Abstract:**

Parkinson's disease (PD) is characterised by severe degeneration of dopamine (DA) neurons innervating the striatum. Spiny projection neurons (SPNs), are the principal type of striatal neuron and belong to either of two classes: the D2 receptor-positive indirect pathway SPNs (iSPNs) and the D1 receptor-positive direct pathway SPNs (dSPNs). The thesis aims at investigating dynamic changes of SPNs and the surrounding glial cells following the loss of dopaminergic innervation. Studies are performed in a mouse model where the toxin 6-hydroxydopamine (6-OHDA) is used to kill DA neurons projecting to the dorsolateral striatum. After establishing that at least 95% of striatal DA fibres are lost 5 days after 6-OHDA injection, we selected 5 and 28 days post lesion (DPL) as representing early vs. chronic stages of DA denervation. Our results show that a loss of dendritic spines occurs in iSPNs already at 5 DPL whereas this process becomes significant in dSPNs only at 28 DPL. In both cell types the dendritic remodeling is accompanied by maladaptive changes in synaptic plasticity and intrinsic electrophysiological properties. We show that caspase-3 is strongly activated at 5 DPL and that a caspase inhibitor can prevent spine pruning and synaptic changes in iSPNs. In another study we show that DA denervation induces a strong transient activation of microglia followed by a sustained activation of astrocytes. This is accompanied by striatal upregulation of pro-inflammatory molecules. At 5 DPL, activated microglial cells form close contacts with SPN dendrites, and these contacts are significantly more abundant on iSPNs compared to dSPNs, suggesting that microglia are involved in the early pruning of iSPN spines. Finally, we show that the antidepressant drug fluvoxamine can partially protect DA neurons from the toxic damage while reducing microglial activation, an effect mediated by the Sigma-1 receptor. Our results shed new light on the coordinated dynamic changes taking place in neurons and glia following DA denervation and provide new clues of therapeutic importance.

**Key words:**

Parkinson’s Disease, 6-OHDA, striatum, dopamine, SPNs, dendritic regression, spine pruning, neuroinflammation, fluvoxamine, microglia, neuroprotection, disease modifying treatment,

Supplementary bibliographical information

**Language** English **Number of pages**: 92

**ISSN and key title**: 1652-8220

**ISBN:** 978-91-8021-588-6

Recipient’s notes Price Security classification



Signature Date 2024-08-09

# Neuronal and glial responses to dopaminergic denervation

Chang Li


LUND
UNIVERSITY

Coverphoto by author using Procreate



Faculty of Medicine
Department of Experimental Medical Science

ISBN 978-91-8021-588-6
ISSN 1652-8220

Printed in Sweden by Media-Tryck, Lund University
Lund 2024

*To my family*

*人生若只如初见，何事秋风悲画扇。--纳兰*

# Table of Contents


Papers and Manuscript ..... 11
Abstract ..... 12
Populärvetenskaplig sammanfattning ..... 13
论文简介 ..... 14
List of Abbreviations ..... 15

**Introduction ..... 17**
Parkinson's Disease ..... 17
The basal ganglia ..... 18
The striatum ..... 18
The SPNs and their expression of dopamine receptors ..... 20
The classic model of the BG circuitry ..... 22
The striatal pathology in the Parkinson's Disease ..... 22
SPN morphological-functional alterations in the PD ..... 23
Neuroinflammation in PD ..... 25
The sigma-1 receptor as a potential target for disease-modifying treatments ..... 26

**Aims of this Thesis ..... 28**

**Materials and Methods ..... 29**
Animals ..... 29
Surgical procedure and drug treatment ..... 30
Animal model of PD ..... 30
Viral Vector injection ..... 30
Drug Treatments ..... 31
Behaviour Tests ..... 31
Ex-vivo slice preparations and Electrophysiological recordings ..... 32
Striatal slice preparation ..... 33
Electrophysiological recordings ..... 33
Two-photon and confocal imaging for SPN morphology ..... 34

Other experimental procedures ....35
Western Immunoblotting (Paper I)....35
Histological procedures, immunohistochemistry and immunofluorescence....36
Apoptosis Assay (TUNEL, Paper I)....37
Quantitative reverse transcription PCR (RT-qPCR, Paper III) ....38
Image analyses and cell counts ....38
Optical density analysis of TH fibres and Stereology counts of DA neurons in SNc (Paper I, II and III)....38
CD68 cell count and discreet TH fibre analysis (Paper IV) ....39
Confocal image analysis (Paper III) ....39
Statistical analysis ....40
**Results....41**
Paper I. Non-apoptotic Caspase-3 activation mediates early synaptic dysfunction of iSPNs in the DA-denervated Striatum ....41
Paper II. Structural-functional alterations in dSPNs at acute and chronic stages of DA denervation....45
Paper III. Glial response dynamics following striatal DA denervation....49
Paper IV. Fluvoxamine induces functional neurorestoration via the Sigma-1 receptor in a mouse model of nigrostriatal dopaminergic degeneration ....56
**Discussion ....63**
Neuronal responses ....64
Glial responses ....66
Harnessing neuronal and glial responses for therapeutic purposes: focus on the Sigma-1 receptor....67
**Summary and conclusions ....69**
**Future perspectives ....70**
**Acknowledgement....72**
**References ....74**

# Papers and Manuscript

(I) **Non-Apoptotic Caspase-3 Activation Mediates Early Synaptic Dysfunction of Indirect Pathway Neurons in the Parkinsonian Striatum.**
Fieblinger T, **Li C**, Espa E, Cenci MA.
*Int J Mol Sci* 2022; 23(10):5470. PMID: 35628278

(II) **Structural-functional properties of direct-pathway striatal neurons at early and chronic stages of dopamine denervation.**
**Li C**, Elabi OF, Fieblinger T, Cenci MA.
*Eur J Neurosci* 2023; e16166. PMID: 37876330

(III) **Glial response dynamics upon striatal dopaminergic denervation.**
**Li C,** Elabi O, Cenci MA.
*Manuscript*

(IV) **Fluvoxamine induces functional neurorestoration via the Sigma-1 receptor in a mouse model of nigrostriatal dopaminergic degeneration.**
**Li C***, Fanni S*, Cesaroni V, Francardo V, Teleuca AE, Espa E, Cenci MA**.**
*Manuscript*

** shared first authorship*

# Abstract

Parkinson's disease (PD) is characterised by severe degeneration of dopamine (DA) neurons innervating the striatum. Spiny projection neurons (SPNs), are the principal type of striatal neuron and belong to either of two classes: the D2 receptor-positive indirect pathway SPNs (iSPNs) and the D1 receptor-positive direct pathway SPNs (dSPNs). The thesis aims at investigating dynamic changes of SPNs and the surrounding glial cells following the loss of dopaminergic innervation. Studies are performed in a mouse model where the toxin 6-hydroxydopamine (6-OHDA) is used to kill DA neurons projecting to the dorsolateral striatum. After establishing that at least 95% of striatal DA fibres are lost 5 days after 6-OHDA injection, we selected 5 and 28 days post lesion (DPL) as representing early vs. chronic stages of DA denervation. Our results show that a loss of dendritic spines occurs in iSPNs already at 5 DPL whereas this process becomes significant in dSPNs only at 28 DPL. In both cell types the dendritic remodeling is accompanied by maladaptive changes in synaptic plasticity and intrinsic electrophysiological properties. We show that caspase-3 is strongly activated at 5 DPL and that a caspase inhibitor can prevent spine pruning and synaptic changes in iSPNs. In another study we show that DA denervation induces a strong transient activation of microglia followed by a sustained activation of astrocytes. This is accompanied by striatal upregulation of pro-inflammatory molecules. At 5 DPL, activated microglial cells form close contacts with SPN dendrites, and these contacts are significantly more abundant on iSPNs compared to dSPNs, suggesting that microglia are involved in the early pruning of iSPN spines. Finally, we show that the antidepressant drug fluvoxamine can partially protect DA neurons from the toxic damage while reducing microglial activation, an effect mediated by the Sigma-1 receptor. Our results shed new light on the coordinated dynamic changes taking place in neurons and glia following DA denervation and provide new clues of therapeutic importance.

# Populärvetenskaplig sammanfattning

Parkinsons sjukdom (PS) är en vanlig neurodegenerativ sjukdom där dopamin-producerande celler i hjärnan förtvinar och dör. Brist på dopamin i en del av hjärnan som heter striatum leder till rubbningar i rörelseförmågan. I denna avhandling undersöker vi hur olika typer av celler i striatum reagerar på dopaminförlust genom att ändra sin struktur eller sina relationer till andra celler. Studier genomförs på möss som utsätts för en skada av dopamin-producerande nervceller med nervcellsgiftet 6-OHDA och som studeras vid olika tidpunkter efter denna toxiska skada. De första två studierna fokuserar på nervceller som kallas för iSPNs och dSPNs och sammanlagt utgör cirka 95% av alla nervceller i striatum. Dessa nervceller är mycket viktiga eftersom de bearbetar rikliga signaler från hjärnbarken, som de tar emot vid små taggar (spines) på sina utskott (dendriter). Våra resultat visar att iSPNs förlorar en del av sina 'taggar' redan inom 5 dagar efter 6-OHDA skadan, medan en liknande förlust syns i dSPNs enbart efter 4 veckor. I båda typer av nervceller sammanfaller förlusten av taggar med funktionella förändringar som sannolikt stör cellernas samspel med hjärnbarken. I andra studier undersöker vi celler som kallas för mikroglia och astrocyter. Våra resultat visar att nedbrytningen av dopaminnervtrådar i striatum triggar en snabb och kraftig (dock övergående) aktivering av mikroglia samt en bestående aktivering av astrocyter. Under de första dagarna efter 6-OHDA skadan uppvisar de aktiverade mikrogliacellerna täta kontakter med striatums nervceller, och speciellt med iSPNs. Detta resultat tyder på att mikroglia deltar i den tidiga nedbrytningen av iSPN taggar vid dopaminförlust. I den sista studien utvärderar vi ett antidepressivt läkemedel (fluvoxamin) för dess förmåga att mildra dopamincellsförlust hos möss utsatta för 6-OHDA skadan. Våra resultat visar att kronisk behandling med fluvoxamin partiellt skyddar dopamin-nervceller, minskar aktivering av mikroglia, och förbättrar mössens motoriska funktion genom att stimulera den s.k. Sigma-1 receptorn. Sammanlagt bidrar våra studier till att förstå konsekvenserna av dopaminförlust på cellulär och funktionell nivå samt bereder ett underlag för utvecklingen av nya behandlingsprinciper.

# 论文简介

帕金森综合症是全球第二大神经退行性疾病，仅次于阿尔兹海默综合症。根据世界卫生组织2019年的报告，全球目前有800万人被诊断为患有帕金森综合症。90%的病例病因无法确定，典型的运动缺陷包括运动迟缓，运动功能减退，肌肉强直和静止震颤。不幸的是疾病的确诊依赖于典型的临床症状，而症状的出现往往起始于病变之后多年，因此当帕金森综合症被诊断出时，患者皮质区的多巴胺神经元往往已经大量丧失，且此病理变化不可逆。这也是神经退行性疾病难以治疗的原因，毕竟神经细胞是人体分化程度最高的细胞，而成年后人脑大部分脑区都已无法再自行生成新的神经细胞。这使得帕金森综合症目前的治疗方式只能治标不治本，主要功效为改善病人的运动缺陷。市面上治疗此病最经典的药物为左旋多巴。长期使用此药物会诱使病人最终发展为异动症。因此，想要更好得治疗此病，在细胞和分子层面了解疾病进程是必不可少的。此论文首先研究了纹状体中受多巴胺神经元控制的脑细胞在丧失多巴胺神经元后产生的结构和功能性的变化。

纹状体中的神经元细胞95%为棘状投射神经元 (SPNs)。根据他们的投射区域及多巴胺受体亚型的表达又分为两类：直接路径棘状投射神经元和间接路径棘状投射神经元。第一类亚型于胞体和树突上大量表达一型多巴胺受体(D1R)，而第二类亚型于胞体和树突上大量表达二型多巴胺受体 (D2R)。在临床病例和动物实验模型中，两类棘状投射神经元均表现出显著的结构和功能性异变，此类变化与帕金森综合症病理症状息息相关，但其在丧失多巴胺神经元支配后异变的时间进程还不曾有人进行过系统研究。除此之外，黑质向纹状体投射的多巴胺轴突在凋亡过程中也会激起神经胶质细胞的活性，主要包括但不限于小胶质细胞和星型胶质细胞。因此刻画这两类细胞活性反应的时间进程对于了解帕金森综合症病理机制有很大意义。此论文也进一步探讨了神经胶质细胞活性与纹状体棘状投射神经元病理变化之间的关系。

最后，此论文研究重点从探索疾病机理转移到探索有前景的临床治疗药物，以求在预临床阶段使用小鼠模型来评估候选药物改善帕金森症神经元及神经胶质细胞恶性变化的效果。被测试药物（氟伏沙明, Fluvoxamine）已在临床批准用于治疗抑郁症。此药后被研究证明对西格玛一型受体(Sig-1R)有很强的亲和性。而这类受体作为细胞内常见的伴侣受体，在调节细胞应激与存活机制中具有不可磨灭的作用。在本论文中，氟伏沙明在模型实验鼠纹状体及黑质中展现了显著的神经保护性以及抗炎症活性，在预临床阶段大力肯定了该药物作为治疗帕金森综合症疾病修正药物的前景。

# List of Abbreviations

| | |
|---|---|
| PD | Parkinson's disease |
| 6-OHDA | 6-hydroxydopamine |
| $A_2$aR | adenosine A2a receptor |
| AC | adenylyl cyclase |
| aCSF | artificial cerebrospinal fluid |
| AMPA | α-amino-3-hydroxy-5-methyl-4-isoxazolepropionic acid |
| AP | action potential |
| BAC | bacterial artificial chromosome |
| BDNF | brain-derived trophic factor |
| BG | basal Ganglia |
| C1q | complement component 1q |
| cAMP | cyclic adenosine monophosphate |
| CD | cluster of differentiation |
| $D_1$R | dopamine D1 receptor |
| $D_2$R | dopamine D2 receptor |
| DA | dopamine |
| DARPP-32 | dopamine and cAMP- regulated phospoprotein |
| DPL | days post lesion |
| DS | delay start |
| dSPN | direct pathway spiny projection neuron |
| eCB | endocannabinoids |
| eGFP | enhanced green fluorophore protein |
| EPSC | excitatory post-synaptic current |
| ER | endoplasmic reticulum |
| GABA | aminobutyric acid |
| GFAP | glial fibrillar acidic protein |
| GluN1 | glutamate ionotropic receptor NMDA type subunit 1 |
| GluN2A | glutamate ionotropic receptor NMDA type subunit 2A |
| GluN2B | glutamate ionotropic receptor NMDA type subunit 2B |
| GPe | globus pallidus pars externa |
| GPi | globus pallidus pars interna |
| HFS | high frequency afferent stimulation |
| Iba1 | ionized calcium binding adaptor 1 |
| IF | immunofluorescent |
| IHC | immunohistochemistry |

| | |
|---|---|
| IL-1α | interleukin-1 alpha |
| IL-1β | interleukin-1 beta |
| IS | immediate start |
| iSPN | indirect pathway spiny projection neuron |
| Kir | inward rectifying potassium channel/current |
| L-DOPA | L-3,4 dihydroxyphenylalanine |
| LTD | long-term depression |
| MFB | medial forebrain bundle |
| mGluR5 | metabotropic glutamate receptor 5 |
| NMDA | N-methyl-D-aspartate |
| PBS | saline phosphate buffer |
| PCR | polymerase chain reaction |
| PFA | paraformaldehyde |
| PKA | protein kinase A |
| PKC | protein kinase C |
| PPR | pair-pulse ratio |
| RMP | resting membrane potential |
| Sig-1R | sigma-1 receptor |
| SNc | substantia nigra pars compacta |
| SNr | substantia nigra pars reticulata |
| SPN | spiny projection neuron |
| STN | subthalamic nucleus |
| SSRI | selective serotonin reuptake inhibitor |
| TH | tyrosine hydroxylase |
| TNF-α | tumor necrosis factor alpha |
| VA | ventral anterior |
| VL | ventral lateral |
| VTA | ventral tegmental area |
| WB | western blotting |
| WT | wild type |

# Introduction

## Parkinson's Disease

Parkinson´s disease (PD) is a relatively common neurodegenerative disorder with unknown aetiology in 90% of the cases. Whether idiopathic or genetically inherited, PD is characterized by cardinal motor symptoms (hypokinesia, bradykinesia, muscle rigidity, resting tremor), which need to be present for the clinical diagnosis (Cardoso et al., 2023). Parkinsonian motor symptoms are mainly due to the degeneration of nigrostriatal dopamine (DA) neurons. The degeneration starts in dopaminergic axons innervating the putamen (the motor part of the striatum), which show a particular vulnerability and degenerate early in PD (Tagliaferro & Burke, 2016). With the progression of disease, the dopaminergic degeneration extends to additional DA projection systems (Gaspar et al., 1991; Pavese et al., 2011). Along with the severe DA neuron loss, brains from PD patients exhibit intraneuronal protein inclusions (Lewy bodies) in disease-affected brain areas (Braak et al., 2003). In addition to the motor symptoms, all PD patients experience non-motor symptoms that include neuropsychiatric problems (cognitive deficits, anxiety, depression, apathy) (Weintraub et al., 2022) and autonomic dysfunctions (Z. Chen et al., 2020). These non-motor symptoms are marginally or not improved by current treatments.

At present, there is no cure for PD. Treatments are symptomatic and focus on managing the motor symptomatology with dopaminomimetic drugs, the most effective being L-DOPA (a DA precursor administered as oral tablets). Unfortunately, within a few years, this treatment induces motor fluctuations and debilitating abnormal involuntary movements (dyskinesia) in most patients (reviewed in (Cenci et al., 2022)). To reduce the dose of L-DOPA, hence the incidence of motor complications, it is common to prescribe adjunctive treatment with DA receptor agonists, most of which have preferential activity at D2/3 type receptors. The use of DA agonists is however associated with a high prevalence of impulse control disorders (ICD), the most frequent being gambling and compulsive shopping (Weintraub et al., 2015). The limitations of current treatments have prompted a development of advanced therapies such as continuous jejunal L-DOPA delivery and deep brain stimulation (DBS) of the subthalamic nucleus. While these treatments reduce the motor complications of oral pharmacotherapy, they can aggravate several neuropsychiatric disturbances (Jahanshahi et al., 2015) and have significant side effects.

The prevalence of PD has doubled in the past 25 years. Global estimates in 2019 showed over 8.5 million individuals with PD. Current estimates suggest that, in 2019, PD resulted in 5.8 million disability adjusted life years (DALYs), an increase of 81% since 2000, and caused 329 000 deaths, an increase of over 100% since 2000.

# The basal ganglia

The basal ganglia refer to a group of subcortical nuclei deeply embedded in the brain hemispheres. These nuclei include the striatum (divided in caudate and putamen nucleus in primates), the globus pallidus (divided in pars externa and pars interna), the subthalamic nucleus (STN) and the substantia nigra (divided in pars compacta and pars reticulata). The basal ganglia form a network together with cortex, thalamus, and brain stem pre-motor regions, enabling the selection and execution of appropriate motor sequences (Nelson & Kreitzer, 2014; Redgrave et al., 1999).

The basal ganglia are generally divided into three parts: input nuclei, output nuclei and intrinsic nuclei (Lanciego et al., 2012). The largest input component is the striatum, which receives abundant inputs from both the cerebral cortex and the thalamus. The output nuclei are structures that send information from the basal ganglia to targets in the thalamus and the brain stem, and consist of the internal segment of the globus pallidus (GPi) and the substantia nigra pars reticulata (SNr). Intrinsic nuclei include the external segment of the globus pallidus (GPe), part of the STN and the substantia nigra pars compacta (SNc). The appropriate functioning of the basal ganglia system requires DA, and dysfunction in DA signalling leads to severe movement disorders, such as difficulties in movement initiation and poverty of movement.

# The striatum

Being the largest structure in the basal ganglia network, the striatum receives a dense glutamatergic innervation from the entire cerebral cortex (Donoghue & Herkenham, 1986; Gerfen, 1984; Redgrave et al., 2010; Selemon & Goldman-Rakic, 1985). Cortical glutamatergic synapses form onto the heads of dendritic spines on the so-called spiny projection neurons (SPNs), which make up over 90% of neurons in the striatum. In addition, these neurons receive thalamostriatal projections with glutamatergic axons forming synaptic contacts on both dendritic spine heads and dendritic shafts (Castle et al., 2005; Dube et al., 1988; Smith et al., 2004). The dopaminergic terminals originating from the substantia nigra pars compacta (SNc) and the ventral tegmental area (VTA) form synaptic contacts on the neck of SPN spines (Surmeier et al., 2007), facilitating modulatory effect on glutamatergic

neurotransmission (Haber et al., 2000; Lynd-Balta & Haber, 1994a, 1994b; Prensa & Parent, 2001). An illustrative schema of striatal and basal ganglia circuitry is depicted in Fig 1.

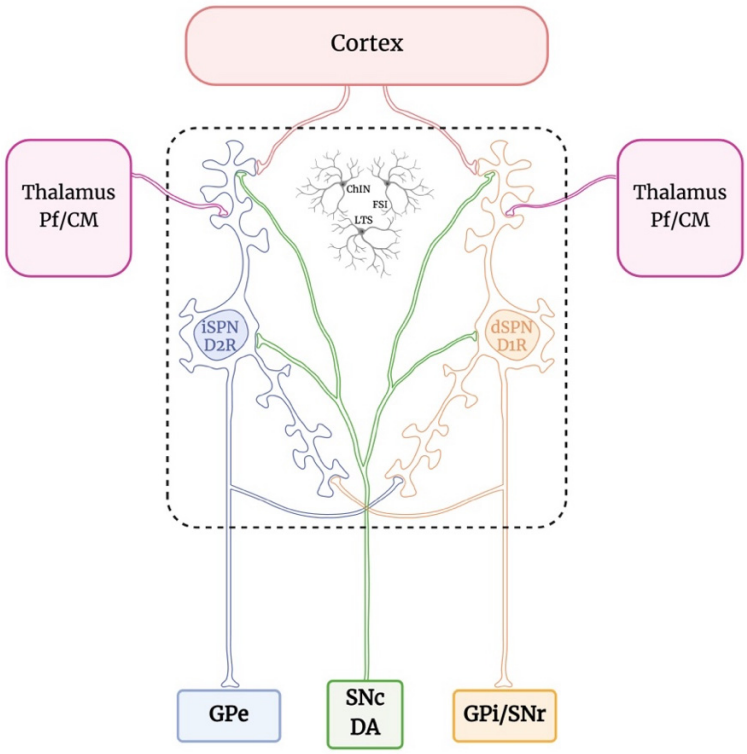


**Figure 1. Schematic representation of striatal neuron afferent and efferent projections**. Striatal iSPNs express $D_2$Rs (blue) and project to GPe, while dSPNs expressing $D_1$Rs (orange) target GPi and SNr. Both subtypes receive cortical glutamatergic inputs (red) formed onto the spine heads. Certain thalamic glutamatergic projections form synaptic contacts mainly on spine neck and dendritic shafts. dSPNs and iSPNs also send axonal collaterals to inhibit each other, together with sparse interneurons (gray) in the striatum, forming a powerful inhibitory local circuitry (Burke et al., 2017; Cenci & Kumar, 2024). Nigral dopaminergic innervation forms axo-somatic, axo-dendritic and axo-spinous boutons on SPNs. Pf/CM, parafascicular and centromedian thalamic nuclei; ChIN, cholinergic interneurons; FSI, fast spiking interneurons; LTS, low threshold spiking interneurons; GPe, globus pallidus pars externa; GPi, globus pallidus pars interna; SNr, substantia nigra pars reticulata; SNc, substantia nigra pars compacta.

Nigrostriatal dopaminergic projection exhibits a powerful control on striatal neurons, as evidenced by both a high expression of DA receptors and an exceptionally dense dopaminergic innervation density in the striatum. In rodent, one dopaminergic axon is estimated to contact around 75000 SPNs, and one SPN is under the coverage of 95-194 dopaminergic neurons (Lanciego et al., 2012; Matsuda et al., 2009). These numbers are even larger in primates, where one dopaminergic neuron can make up to 1 million synaptic contacts onto striatal neurons (Lanciego

et al., 2012). Such an abundance of nigrostriatal axonal arborizations emphasizes the vital modulatory effect exerted on striatal neurons by their dopaminergic input. When the sophisticated nigrostriatal DA axon network degenerates in PD, dramatic changes occur to the function of striatal neurons and their projections to other basal ganglia nuclei.

Within the striatum, there are two main divisions, the dorsal and the ventral striatum, in which the former is primarily involved in control of movements and cognitive executive functions, whereas the latter (ventral striatum) is responsible for affective functions, such as the response and sensitivity to reward and aversion (Young et al., 2024).

A large body of studies implicate the striatum in motor control, including both the generation and the inhibition of movements (Kravitz & Kreitzer, 2012). As early as in 1940s, Mettler described bilateral striatal lesions would cause animals to run forward without regard to obstacles or walls in their paths (Mettler, 1945; Mettler & Mettler, 1940, 1942). Similar phenomena were observed in parkinsonian patients who were described as unable to stop running at times, sending themselves headlong into walls and furniture (Martin, 1966). James Parkinson in his work "An Essay on the Shaking Palsy" also described such behaviour as "an inability for motion, except in a running pace" (Parkinson, 2002). A large number of animal studies have proven that either loss or excess of DA in the striatum results in movement disorders (either poverty of movement, ie hypokinesia, or uncontrolled abnormal movements, ie dyskinesia) (Blume et al., 2009; Bove & Perier, 2012; Lundblad et al., 2002; Lundblad et al., 2004; Lundblad et al., 2005; Sedelis et al., 2001).

## The SPNs and their expression of dopamine receptors

As mentioned above, well-coordinated movement control is achieved partially due to a heterogeneous composition of neuronal populations in the striatum (often mutually inhibiting or counterbalancing), 90% of which are projection neurons (SPNs) (Kawaguchi, 1997) and 10% are the interneurons. As the principal neurons of the striatum, SPNs were termed so due to their medium size of cellular soma (20 μm in diameter) and multipolar dendritic arborizations densely interspersed with postsynaptic specializations, so called dendritic spines. They are also proven to be inhibitory neurons which use GABA as their neurotransmitter.

Although almost indistinguishable in appearance, striatal SPNs divide into two subpopulations according to their projection targets and selective expression of different dopamine receptors. Those innervating GPe nucleus express the dopamine receptor subtype 2 ($D_2R$), and the other SPNs projecting to the output nuclei GPi and SNr express exclusively dopamine subtype 1 receptors ($D_1R$) (Gerfen et al., 1990). When dopamine binds to $D_1Rs$, which are positively coupled to the G-protein

$G_{olf}$(Herve et al., 1995), adenylyl cyclase (AC) is activated leading to the production of the secondary messenger cyclic adenosine monophosphate (cAMP), the activation of protein kinase A (PKA) and the phosphorylation of different substrates. Among all substrates, DARPP-32 (DA and cAMP-regulated phosphoprotein) is one of the most well studied. It regulates neuronal excitability and glutamatergic transmission (Surmeier et al., 2007). When $D_2$Rs are stimulated by dopamine, multiple modulatory effects are activated. First, $D_2$R-coupled $G_{i/o}$ proteins negatively modulate the AC levels (Stoof & Kebabian, 1984) and cAMP signalling. In parallel, $D_2$R activation, via the $G_{\beta\gamma}$ subunits and subsequential activation of protein kinase C (PKC) (Surmeier et al., 2010), reduces L-type $Ca_2^+$ currents (Cav1.3 $Ca^{2+}$ channels) (Day et al., 2006; Hernandez-Lopez et al., 2000) and boosts inward rectifying potassium (Kir) currents (Cazorla et al., 2012; Gardoni & Bellone, 2015), leading to a decrease of neuronal excitability (Surmeier et al., 2007). Presynaptic location of $D_2$Rs on the glutamatergic axons also influence excitatory neurotransmission via the presynaptic $Ca_2^+$ influx (Higley & Sabatini, 2010).

SNr-derived dopamine exerts an opposite modulatory effect on the cellular excitability of dSPNs and iSPNs. To be more specific, activation of $D_1$R usually leads to the potentiation of NMDA receptor-mediating currents and a higher excitability, both via the L-type $Ca_2^+$ channels and through more active postsynaptic membrane trafficking of NMDAR subunits (Blank et al., 1997; Cepeda et al., 1993; Cepeda & Levine, 1998; Dunah et al., 2004; Hallett et al., 2006; Levine et al., 1996; Liu et al., 2004; Murphy et al., 2014; Surmeier et al., 2010; Vergara et al., 2003). Jocoy, E. L and colleagues in their work (Jocoy et al., 2011) dissected the contribution of GluN1 and GluN2A/B subunits to NMDA currents and their dopaminergic modulation upon stimulation on $D_1$Rs and $D_2$Rs. To summarize, genetic knockout of GluN1 subunits significantly reduces $D_1$R-mediated potentiation of NMDA currents. In comparison, genetic deletion of GluN2A subunits enhances such $D_1$ modulation, whereas pharmacological blockage of GluN2B subunits reduces this potentiation, indicating counteracting roles played by GluN2A/B subunits regarding regulating NMDA receptor responses. Moreover, they have also shown a higher contribution of GluN2A subunits to NMDA receptors in dSPNs, and more attributes of GluN2B subunits to iSPNs. In addition, $D_1$R activation also modulates conductance of other ion channels, including sodium (Scheuer & Catterall, 2006; Surmeier & Kitai, 1993) and calcium (Kisilevsky et al., 2008) channels. As for $D_2$R signalling, its activation reduces the excitability of $D_2$R-expressing SPNs. In detail, activation of $D_2$Rs not only decreases α-amino-3-hydroxy-5-methyl-4-isoxalone propionic acid (AMPA) receptor currents (André et al., 2010; Cepeda et al., 1993; Hernández-Echeagaray et al., 2004), but also diminishes pre-synaptic glutamate release (Bamford et al., 2004). Besides, $D_2$R activation also reduces opening of voltage-dependent $Na^+$ channels (Surmeier & Kitai, 1993) and promotes the opening of $K^+$ channels (Greif et al., 1995). Taken altogether, the $D_1$R signalling is considered to promote the excitatory pathway, and the $D_2$R signalling assumes an inhibitory function.

# The classic model of the BG circuitry

As mentioned in the previous sections, the BG circuitry exerts a key function in movement control. Striatum acts as a hub receiving motor signals from the cortex and the thalamus, weighs these signals, and selects the most relevant movement command to be implemented while filtering and tuning down the "noise" signal that may interfere with proper motor control. How do the intrinsic nuclei (in comparison to the input and output nuclei of the BG network) and the striatum do so? The classic model of BG network defines the "direct pathway" as originating from the $D_1R^+$ SPNs (dSPNs) and projecting directly to the output nuclei (GPi and SNr). In line with this nomenclature, the "indirect pathway" initiates from $D_2R^+$ SPNs (iSPNs) reaching to the output nuclei by first projecting to GPe and STN. In other occasions, dSPNs are also termed as striatonigral neurons, and iSPNs called striatopallidal neurons.

When dopamine is released in the striatum via the nigrostriatal axons, dSPNs are excited to send inhibitory projections to the GPi/ SNr, in which the GABAergic inhibitory neurons further project to ventral anterior (VA) and ventral lateral (VL) thalamus where glutamatergic excitatory neurons project to the motor cortex. In this way, the "direct pathway" inhibits GPi which in turn stops inhibiting the thalamus. Thereby, the VA/VL thalamus are "disinhibited" and are able to excite the motor cortex and promote movement (Kravitz et al., 2010; Young et al., 2024). In comparison, dopamine reduces the activity of iSPNs that innervate the GABAergic inhibitory neurons in the GPe, and GPe further inhibits STN, the excitatory neurons in which project to GPi/SNr. The same as above, the GPi negatively governs the VA/VL of the thalamus. In this way, the activation of the "indirect pathway" stimulates the GPi which then suppresses thalamus's activity, in this end inhibiting movement (Durieux et al., 2009; Sano et al., 2003; Young et al., 2024). So far, the classic model of dopaminergic modulation of BG circuitry and movement selection had been set up, until Costa and colleagues demonstrated that concurrent activation of both dSPNs and iSPNs is required for movement initiation (Cui et al., 2013). This first line of evidence challenged the classic view that two pathways counteract to control BG output, and proposed a coordinated manner for movement control.

# The striatal pathology in the Parkinson's Disease

One of the most significant hallmarks of PD is the loss of dopaminergic innervation of the striatum. As mentioned above, loss of dopaminergic input is expectable leading to a hypoactivity in dSPNs and a hyperactivity in iSPNs (Albin et al., 1989; Surmeier et al., 2014). Indeed, in animal models of PD, such cell type-specific changes were observed (Kravitz et al., 2010; Mallet et al., 2006) after striatal dopamine depletion. Thereby, the suppressed motor symptoms observed in PD

patients can be at least partially explained by the disturbed and imbalanced BG circuitry.

The importance of the striatal dopaminergic modulation in movement control is now beyond any doubt, as we discussed before. The next to ask is: how does the BG network respond to or adapt to such aberrant perturbations? Clinical investigations have shown that both initiation and progression of parkinsonian symptoms take years to develop in patients. By the time that clinical symptoms start to surface, merely around 50% of DA neurons in midbrain and 30% of striatal DA content remains (Bernheimer et al., 1973; Fearnley & Lees, 1991; Tagliaferro & Burke, 2016). Considering that the brain is a plastic organ containing millions of neurons and synaptic connections it is conceivable that it would reorganize its structure and functionality in order to develop novel mechanisms to compensate for any kind of deficiency or loss of functions in pathological conditions (Hurst, 1965; Johnston et al., 2009). Such kind of adaptive mechanisms underlying neuroplasticity are termed as "homeostatic adaptations" in a lot of occasions, specifically referring to the ability to restore the lost balance.

## SPN morphological-functional alterations in the PD

In the context of parkinsonism, bi-directional compensatory mechanisms render reduced intrinsic excitability of iSPNs and elevated intrinsic excitability of dSPNs, as a result of their hyper- and hypo- activity, respectively, following DA depletion in the striatum over time (Fieblinger, Graves, et al., 2014). In addition to changes in the basic electrophysiological properties, postsynaptic spine structures have also been discovered to be substrates for homeostatic plasticity. To be more specific, iSPNs substantially lose dendritic spines up to 30% following striatal DA depletion (Day et al., 2006; Fieblinger, Graves, et al., 2014; Fieblinger et al., 2022; Nishijima et al., 2014; Suarez et al., 2014). Theoretically, reduced number of spines in iSPNs provide fewer anatomical sites for excitatory input from the corticothalamic circuit, thereby it fits the general principal of homeostasis that spine pruning helps to restrain the over-active iSPNs in a lack of $D_2R$ signalling. Unlike iSPNs, spine stripping in dSPNs reported in previous studies using experiment models has remained a matter of debate. Discrepancies in whether dSPN spines are pruned or not probably can be explained by the choice of parkinsonian model creation, by the duration of dopamine depletion in a certain model, and lastly by different methods which were used to acquire morphological images. Two studies discovered no decline in spine density at 3- 4 weeks after the onset of 6-OHDA lesion (Day et al., 2006; Fieblinger, Graves, et al., 2014) using two-photon laser visualization of neurons alive. One study from the same group using the same methods claimed a spine loss in dSPNs at a more chronic stage, 2 months following the lesion (Graves & Surmeier, 2019). Other studies performed in 6-OHDA lesioned mice reported a dSPN spine loss as early as 4 weeks post toxin infusion, however such observation

was achieved by using conventional confocal imaging (Gagnon et al., 2017; Li et al., 2024; Suarez et al., 2014). Moreover, investigations from a genetic mouse model of DA depletion and a primate model based on MPTP have both displayed a comparable degree of spine loss in both iSPNs and dSPNs (Suarez et al., 2018; Villalba et al., 2009). Regardless of the uncertain timing of the event, hypoactivity in dSPNs should not warrant a decrease in glutamatergic synapses hypothetically on a base of homeostatic response. In other words, different mechanisms underly post-synaptic remodelling in two populations of SPNs, where the one in dSPNs could be "maladaptive".

Spine protrusion and retraction in the adult age is a common form of morphological remodelling and synaptic plasticity in neurons. The temporal course of that is relatively rapid and acute in comparison to the regression or atrophy of dendritic arbour. More than three decades ago, a shorter length of dendrites in striatal SPNs was described in deceased cases of PD (McNeill et al., 1988; Stephens et al., 2005; Zaja-Milatovic et al., 2005). The authors from the above studies even suggested that the dendrite regression observed in SPNs was a highly potential suspect of declining efficacy of DA replacement therapy in late-stage PD patients. Considering multiple methodological limitations in the human post-mortem studies, animal experimental models, especially transgenic mice with genetically edited expression of fluorophore reporters under $D_1$R- and $D_2$R/$A_2$aR- promoters, were developed to distinguish between dSPNs and iSPNs (Gong et al., 2003). Another great advantage of using an experimental setting to model PD lies in the possibility to individually manipulate all relevant factors that may influence the progression of a pathological condition under a tight control. Two studies using 6-OHDA lesion model in mice have shown that severe loss of DA inputs to striatum recapitulated similarly pronounced reduction of dendritic complexity, as observed in human studies, in both pathways of striatal SPNs (Fieblinger, Graves, et al., 2014; Gagnon et al., 2017). Same phenomena were also described in the aphakia mouse, a genetic model lacking striatal DA content from at birth (Suarez et al., 2018). It is noteworthy to point out that in above-mentioned cases, both dSPNs and iSPNs exhibited a similar temporal course in dendrite degeneration, differing from the delayed timing of spine pruning observed in dSPNs, in comparison to that in iSPNs. The unidirectional changes of dendritic arbour and their irreversibility by DA supplement treatment (Levodopa, L-DOPA) inevitably point to a pathological mechanism rather than DA-dependent homeostatic adaptations. One hypothesis could be deficient trophic factor support, such as brain-derived trophic factor (BDNF) (Andreska et al., 2023).

Long-term changes in the synaptic strength are the well-characterized types of synaptic plasticity in the striatum. One of the most robust observations is that $D_2$R signalling promotes the induction of LTD at corticostriatal synapses in iSPNs (Surmeier et al., 2014). Studies from the 1990s showed that high frequency afferent stimulation (HFS) in *ex vivo* slice preparation induces a long-lasting decrease in the amplitude of excitatory postsynaptic potentials in SPNs (Mathur & Lovinger, 2012;

Walsh, 1993). As a Hebbian form of long-lasting synaptic plasticity, induction of such requires HFS coupled with postsynaptic depolarization (Calabresi et al., 1992; Choi & Lovinger, 1997). Concomitant activation of postsynaptic L-type voltage-gated $Ca_2^+$ channels (VGCCs, Cav1) combined with metabotropic glutamate receptor 5 (mGluR5) promotes the production and release of endocannabinoids (eCB), which bind to presynaptically localized CB1 receptors as a retrograde messenger (Gerdeman et al., 2002), leading to a long-lasting decline in probability of glutamate release (Lovinger et al., 1993; Surmeier et al., 2014; Zhai et al., 2019). In iSPNs, $D_2$R signalling diminishes PKA stimulation of RGS4, disinhibiting mGluR5-mediated production of eCB, thereby promoting LTD (Lerner & Kreitzer, 2012). Another study also reavealed an opposing regulatory effect between $D_2$R and $A_2$aR activation, where the former promotes LTD and the later promotes LTP (W. Shen et al., 2008).

## Neuroinflammation in PD

Initially, researchers in the field of PD used to constrain their attention merely to cellular mechanisms within neurons underlying DA neuronal death. Over the past several decades, growing evidence suggests a pivotal role also played by neuroinflammation in the pathogenesis of PD. Ever since neuroinflammation had taken the "hotspot" in the field of PD research, numerous studies have focused on SNc where nigrostriatal DA neuronal soma are located. However, neuroinflammatory reactions in the striatum, the gateway nuclei of BG circuit where corticothalamic motor and sensory inputs converge to filter input signals, has been largely neglected. Moreover, dopaminergic modulation of movement control is mainly achieved by innervating striatal neurons of two opposing pathways with distinct expression of DA receptor categories. This further questions what effects assumed striatal neuroinflammatory process would impose on SPNs. Taken together, characterizing the neuroinflammatory profile in the parkinsonian striatum would deepen the understanding of pathogenesis of PD and further provide potential subjects for disease-modifying therapeutic strategies in the future.

The earliest record of the "activated" microglial phenotype stems back to 1988 by McGeer and colleagues (McGeer et al., 1988), in which they detected large numbers of HLA-DR-positive reactive microglia in the SN of post-mortem PD cases. Later on, more studies discovered additional reactive features of microglia, such as upregulated levels of phagocyte marker CD68 and complement receptor CR3 in PD-affected regions including SN and putamen (Banati et al., 1998; Croisier et al., 2005; Imamura et al., 2003). Additionally, reactive astrocytes marked by glial fibrillar acidic protein (GFAP) and Vimentin were also noted in the brains of PD patients (Banati et al., 1998; McGeer et al., 1988; Yamada et al., 1992).

Microglial cells, as the brain resident macrophages, are the first line of immune surveillance, pathogen defence and maintenance of homeostasis (Hanisch &

Kettenmann, 2007; Kuter et al., 2020; Nimmerjahn et al., 2005; Streit, 2002). Microglia respond to external insults or stimuli by engaging in divergent morphological and phenotypical changes (Kreutzberg, 1996; Ransohoff & Perry, 2009; Vidal-Itriago et al., 2022; Wolf et al., 2017). Morphological shift from highly ramified to an amoeboid soma is a common evident marker of microglial activation (Kreutzberg, 1996). Depending on specific pathological conditions, different profiles of transcriptional factors (Holtman et al., 2017) push microglia into either neuroprotective or neurotoxic directions (Hanisch & Kettenmann, 2007; Tang & Le, 2016). The classic view of the deleterious phenotype, often referred as M1-microglia, produces pro-inflammatory cytokines, including tumor necrotic factor- α (TNF-α), IL-6, IL-12, and IL-1β (Martinez & Gordon, 2014; Tang & Le, 2016). In contrast, M2-microglia produce anti-inflammatory molecules, such as transforming growth factor (TGF)-β and IL-4, IL-10 and IL-13, and display immune-depressive or tissue repairing features (Martinez & Gordon, 2014; Wolf et al., 2017). In the experimental models of PD, mixed populations of both M1- and M2- microglia may co-exist in the early stage (Haas et al., 2016; Kuter et al., 2020; Lofrumento et al., 2011; Nagatsu et al., 2000; Pisanu et al., 2014).

Astrocytes, initially classified as a supportive cell population (Seth & Koul, 2008) in the central nervous system (CNS), play a variety of roles at physiological conditions including neurotransmitter clearance, control of cerebral flow, inotropic balance and maintenance of the blood-brain barrier (BBB) integrity (Halassa et al., 2007; Halassa & Haydon, 2010; Haydon & Carmignoto, 2006; Kuter et al., 2020; Seth & Koul, 2008). Interestingly, in the case of putative deficiency in the striatal trophic factors which was postulated as mediating striatal dendritic atrophy (as mentioned in previous sections), astrocytes are known to release neurotrophic factors (GDNF, FGF-2, VEGF) and promote neuronal survival and plasticity (Tome et al., 2017). Like microglia, astrocytes are also able to adopt A1- versus A2-reactive phenotypes in the immune response but more as a response to microglia-released signals or stressed neurons (Ding et al., 2021; Liddelow & Barres, 2017; Liddelow et al., 2017; Yun et al., 2018).

## The sigma-1 receptor as a potential target for disease-modifying treatments

The Sigma-1 receptor (Sig-1R) is a small (28 kDa) transmembrane protein located in the endoplasmic reticulum (ER) membrane, specifically enriched in the ER subregion contacting mitochondria, called the mitochondrial-associated membrane (MAM) (Hayashi & Su, 2003; Nguyen et al., 2015). Multiple CNS cell types express Sig-1Rs, including astrocytes, microglia, oligodendrocytes and neurons. In response to ligand binding, Sig-1Rs can migrate between organellar and cellular membranes (Hayashi & Su, 2007; Su et al., 2010), regulating the activity of a large variety of ion channels, signalling molecules, and other receptors. As a chaperone protein that

accommodates numerous client proteins at various membranous sites, Sig-1Rs often exert multifaceted neuroprotective effects via several cellular mechanisms: i) regulation of intracellular calcium levels and prevention from glutamate excitotoxicity (Behensky et al., 2013; DeCoster et al., 1995; Griesmaier et al., 2012; Hayashi & Su, 2007; Y. C. Shen et al., 2008; Shimazu et al., 2000; Tchedre et al., 2008; Tchedre & Yorio, 2008); ii) modulation of mitochondrial dysfunction and ER stress (Luty et al., 2010; Miki et al., 2014; Mori et al., 2013; Shimazawa et al., 2015; Wegleiter et al., 2014); and iii) attenuation of neuroinflammation and reactive astrogliosis (Dong et al., 2016; Peviani et al., 2014; Robson et al., 2013; Robson et al., 2014; Wu et al., 2015). Taken together, Sig-1R ligands may be able to facilitate coordinated responses across cell types by activating several neuroprotective/anti-inflammatory pathways simultaneously, to achieve therapeutic outcomes (Nguyen et al., 2017). Indeed, pharmacological stimulation of Sig-1Rs is currently under clinical consideration as a potential neuroprotective treatment in several neurological diseases (Allahtavakoli & Jarrott, 2011; Behensky et al., 2013; Hyrskyluoto et al., 2013; Lahmy et al., 2013; Mori et al., 2012; Sato et al., 2014; Villard et al., 2009).

# Aims of this Thesis

I. To examine potential correlate of non-apoptotic caspase-3 activation in early synaptic dysfunctions in iSPNs following striatal DA denervation. (*paper I*)

II. To investigate temporal dynamics of structural-functional alterations to dSPNs in 6-OHDA lesioned mice and to explore potential mechanisms underlying those changes. (*paper II*)

III. To define a temporal profile of glial reactivity in the dorsal striatum at both acute and chronic stages following DA denervation, and to examine close appositions (physical contacts) between microglia and the two SPN populations in the same temporal frame (*paper III*)

IV. To preclinically evaluate a candidate drug treatment acting on Sig-1R with particular regard to amelioration of behavioural deficits, neuronal degeneration and maladaptive glial responses in a 6-OHDA mouse model of PD (*paper IV*)

# Materials and Methods

All the details about experiments if not included here can be found in the corresponding paper.

## Animals

Mouse model of PD was used in the present thesis. Both wild type (WT) and genetically engineered transgenic mice were used within these four studies. Specifically, two heterozygous strains of bacterial artificial chromosome (BAC) transgenic mice were used in Paper I to selectively target the iSPN population in the striatum: BAC-*Adora2a*-GFP (A2a-eGFP, GENSAT project, founder line KG139) and BAC-*Adora2a*-Cre (A2a-Cre, GENSAT project, founder line KG139). Paper II used both WT mice and one heterozygous transgenic mouse line BAC-*Drd1a*-tdTomato (D1-tdTomato, GENSAT project, founder line EY262) to specifically target dSPN population. Paper III contained WT mice, above-mentioned transgenic strain A2a-Cre and a new heterozygous transgenic strain BAC *Drd1a*-Cre (D1-Cre, GENSAT project, founder line EY262). Cre-lines entail a selective expression of Cre proteins in specific neuronal population by genetically edited under a cell type-specific promoter. A2a-eGFP and D1-tdTomato fluorophore-reporter lines specifically "light up" iSPNs and dSPNs by different wavelength of fluorescence. Paper IV utilized both WT male mice and Sig-1R knockout mice, which were derived from a well-characterized $\mathrm{Sigmar1}^{\mathrm{Gt(OST422756)Lex}}$ mouse strain (Chevallier et al., 2011; Mavlyutov et al., 2010; Sabino et al., 2009).

All the transgenic mouse strains were originally purchased from the Mutant Mouse Resource Regional Centre (MMRRC) at the University of California, Davis (CA), and they are all bred on a C57bl6J background. WT mice were purchased from Charles River Laboratories. Mice of 10-12 weeks old of the age at the beginning of the experimental procedures were used for all studies. Both male and female mice were adopted unless otherwise stated (Paper IV). Mice were housed under 12-hour light/dark cycle with *ad libitum* access to food and water.

**Table 1. Overview of transgenic mouse strains**

| *Mouse colony* | *Promoter* | *Transgene* | *Description* | *Paper* |
|---|---|---|---|---|
| *Adora2a-GFP* | Adora2a | GFP | iSPN reporter | I |
| *Adora2a-Cre* | Adora2a | Cre | iSPN reporter | I, III |
| *Drd1a-tdTomato* | Drd1a | tdTomato | dSPN reporter | II |
| *Drd1a-Cre* | Drd1a | Cre | dSPN reporter | III |
| *Sig-1R$^{KO}$* | Sigma1 | - | Sig-1R is knockout in the whole brain | IV |

# Surgical procedure and drug treatment

## Animal model of PD

Chronical striatal DA denervation in mice was induced through the injection of the neurotoxin 6-hydroxidopamine (6-OHDA, Sigma Aldrich) into the right medial forebrain bundle (MFB; Paper I-III), or in the right hemisphere of striatum (Paper IV) (Cenci & Lundblad, 2007; Francardo et al., 2011). Briefly, the toxin was dissolved in sterile saline containing 0.02% ascorbic acid at a concentration of 3.2 µg 6-OHDA (free base)/µl. One µl of this solution was injected to right MFB at the following coordinates (in mm relative to bregma and the dura surface): anterior-posterior (AP): -0.7, medial-lateral (ML): 1.2, dorsal-ventral (DV): -4.7 (Paper I-III) (Francardo et al., 2011). Two µl of the same solution (1 µl/site) was injected to the right striatum at the following coordinates: (1) AP: +1.0, ML: -2.1, DV: -2.9; (2) AP: +0.3, ML: -2.3, DV: -2.9 (Paper IV) (Francardo et al., 2011). Successful MFB-lesioned mice of chronic DA depletion (survived at least 2 weeks (Paper II and III) should pass the threshold of <35% contralateral forelimb use in the cylinder test (Lundblad et al., 2004). The striatal regions of these mice often exhibited > 90% depletion of dopaminergic fibres compared to sham-lesion control mice.

## Viral Vector injection

Cre-inducible AAV vectors were injected in the striatum (Paper I and III) to particularly mark two SPN populations, respectively. In Paper I, AAV5-hSyn-DIO-EGFP-WPRE was injected into the right striatum at two sites (0.5 µL each): AP = +1, ML = −2.1, DV = −2.9; and AP = +0.3, ML = −2.3, DV = −3.0 (Alcacer et al., 2017). In Paper III, AAV5-flex-GFP was injected into the right striatum at adjusted-coordinates (compared to Paper I) (1 µl/site): AP = +1, ML = −2.1, DV = −2.6; and AP = +0.3, ML = −2.3, DV = −2.6. All vectors were produced at the Lund University AAV Vector Core.

### Drug Treatments

Systematic treatment of different drugs was administered in two studies. In Paper I, a pan-caspase Inhibitor is only applicable to laboratory settings, not clinical. In Paper IV, fluvoxamine is a clinically approved drug to treat depression, here we designed to study its potential neuroprotective or neurorestorative effect in PD conditions. **Paper I**: pan-caspase inhibitor QVD-OPh (APExBio, Cat.No.: A1901) was dissolved first in DMSO and then diluted to the final concentration (2 mg/mL, 50% DMSO) with saline. Mice received injections of 10 mg/kg s.c., twice daily, with an injection volume of 5 ml/kg of the body weight. **Paper IV**: fluvoxamine maleate (HelloBio Ltd., Republic of Ireland) was freshly dissolved in saline solution and injected s.c. at the volume of 100 µl/10 g body weight. Two fluvoxamine doses were chosen based on previous studies. The lower dose (0.3 mg/kg/day) corresponds to the most effective dose of high-affinity Sig-1R agonists (Francardo et al., 2014; Francardo et al., 2019). The higher dose (20 mg/kg/day) represents the mouse equivalent of an effective antidepressant dosage of fluvoxamine in human subjects (Dalle et al., 2017a; Dalle et al., 2017b). Two types of treatment regimens were designed, the "immediate start" (IS) treatment entails the first injection immediately upon completing the 6-OHDA infusion, whereas the "delay start" (DS) treatment gave mice the first injection 7 days after the surgery. The second design is to mimic the clinical condition where the degeneration of neurons, susceptible to various risk factors, often initiates with no evident clinical symptoms, and comes into patients' realization when the pathology has progressed to certain stage.

## Behaviour Tests

Note that cylinder test was used throughout the whole thesis work, however the purpose of which differs in individual papers. For Paper I-III, the cylinder test was used as a manner to validate the success of lesion, especially prior to the patch clamp experiments, which is known as a low output technique. We intend not to apply such expensive technique on mice bearing suspicious quality of lesion. For Paper IV, the cylinder test was a main method used to evaluate the severity of voluntary asymmetric forelimb use in the striatal lesioned mice. It is an important readout of behaviour recovery to test the effect of the treatment.

Two behaviour tests used in the papers are as below:

- *Cylinder test*: This is a test of spontaneous forelimb use during vertical exploratory behaviour (Francardo et al., 2014; Francardo et al., 2019). Briefly, a glass cylinder (10 cm diameter, 14 cm height) was placed in front of two vertical mirrors to visualize the mouse movements from all angles. Mice were gently placed into the cylinder and video-recorded for 3 min. The number of supporting wall touches (contacts made with fully extended

digits) executed using left and right paws was manually counted off-line. Animals performing less than 9 touches were recorded for additional two minutes. Results were expressed as the percentage of the paw contacts performed by the forelimb contralateral to the lesion (left paw) divided by the total number of contacts.

- *Stepping test*: This test was used to assess asymmetries in adjusting steps during experimentally imposed movements (Blume et al., 2009), and was performed as described in (Francardo et al., 2019). Mice were placed at the entrance of a customized corridor (7 cm wide, 1 m long, flanked by 10-cm-high walls) and allowed to grasp the edge with forelimbs for ~2 s. The experimenter lifted the lower part of the mouse body by grabbing the tail, then pulled the mouse backwards at a steady pace (0.25 m/s) until reaching the opposite end of the corridor. The whole session was video-recorded and the number of adjusting steps executed with each forelimb was analysed offline.

## Ex-vivo slice preparations and Electrophysiological recordings

Patch clamp electrophysiological recordings were performed in Paper I and II. The slices were prepared in almost identical way. The differences are that patch clamp experiments in **Paper I** focuses on long-term plasticity (LTD) recording in iSPNs, which requires simultaneous presynaptic electrical stimulation and postsynaptic membrane depolarization. Besides, this type of electrophysiology recordings is empirically performed at physiological temperature, the *ex vivo* slice quality at which usually deteriorates faster than at the room temperature. Whereas in **Paper II**, one set of whole-cell recordings was merely to study the very basic intrinsic electrophysiological properties, the protocol of which in three repetitions took less than 2 mins to complete. What was truly time-consuming in this experimental configuration was the 2-Photon laser image acquisition of dendritic z-stacks (4 quadrants per cell), which could count up to one hour of waiting time once a whole-cell configuration was achieved. During the whole image acquisition process, the patch pipette and the cell on target ideally should be anchored tightly at the same spot with the minimal drift in the bath solution. In the meanwhile, the viability and relatively healthy status of the neuron needs to be guaranteed, this is in order for the dendrite morphology to suffice certain criteria for the subsequent reconstruction analysis. The second set of whole-cell experiments involves channel-specific current recordings, which includes 15-min of bath application of a channel blocker before the second recording session starts. In total, this type of experiment was also relatively long (around 45 mins).

## Striatal slice preparation

Acute sagittal slices were prepared as previously described (Fieblinger, Graves, et al., 2014; Sebastianutto et al., 2017). Briefly, mice were anesthetized with pentobarbital (240 mg/kg body weight, i.p.) and perfused with ice-cold artificial cerebrospinal fluid (aCSF, pH: 7.4; 300-310 mOsm). The brain was rapidly extracted, placed in ice-cold aCSF, and cut into 275 µm thick parasagittal slices using a vibratome (VT1200s, Leica, Germany). Slices were first incubated at 34°C in aCSF for 30 min, followed by 30 min of recovery at room temperature.

## Electrophysiological recordings

- *LTD recordings in iSPNs (Paper I)*: Long term synaptic plasticity in the central nervous system lays the foundation for learning and memory (Fusi et al., 2005; Kandel, 2001). Despite various underlying mechanisms (both pre- and post-synaptic wise), LTD (or LTP) has become one of the most common standards to assess the functionality and proper health status for a large variety of neuronal types. In our case, HFS-induced LTD in striatal iSPNs is the most well-established subtype, the protocol of which in *ex vivo* slice settings has been validated over and over again (Bagetta et al., 2011; Kreitzer & Malenka, 2007; Lerner & Kreitzer, 2012). We adopted the protocol and tested in our hemi-parkinsonian mouse model. In brief, the stimulation electrode was placed right underneath the corpus callosum in the dorsal striatum, and the excitatory post-synaptic currents (EPSCs) were recorded in time series from eGFP-expressing cells of mice from Sham, 6-OHDA + vehicle, and 6-OHDA +QVD groups.
- *Intrinsic excitability recording in dSPNs (Paper II)*: Intrinsic excitability is overall defined as a neuron's capability to generate action potentials (APs) in response to synaptic or somatic stimulation (L. Chen et al., 2020). There are several key parameters that could impact AP generation, such as resting membrane potential (RMP) and afterhyperpolarization (AHP). In our settings, somatic current injections of different magnitude were applied to td-Tomato expressing dSPNs for 500 ms, and the traces of AP response were recorded under the current clamp. Relevant parameters regarding intrinsic excitability were calculated as previously described (Sebastianutto et al., 2017), including but not restricted to: number of APs, RMP, amplitude/ duration/ kinetics of APs and AHP.
- *Kir-channel recordings in dSPNs (Paper II):* The inward rectifying potassium channels (Kir) are highly expressed and tonically active in striatal SPNs as a key factor to modulate the intrinsic excitability (Nisenbaum & Wilson, 1995; Wang et al., 2024). To test our hypothesis that alterations in Kir channel conductance influence dSPNs excitability in

parkinsonian mice, hyperpolarized voltage step protocols were applied to whole-cell recording cells, as in previous published studies (Cazorla et al., 2012; Gertler et al., 2008; Sebastianutto et al., 2017). Briefly, dSPNs were held at -70mV in voltage clamp and then probed in a voltage range from -150 mV to -60 mV using 100 ms test pulses with 10 mV incremental steps. Net Kir currents were calculated by subtracting the remaining currents recorded after bath application of 3 mM cesium chloride (CsCl, blocker for Kir channel) for 15 mins.

## Two-photon and confocal imaging for SPN morphology

- *Spine image acquisition and analysis (Paper I)*: As mentioned in previous section, spine loss has been characterized in both dSPNs and iSPNs in parkinsonian mouse models. In order to characterize the spine density on both iSPNs (*Paper I*) and dSPNs (*Paper II, later, using a different method*) at the "pre-mature" (referring to 5 days post 6-OHDA MFB lesion) stage after DA denervation in the striatum, two-photon imaging was performed on patch clamped cells, using a confocal microscopic settings (Sebastianutto et al., 2017). SPN morphology was revealed by addition of 50 μM of AlexaFluor-568 (excitation wavelength: 780 nm) to the internal recording solution. Dendritic segments bearing clear signals of spines, at a mid-distance from the soma (typically 50–100 μm) were shot as z-stack images for off-line spine counting analysis. For each neuron, 2–3 dendrites were analyzed and an average was taken as the final value of a cell.
- *Dendrite image acquisition and analysis (Paper II)*: For the comparison of dendrite excitability in dSPNs at acute and chronic stages after DA denervation, exactly the same two-photon imaging method as in Paper I was adopted, with only minor adaptation of changing the Fluorophore from AlexaFluor-568 to Alexa Fluor 488 (laser wavelength of 750 nm). As one of the biggest advantages of two photon-imaging, signals with adequate resolution were possible to be detected from dendritic structure of approx. 150 μm depth under the slice surface. Four z-stack images as quadrants around the soma were acquired for each neuron, stitched offline (Cazorla et al., 2012; Fieblinger et al., 2018; Sebastianutto et al., 2017). Dendritic tracing analysis was carried out on the stitched image stacks using Imaris (v7.6.1, Bitplane, AG Zurich, Switzerland). The same software was also used to perform Sholl analysis and obtain other basic features, such as: total dendritic length, number of branching points and so on.
- *Spine image acquisition and analysis (Paper II):* Due to several practical reasons in the experimental settings, dendrite morphology and spine analysis from dSPNs examined at early and late stages after DA denervation were studied using different methods. The previous was described as above,

the latter was done using slices from patch clamp recordings of Kir currents. This is because the dendrite acquisition alone using two-photon imaging, as mentioned before, takes almost one hour to complete; and dendritic segment acquisition for spines (consider 3 pieces of dendrites per cell) warrants extra 15-20 minutes. Note that reasonably good morphology of spines with a crisp signal-to-noise ratio is necessary for an accurate counting of spine numbers; and neurons examined under two-photon image settings are required alive and presenting intact dendrite structures throughout the whole image session. Thereby, instead of adding more risks and difficulties to the current experiment design, we added neurobiotin to the internal solution for Kir channel recording in whole-cell configuration, and post-fixed the used brain slices with 4% paraformaldehyde (PFA). After staining the fixed slices with streptavidin-conjugated Alexa Fluor 488, dSPN structures were examined under a normal confocal microscopic configuration, and the image acquisition parameters were set with a higher resolution to obtain better quality compared to the parameters used in two-photon settings, which obviously takes more time.

# Other experimental procedures

## Western Immunoblotting (Paper I)

Based on the hypothesis of Paper I, the striatal content of active caspase-3 (the cleaved form) is expected to increase as the striatal content of DA (or TH, as a well-verified surrogate marker of dopaminergic neuronal axons) decreases. Various experimental methods are available at choice to quantify the content of proteins. We took Western Immunoblotting simply due to easy accessibility to laboratory devices and commercial agents. Mouse striata samples were collected per previous study (Fieblinger, Sebastianutto, et al., 2014). Acute sagittal slices were cut with vibratome as prepared for Electrophysiology in ice-cold aCSF. Dissected striata were rapidly frozen on dry ice and stored at -80°C until further use. Under protease and phosphatase inhibited condition, striatal tissue was homogenized and the protein concentration was measured using a BCA Kit (Thermo Scientific). Samples were loaded on a 7.5% SDS gel and transferred on PVD membranes. Membranes were blocked with 5% nonfat dry milk and incubated overnight with the primary antibodies (Table 2). HRP-linked secondary antibody incubation was carried out and bands were visualized by chemiluminescence using an ECL kit (Thermo Scientific). Images were acquired using a CCD camera (LAS1000 system, Fuji Films, Japan) and analyzed with ImageJ (National Institutes of Health, USA). After image acquisition, membranes were stripped and re-blotted for loading controls.

## Histological procedures, immunohistochemistry and immunofluorescence

All the studies contained in this thesis had strictly defined temporal endpoints. Particularly, Paper I, II and III required hemi-parkinsonian brains punctually harvested at 5 days and 28 days post lesion, although more time points were tested in some parts of experiments (*Paper I and III*). For Paper IV, mice were supposed to be sacrificed at 35 days and 42 days based on the IS and DS treatment regimen, respectively. Upon reaching the endpoint, mice under deep anesthesia underwent a transcardial perfusion of saline phosphate buffer (PBS, pH 7.4) containing 4% PFA. Extracted mouse brains were post-fixed overnight in the same solution, and transferred to 25% sucrose-containing PBS until completely soaked. 30 μm-thick coronal sections spinning striatum and SN were cut with the vibratome used for Electrophysiology in the same PBS solution. Sequential sections were collected in plastic wells and stored at -20°C in antifreeze solution composed of ethylene glycol, glycerol and 0.1 M sodium phosphate buffer.

Protocols for staining of free-floating sections were all the same by principle. Immunolabeling of antigen-specific cell markers was achieved by commercial primary antibodies (Table 2). The difference between immunohistochemistry (IHC) and Immunofluorescent staining (IF) mainly starts from the choice of secondary antibodies, with the previous using the biotin-conjugated whereas the latter adopting fluorescent ones (Table 3), except for an additional step in IHC, to get rid of the endogenous peroxidase activity (so-called "quench", with 3% $H_2O_2$ and 10% methanol) prior to the blocking step. IF staining ends by secondary antibody incubation, and after rinsing off residual agents with PBS, sections were ready to be mounted. IHC staining entails an extra incubation step with an avidin-biotin-peroxidase solution (Vector Laboratories), followed by visualization of the immunocomplexes using 3,3-daiminobenzidine (DAB) and $H_2O_2$ (0.05% and 0.04%).

**Table 2. list of primary antibodies used in immunohistochemistry, immunofluorescence, and Western Blot**

| *Antibody* | *Host Species* | *Supplier* | *Application* |
|---|---|---|---|
| *Tyrosine Hydroxylase* | Rabbit | Pel-Freez | WB, IHC, IF |
| *Caspase-3* | Rabbit | Cell Signalling | WB, IHC, IF |
| *β-Actin* | Mouse | Sigma Aldrich | WB |
| *Caspase-3* | Mouse | BD Transduction Laboratories | IHC, IF |
| *S100β* | Mouse | Sigma Aldrich | IF |
| *Iba1* | Chicken | Synaptic Systems | IHC, IF |
| *Iba1* | Rabbit | Wako | IHC, IF |
| *GFAP* | Mouse | Chemicon | IHC, IF |
| *GFP* | Rabbit | Abcam | IF |
| *CD68* | Rat | Bio-Rad | IHC, IF |
| *DAPI* | | Invitrogen | IF |
| *TO-PRO3* | | Invitrogen | IF |

**Table 3. list of seconday antibodies used in immunohistochemistry, immunofluorescence, and Western Blot**

| *Antibody* | *Host Species* | *Supplier* | *Application* |
|---|---|---|---|
| *HRP-linked anti-biotin* | Goat | Cell Signalling | WB |
| *HRP-linked anti-rabbit* | Goat | Cell Signalling | WB |
| *HRP-linked anti-mouse* | Horse | Vector Laboratories | IHC |
| *HRP-linked anti-rabbit* | Goat | Vector Laboratories | IHC |
| *HRP-linked anti-rat* | Rabbit | Vector Laboratories | IHC |
| *HRP-linked anti-chicken* | Goat | Vector Laboratories | IHC |
| *Alexa 488 anti-rabbit* | Goat | Invitrogen | IF |
| *Alexa 647 anti-mouse* | Donkey | Invitrogen | IF |
| *Alexa 647 anti-chicken* | Donkey | Jackson ImmunoResearch | IF |
| *Alexa 488 anti-chicken* | Goat | Invitrogen | IF |
| *Alexa 555 anti-rabbit* | Goat | Invitrogen | IF |
| *Cy3 anti-rat* | Goat | Jackson ImmunoResearch | IF |
| *Cy5 anti-mouse* | Goat | Jackson ImmunoResearch | IF |

## Apoptosis Assay (TUNEL, Paper I)

Both pro-forms and active forms of caspase-3 have been quantified using Western Blot and IHC in DA-denervated striatum within the first five days after intracranial infusion of 6-OHDA. However, caspase-3 is known for playing a vital role in the programmed cell death cascade, so-called “apoptosis”. Large extent of caspase-3 activation in the biological organs usually concurs with cell death. Sub-lethal levels of caspase-3 activation, when spatially restricted to sub-cellular areas (such as: rerouting/ degenerating tips of axons and dendrites or post-synaptic sites), mediate non-apoptotic functions, including synapse plasticity (Dehkordi et al., 2022). In order to prove that the observed upregulation of caspase-3 in the acute DA-denervated striatum only serves a non-apoptotic function, paraffin-embedded mouse striatal sections (5 µm-thick) were prepared and a commercial assay attesting the presence of apoptosis was applied accordingly. Terminal deoxynucleotidyl transferase (TdT)-mediated biotinylated dUTP nick end labeling (TUNEL) was designed to detect apoptotic cells that undergo extensive DNA degradation during the late stages of apoptosis (Kyrylkova et al., 2012). In principle, TdT access the break ends of double-stranded DNA, then the precipitation of TdT is either quantified in a colorimetric manner or labeled/displayed using IHC or IF staining. We chose a product from Roche where quantification of DNA breaks was illuminated by fluorescence of Alexa Fluor 488. A bottom neck when applying this technique in our experiments is to ascertain that this particular TUNEL kit works on our sample preparations, the best way to prove which is providing a positive control prepared in the same procedure, namely a brain region where apoptosis is known to take place. Options are paraffin-embedded sections encompassing midbrain or MFB, the site where neurotoxin was infused.

### Quantitative reverse transcription PCR (RT-qPCR, Paper III)

In Paper III, one of our investigational targets is to compare the expression profile of the most relevant cytokines or immunomodulatory factors in a series of time points of MFB infusion of neurotoxin. The most prevalent and classic method to study cytokine mRNA levels undeniably is the quantitative real time PCR, the advantage of which includes both a large detection range and a reasonably good sensitivity. Tissue preparation procedure resembles that of WB, except for a requirement of extra causion in sanitary care, including autoclave all the metal tools, use none-nuclease water and agents and so on. By principle, this technique elutes mRNA from tissue homogenates, afterwards reverse transcribe those mRNA into complementary DNA (cDNA) and lastly amplify specific cDNA targets (picked up by specific primers) using a polymerase chain reaction (PCR). The development of devices and analytical software to carry out this technique has matured and been well verified, thereby the results turned out accurate and reproducibly reliable. In the end, the mRNA levels of target molecules were expressed as fold change over a housing keeping gene.

## Image analyses and cell counts

### Optical density analysis of TH fibres and Stereology counts of DA neurons in SNc (Paper I, II and III)

Densitometry analysis of TH fibres is a measurement of immunocomplex precipitation. Images of striatal sections were taken by a bright field Nikon microscope under low magnification. Optical density of TH fibres was measured using the freeware NIH ImageJ. An average value taken from three rostro-caudal levels was calculated in each animal (*Paper I and II*). Besides axonal density, the number of DA neuronal soma in the SNc was also estimated by unbiased stereology using a software newCast (Visiopharm) (*Paper I, II and III*) (Francardo et al., 2011; West, 1999). Shortly, nigral sections were mounted on the stage of the software-controlled Nikon microscope. The SNc was outlined under a 4x objective, and the counting of neurons was done under a 100x objective under the command of software using a random sampling. Counted numbers from four rostro-caudal levels were summed up, and put in a pre-determined formula composed of relevant factors. As convention, stereological counting of DA neurons is a gold standard to estimate DA cell loss in studies of PD.

## CD68 cell count and discreet TH fibre analysis (Paper IV)

In paper IV, a phagocytotic marker of microglia (CD68) was selected to assess the treatment effects in the regard of neuroinflammation. As a continuation of chapter three following two previous studies (Francardo et al., 2014; Francardo et al., 2019) published by our lab on the same topic (Sigma-1 receptor), we adopted the same marker and the same protocol of analysis as in the other two previous papers. Thereby, although this technique is rather time and labor consuming, and there are other methods available, we still sticked to the old ones, so that data across three studies could be more comparable. CD68-stained cells were manually counted with a scrutiny looking for certain morphological patterns of activated microglia, that is, densely labeled cell bodies with processes, where the signals of CD68 were usually in connected dots, stretching into the filament-shape. Such discrimination was subjected to human observation as to achieve an optimal accuracy.

Still in paper IV, another challenging readout is the measurement of TH axonal density in a postulated fibre-resprouting area (ventrolateral striatum) where the degeneration of DA fibres (at 35 days or above upon intrastriatal 6-OHDA lesion) was proven to be severe but yet spared with a subtle amount of remainder. How to detect small differences among different groups in a sparse fibre populated area? First, we visualize ventrolateral striatum in the highest magnification using 100x objective; then select as highest resolution as possible. Taken together, an image segmentation analysis using Visiopharm was adopted where distinct TH-positive fibres were distinguished from the background using a Bayesian algorithm-based pixel classifier (Westin et al., 2006). This method is not suitable to be applied to DA axon-intact striatum.

## Confocal image analysis (Paper III)

In paper I, confocal images of caspase-3 co-localizing with SPN dendrites/glial cells were only shown as a proof of concept. In paper III, co-localization of a Iba1 with GFP was quantified as physical contacts/ interactions between microglia and SPN dendrites. Note that co-localization detected by the confocal microscopy could result from approximation of two fluorescent particles, because of the scattered light signals of fluorophores). Other studies have also used confocal imaging to demonstrate intermingled or overlapped objects in specimens, for example in the ground-breaking study carried out by (Liddelow et al., 2017). Super resolution microscopy can be a better option if a confocal microscope is proven inadequate. Electron microscope can be considered as well, although the analysis of discriminating different subcellular structures and organelles requires certain level of training in experimenters.

- *Quantification of microglia-dendrite interaction:* To test our hypothesis that microglia help with spine pruning or dendrite regression in SPNs, we

filled up the SPN dendrites and post-synaptic spines with GFP via viral vector transfection. If microglia engulf constitutive elements of spines and dendrites, it is inevitable to take up GFP together with cellular contents. Thereby, a shape-delineating marker of microglia (Iba1) is expected to overlap with GFP signals. Co-localized signals were first highlighted at each confocal plan of z-stack images with a colocalization plugin, and then quantified as number of pixels using the fraction tool in ImageJ. Absolute value of contact points in each z-stack was further normalized to the number of GFP-positive pixels. We have also verified that in intact mice, basal levels of physical contact points between microglia and SPN dendrite/spine are quite comparable in GFP-expressing iSPNs and dSPNs.

- *Microglia cell count and CD68 expression:* A rapid increase in the number of microglia was expected in the striatum from 6-OHDA lesioned mice. Quantification of Iba1 and DAPI-positive cells in confocal z-stack images was performed with the analyse-particle tool in ImageJ. If microglia carry out the removal and digestion of post-synaptic or dendritic compartments under a pathological condition, an elevated phagocytic activity is expected. Thereby, as a marker of that, percentage of CD68 expression within the territory of $Iba1^+$ microglia was calculated in the same way as quantify the density of physical interactions as above.
- *Activation score of microglia:* Classic criteria to assess microglial activation usually consider transitions from "ramified" to "ameboid" morphology. In our scenario, how "ameboid" has the soma become and how "shrank" the processes are, were estimated via one parameter: activation index. It is calculated as a ratio of process-occupied pixels divided by cell body-occupied pixels. The more active the microglia, the lower the index value. The tubeness plugin of ImageJ was used to delineate microglial processes, and factional tool was used to quantify the number of pixels occupied by processes and cell bodies, respectively.

## Statistical analysis

The choice of statistical comparisons was based on the nature and distribution of the data. Statistical analysis was carried out using the software GraphPad Prism. Two-way ANOVA with Tukey's post hoc test was used to compare experimental groups on two factors (*Papers II, III),* and repeated measure ANOVA was used to compare the same groups over multiple time points *(Paper IV*). Kruskal-Wallis test or one-way ANOVA were applied as appropriate to compare multiple groups on one variable, the choice depending on whether or not the dataset passed the normal distribution tests provided by the software (*Paper I, II, III and IV*). The significance level was set as 0.05.

# Results

## Paper I. Non-apoptotic Caspase-3 activation mediates early synaptic dysfunction of iSPNs in the DA-denervated Striatum

### Caspase-3 is transiently upregulated in the DA-denervated striatum in a non-apoptotic manner

Chronic striatal DA denervation in mice was induced through the injection of 6-OHDA in the right MFB. An exponential decay of striatal TH levels was detected within the first 5 days after the lesion (Data not shown here). Concomitantly, we also discovered a surge increase of caspase-3 proteins, both the pro-caspase-3 and the cleaved active enzymatic form, in the same time course, as in Fig 2. A, B. More interestingly, IHC staining in the dorsolateral striatum revealed that the peak of caspase-3 upregulation was achieved at 5 days post lesion, followed by a rapid decline already at 7 days post lesion (Fig 2. C, D-G').

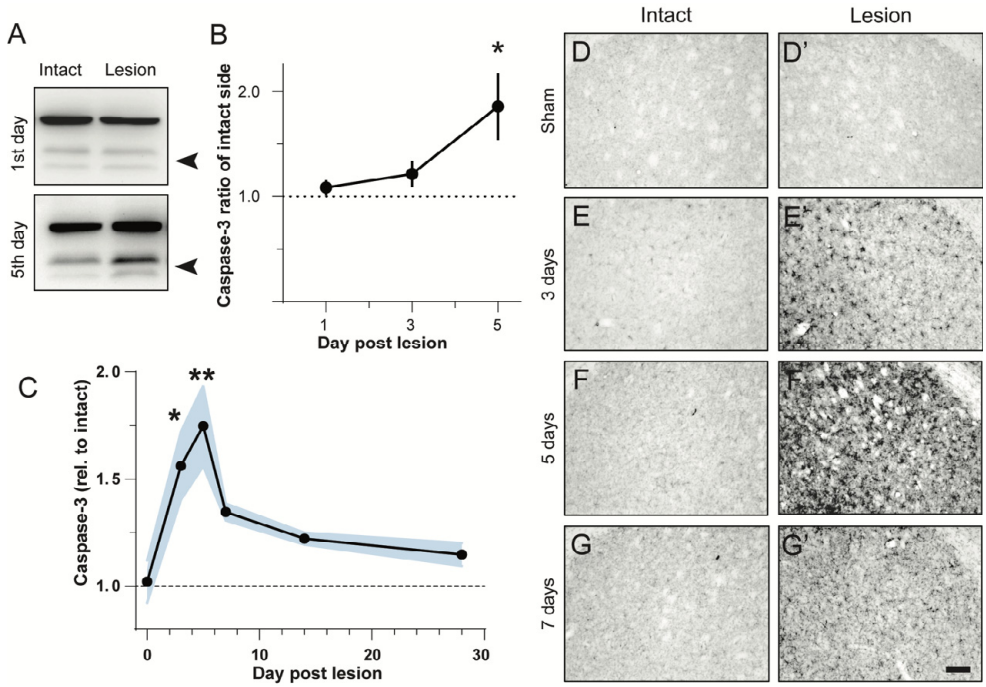


**Figure 2**. Striatal levels of caspase-3 following an acute DA denervation. (A) Examples of caspase-3-stained blots. Bands on the top indicate pro-caspase-3 protein (35 kDa), and two bands on the bottom of a weaker intensity correspond to cleaved caspase-3 (17 and 19 kDa, arrow head). (B) Western blot analysis of striatal caspase-3 content was assessed as a ratio of the cleaved over the none-cleaved form of the protein. The ratios from the lesion side are normalized to its own intact side. * $p < 0.05$ vs. one day post-lesion, ANOVA and post hoc Bonferroni test, N=6-7. (C) Densitometric analysis of caspase-3 levels in the DA-denervated striatum revealed a rapid increase at three- and five-days post-lesion, as compared to sham-lesioned animals (represented by "Day 0" datapoint). * $p < 0.05$, ** $p < 0.01$ vs. Sham, ANOVA and post hoc Bonferroni test, N=4-7. (D-G') Representative sections of dorsolateral striatum immunostained with a caspase-3 antibody depict the course of activation of caspase-3 in the DA-denervated striatum (D'-G'), in comparison to the intact side (D-G), within the first 7 days post-6-OHDA lesion. Scale bar: 100 µm.

## Early spine loss and absence of HFS-LTD in iSPNs from DA-denervated striatum are rescued by a caspase inhibitor

As previously reported, iSPNs lose their postsynaptic spines as early as 5 days following a nigrostriatal lesion (Day et al., 2006). Our two-photon imaging on iSPNs in a whole-cell configuration demonstrated a significant spine loss (Fig 3. A, B). Moreover, a systemic treatment with pan-caspase inhibitor managed to restore the loss of spines in iSPNs to a comparable level as observed in sham-lesioned control mice (Fig 3. A, B-b'').

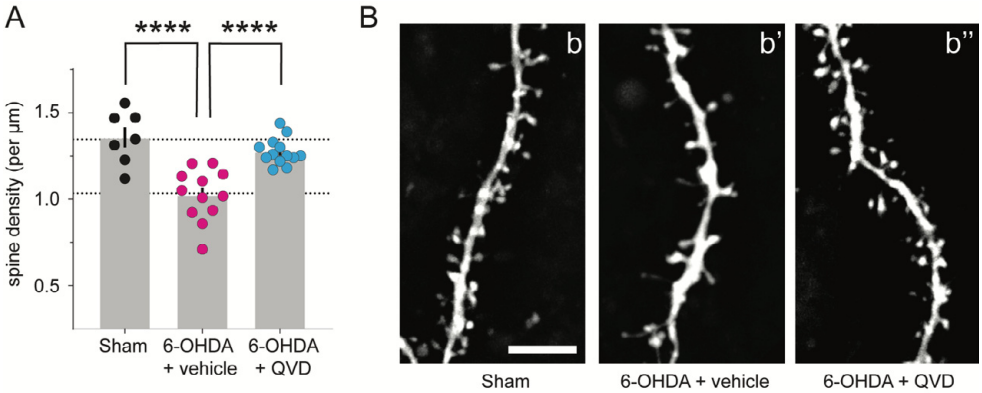


**Figure 3.** Spine loss of iSPNs following an acute DA denervation is restored by a treatment of caspase inhibitor. (A) Dendritic spine density of iSPNs is reduced at 5 days post-6-OHDA lesion, and this loss is prevented by pharmacological treatment with Q-VD-OPh (QVD). **** $p < 0.0001$ vs. 6-OHDA + vehicle, ANOVA and post hoc Bonferroni tests. N = 7-13 cells. (B) Two-photon images of iSPN dendrites, visualized after filling neurons with AlexaFluo-568 through the patch pipette. Maximum-intensity projections of dendrites from (b) Sham, (b') 6-OHDA-lesioned mice treated with vehicle and (b'') treated with QVD. Scale bar: 5 µm.

One of the most well studied functional properties in SPNs is LTD, induced by high frequency stimulation (Fig 4. A) (Bagetta et al., 2011; Kreitzer & Malenka, 2007; Lerner & Kreitzer, 2012). Here we evaluated this in iSPNs by *ex vivo* slice electrophysiology. A loss of functional LTD was revealed in 6-OHDA lesioned mice at 5 days post lesion, fitting the same time course as the loss of spines. The average traces of normalized EPSCs over a 25-min recording session from the Sham, 6-OHDA lesion, and 6-OHDA+ QVD treatment groups were presented in Fig. 3B. Again, the treatment with caspase inhibitor largely prevented the loss of LTD.

Short-term plasticity was also tested in the current experimental settings. Two electrical stimuli with short interstimulus interval (ISI) often facilitates short-term plasticity at cortico-striatal synapses (Choi & Lovinger, 1997; Gerdeman et al., 2002). As a measurement of such, pair-pulse ratio (PPR) was calculated as dividing the amplitude of the second EPSC by that of the first EPSC. Under the normal physiological condition, PPR increased after HFS, indicating a reduced probability of glutamate release from presynaptic axonal terminals (Fig 4. E). However, such increase was eliminated by removing DA inputs to the dorsolateral striatum, and regained by co-treatment with caspase-3 inhibitor.

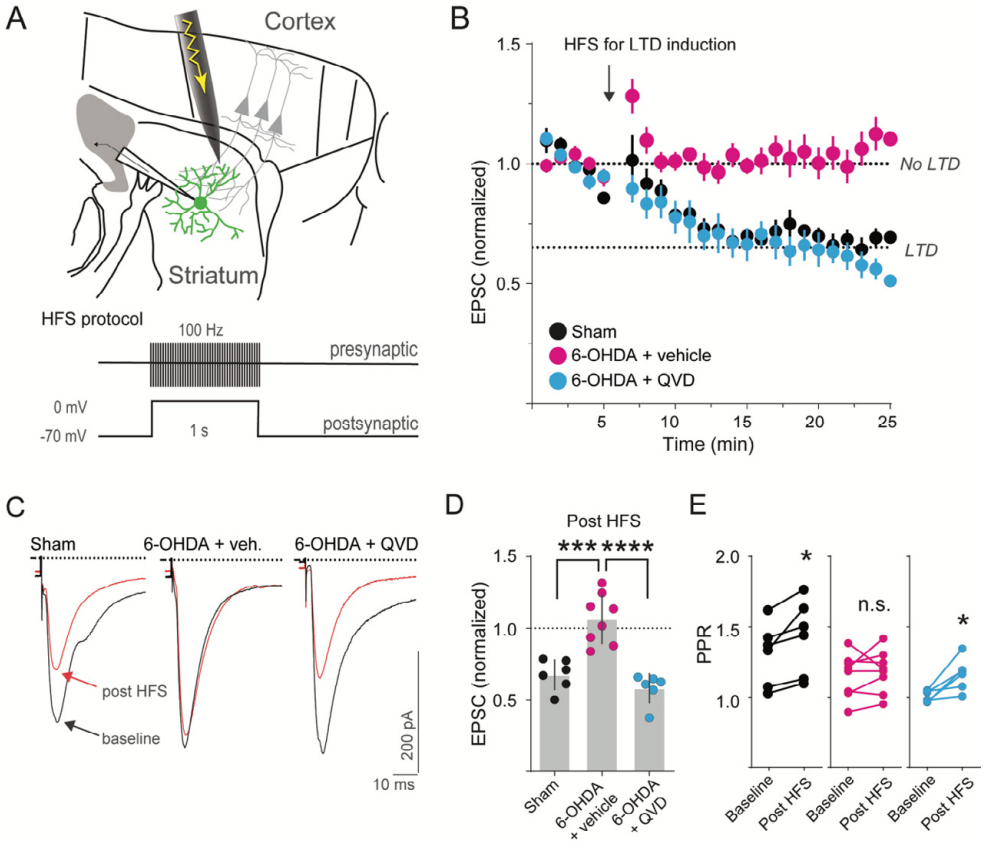


**Figure 4**. Functional LTD in iSPNs was completely lost in 6-OHDA lesioned mice, but was rescued by the treatment of QVD. (A) Illustration of the LTD recording paradigm. GFP-positive iSPNs were patched in the dorsolateral striatum and the stimulus electrode was placed under the corpus callosum. LTD was induced by high-frequent input stimulation (1 s at 100 Hz) pairing with a postsynaptic depolarization. (B) The amplitude of cortico-striatal EPSCs in iSPNs is reduced using above protocol in sham-lesioned mice (black), whereas EPSC amplitude is unchanged after HFS in 6-OHDA lesioned mice at 5 days post lesion (magenta). QVD treatment rectified the loss of LTD (cyan). (C) Representative traces of single EPSCs from before (black) and after (red) HFS in three groups. (D) Quantification of post-HFS EPSC amplitude normalized to that of pre-HFS EPSCs, from three experimental groups. *** $p < 0.001$, **** $p < 0.0001$ vs. 6-OHDA + vehicle, ANOVA and post hoc Bonferroni test, N = 6-8 cells. (E) Pair-pulse ratios (PPR) in iSPNs are increased after HFS in control mice (black), and remain unchanged in the lesioned mice (magenta). Treatment with QVD rescued the lost increase of PPRs in iSPNs from 6-OHDA lesioned mice (cyan). * $p < 0.05$, paired *t*-test, N = 6-8 cells.

In order to rule out the possibility that the treatment with the caspase inhibitor exerted an anti-degenerative effect on the impaired nigrostriatal DA systems, densitometry analysis of DA fibres in the lesioned striatum and stereological counts of nigral DA neurons were compared between vehicle-treated and QVD-treated mice that were lesioned by 6-OHDA. Results showed no difference in the severity of DA fibre loss or in DA cell body loss was spotted comparing groups with or without caspase inhibitor treatment (Data not shown here).

**Summary:**

Our results show an early loss of spines and synaptic functionality in iSPNs in the dorsolateral striatum following deprivation of DA input. These changes took place at the interval of peak caspase-3 upregulation. Such synaptic reorganizations in iSPNs were reversed by treatment with a pan-caspase inhibitor, pinpointing that caspases play a pivotal role in mediating above-mentioned pathophysiological processes in striatal neurons.

# Paper II. Structural-functional alterations in dSPNs at acute and chronic stages of DA denervation

## The loss of DA fibres in the striatum was complete by 5 days following a 6-OHDA lesion in the right MFB

Using the same model as *Paper I*, we set out to investigate morphological and functional changes in the other major striatal neurons, dSPNs. We fist confirmed that nigrostriatal DA fibres were already massively lost, with less than 10% remained, within 5 days after 6-OHDA lesion in the MFB (Fig 5. A', B). Such severe fibre loss wasn't further aggravated but for the minor remainder in the medial and ventral (close to nucleus accumbens, NA) striatum (Fig 5. A'', B).

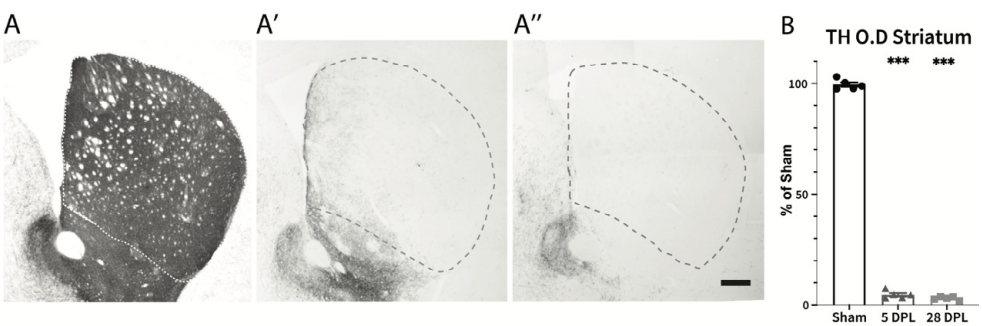


**Figure 5**. Loss of striatal dopaminergic fibres is equivalent at early and chronic phases after 6-OHDA lesion in the MFB. Representative images of TH-stained striatum from sham-lesioned (A), 5 days (A') and 28 days (A'') post lesion (DPL) mice. Scale bar: 400 µm. (B) Densitometry analysis of TH-positive fibres in the ipsilateral striatum shows no difference in the extent of striatal DA denervation between 5 and 28 DPL. Data shown as group mean with standard error of the mean (SEM). One-way ANOVA with Tukey's multiple comparison test. *** $p < 0.001$ vs. Sham.

## dSPNs only loss dendritic complexity and spines in the chronic stage of DA depletion

Seeing that the rapid DA denervation took place in the dorsolateral striatum as early as 5 days after MFB lesion, it inevitably raised the question: what morphological changes had occurred at such an early stage following acute lesion. We first studied the complexity of the dendritic arbour in dSPNs, see (Fig 6). None of the relevant parameters (Sholl analysis, the total dendritic length, and the number of branching points, seen in Fig 6. B-E) were changed at 5 DPL, but only reduced by 28 DPL. What happened to dSPNs spines? Our data suggested that the loss of spines in dSPN coincide the same temporal course as the degeneration of dendrite structures (Fig 7. A, B), only that the image stacks were acquired with a confocal microscopy instead of two-photon imaging.

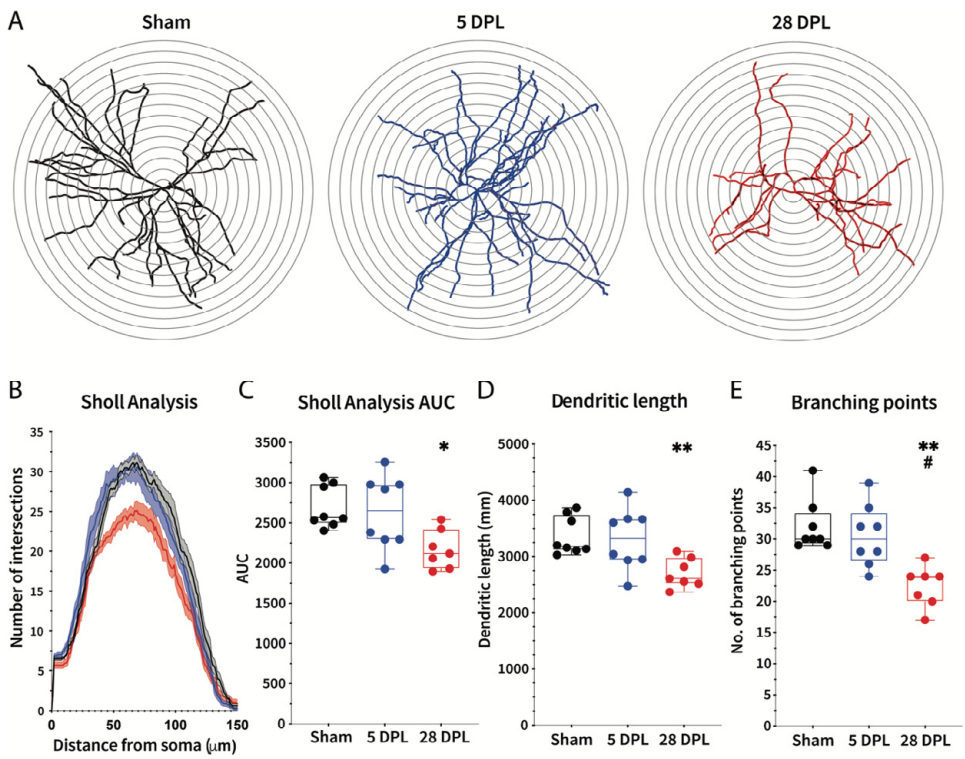


**Figure 6.** The dendritic complexity of dSPNs is only reduced in the chronic but not the early stage of DA denervation. dSPNs were patched and filled with AlexaFluor-488, two-photon images of whole dendritic arbour were obtained and reconstructed with Imaris software. (A) Representative dendrite reconstructions of dSPNs from sham-lesioned, 5-DPL and 28-DPL mice. (B) Sholl analysis of reconstructed dSPN dendrites. Solid lines represent the mean with shaded regions illustrating SEM. (C) Area under curve of Sholl analysis from Sham, 5-DPL and 28-DPL mice. (D) Total dendritic length of dSPN from three experimental groups. (E) Number of branching points from same groups. N = 7-8 cells. Kruskal-Wallis with Dunn's multiple comparison test: ** p< 0.05, ** p < 0.01* vs. Sham; *# p < 0.05* vs. 5 DPL.

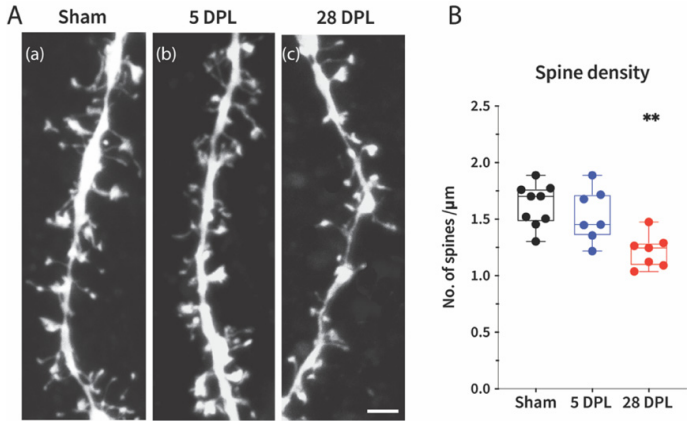


**Figure 7.** The spine density of dSPNs is only reduced in the chronic but not the early stage of DA denervation. (A) Confocal images of dendritic segments with spines from sham-lesioned (a), 5-DPL (b), and 28-DPL (c) mice are shown in maximum-intensity projection. Scale bar: 2 µm. (B) dSPN spine density is reduced at 28 DPL compared to that in the sham-lesion and 5-DPL mice. N = 7-9 cells. ** $p < 0.01$ vs. Sham. Kruskal-Wallis with Dunn's multiple comparison test.

## dSPNs have shown an increased intrinsic excitability and reduced Kir currents only in the chronic stage of DA depletion

After the assessment in structural alterations, we moved on to evaluate the electrophysiological properties of dSPNs by looking into their intrinsic excitability and the major factor that helps to shape such properties of SPNs, inward rectifying potassium channels (Kir) (Gerfen & Surmeier, 2011; Karschin et al., 1996). Somatic current injection-induced action potential (AP) curves comparing the cell excitability of dSPNs at 28 DPL to that under the sham-condition showed a leftwards shift (Fig 8. A, B), indicating an upregulated intrinsic excitability in companion with a higher input resistance and a lower rheobase current level (data not shown). However, such trendy alterations were not yet significantly evident by 5 DPL.

As for Kir channel currents, the same temporal patterns applied as well. Reduced Kir conductance was only detectable in the chronically DA-denervated state, not in the acute (Fig 8. C, D). Bear in mind that Kir channels are those potassium channels that help to combat depolarizing currents at sub-threshold membrane potentials. Reduction in such currents high likely serves as a causality link to the observed elevated intrinsic excitability in dSPNs.

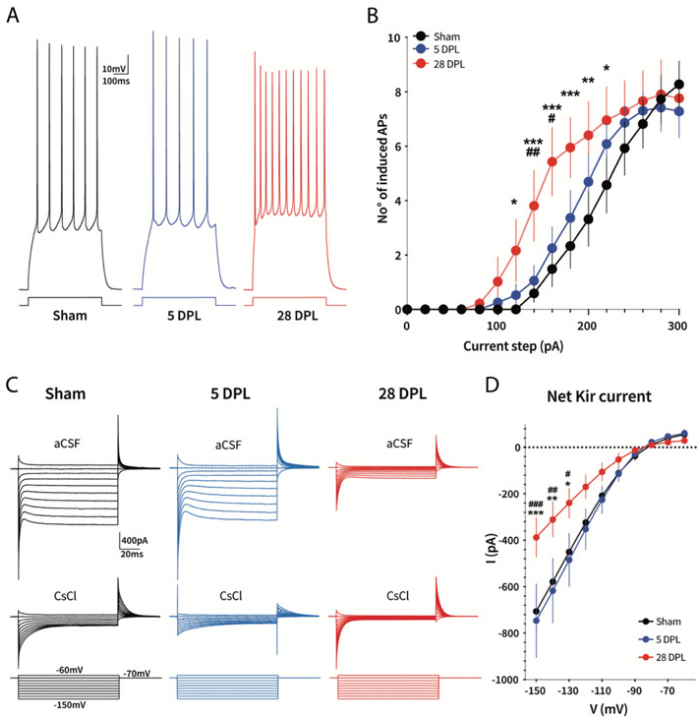


**Figure 8**. Electrophysiological properties of dSPNs are altered in the chronic but not the early stage of DA denervation. (A) Action potential (AP) response of dSPNs from sham-lesion (black), 5 DPL (blue) and 28 DPL (red) groups. (B) Number of induced APs is increased in dSPNs from 28 DPL mice compared to sham-lesioned and 5-DPL mice. Vertical lines represent SEM. N = 6-11 cells. Two-way ANOVA with Tukey's post hoc comparison test. * $p < 0.05$, ** $p < 0.01$, *** $p < 0.001$ vs. Sham; # $p < 0.05$, ## $p < 0.01$ vs. 5 DPL. (C) Top: representative recordings of potassium inward rectifying current (Kir) in aCSF bath solution from Sham, 5 DPL and 28 DPL mice. Current traces recorded in aCSF containing 3 mM CsCl (Kir channel blocker) are shown below. Bottom: Voltage step protocol from -150 to -60 mV. (D) Net Kir current ($I_{Net} = I_{aCSF} - I_{CsCl}$) in dSPNs is decreased at 28 DPL compared to Sham and 5 DPL. N = 7-9 cells. Two-way ANOVA with Tukey's post hoc comparison test. * $p < 0.05$, ** $p < 0.01$, *** $p < 0.001$ vs. Sham; # $p < 0.05$, ## $p < 0.01$, ### $p < 0.001$ vs. 5 DPL.

## Summary:

In comparison to iSPNs, dSPNs develop spine loss in a rather delayed state of DA depletion. Other structural and functional adaptations in dSPNs, such as a dendrite atrophy, an elevated intrinsic excitability and reduced Kir currents, were also found to take place in the same temporal frame as the loss of spines. Taken together, these changes are predicted to profoundly alter the functional properties of dSPNs and their response to incoming excitatory inputs.

# Paper III. Glial response dynamics following striatal DA denervation

## Pattern of microglial and astrocytic reactivity in response to DA loss in the striatum

Besides in *Paper I and II*, we focused on the major neuronal adaptations under the condition of perturbed striatal DA transmission. In the current study, we moved on to investigate inflammatory aspects using exactly the same model as in the previous two studies. In this way, neuronal and glial response dynamics can be readily compared within a uniform temporal frame. We embarked our journey by characterizing dynamics of microglia and astrocytes over a 28-day time course following MFB 6-OHDA lesion, with short intervals in the first week after the lesion. Three to five mice sustaining toxin infusion were sacrificed at each time point, including 1-, 3-, 5-, 7-, 14- and 28-days post lesion, as in comparison to the sham-lesioned mice. Fixed striatal sections were respectively stained against CD68, ionized calcium binding adaptor 1 (Iba1), and glial fibrillary acidic protein (GFAP), as seen in Fig 9. Both CD68 and Iba1 immunoreactive complexes suggest that striatal microglia reacted to DA loss rather fast, noticeably reaching a peak level at 3 DPL, but readily died down already at 5DPL. By 14 days post lesion, microglia almost completely subsided. Contrarily, astrocytes exerted a relatively sustained response. A surge in their reactivity was initiated from 3 DPL, continuing climbing to the maximum level at 5-7 DPL, and followed by a slow decline, with residual reactivity present at 28 DPL.

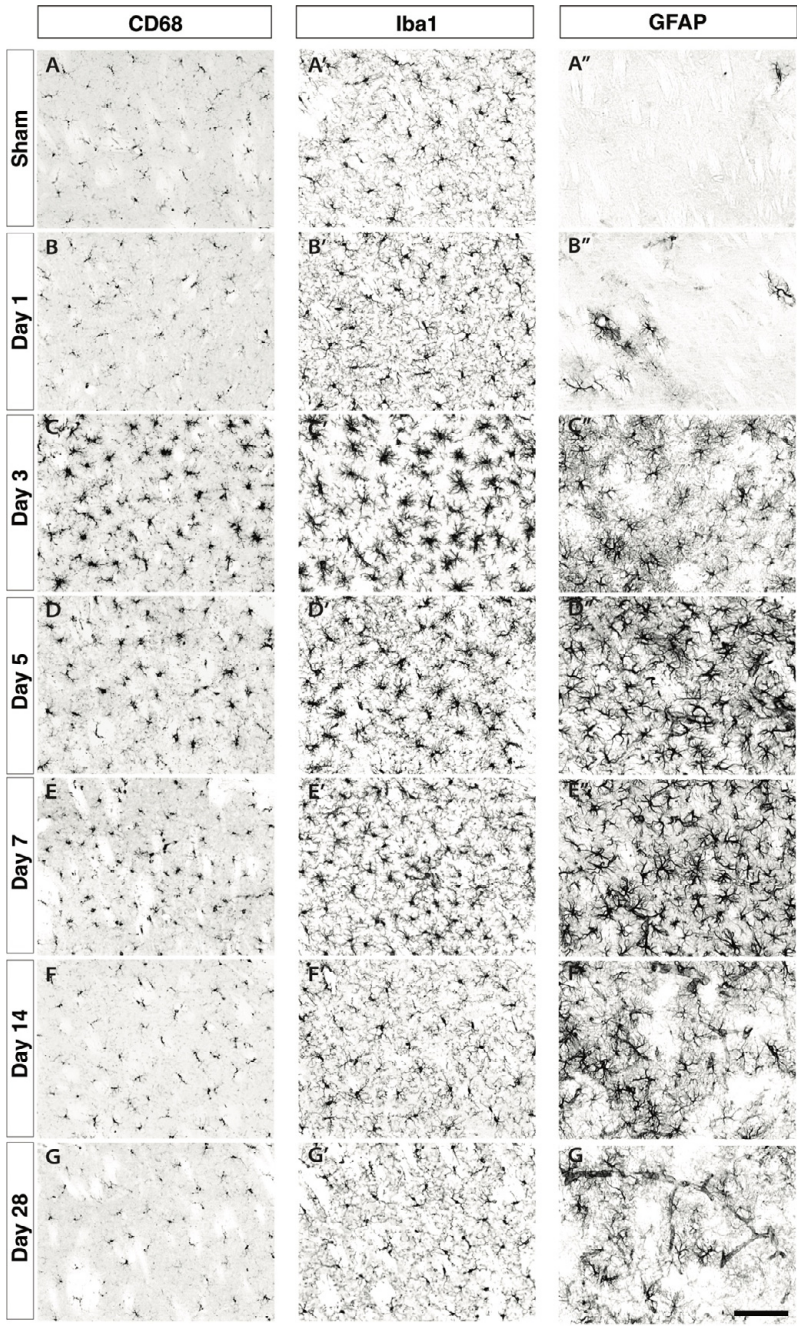


**Figure 9**. Reactivity pattern of microglia and astrocytes at different time points following 6-OHDA lesion in the MFB. Photomicrographs show the dorsolateral striatum on the lesion side immunostained for (A-G) CD68, marker of phagocytic activation in microglia and related cells; (A'-G') Iba1, a pan microglial marker; (A''-G'') GFAP, marker of astrocytic reactivity. The pictures represent sham-lesioned mice (A-A'') and mice sacrificed at 1 day (B-B''), 3 days (C-C''), 5 days (D-D''), 7 days (E-E''), 14 days (F-F''), or 28 days (G-G'') post 6-OHDA lesion (number of mice analyzed per time point, n = 3-5 animals, all showing consistent patterns). Scale bar: 100 µm.

## Microglial and astrocytic dynamics coincide with degenerating DA axons

From *studies I and II*, we know that 6-OHDA infusion in the MFB completely wipes out nigrostriatal DA transmission as early as 5 days post lesion. How do the degenerating DA fibres temporally correlate with reactive microglia and astrocytes? Triple-immunofluorescent staining of TH, Iba1 and GFAP (Fig 10) reveals that the fine mesh of TH-positive fibres was well preserved at 1 DPL, whereas neither microglia nor astrocytes exerted evident reactivity. When the first sign of TH fibre breakdown was noticed at 3 DPL, the fine mesh of TH-positive fibres became discontinuous, and axonal spheroids (indicating dystrophic axonal endings)(Morales et al., 2015) became evident. In the meanwhile, microglia reached their peak reactivity but GFAP-positive astrocytes only mildly manifested. By the point when TH-positive fibres almost completely vanished, microglia were found out having recovered from the fully active ameboid morphology and fewer in numbers, but not yet to the total quiescent state, as observed in the intact striatum. On the other hand, astrocytes kept on mounting in number and reactive intensity.

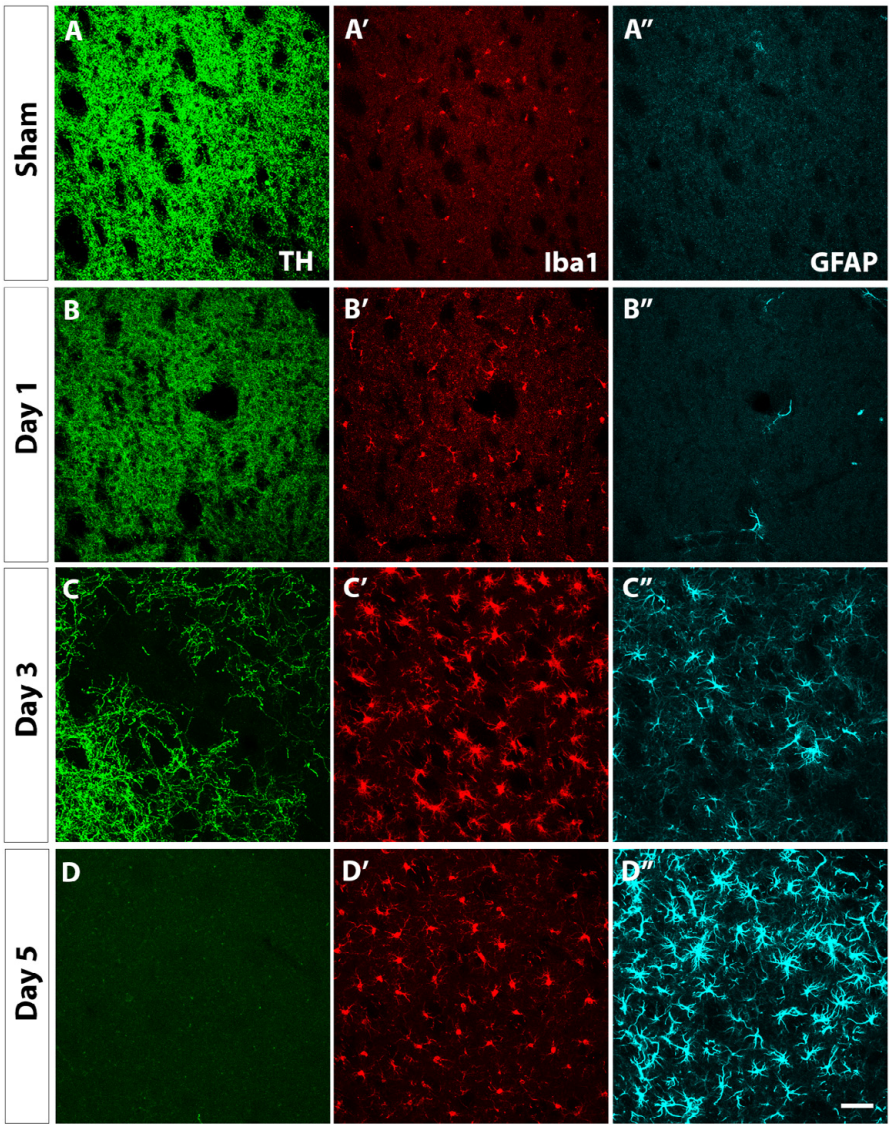


**Figure 10.** The degeneration of dopaminergic fibres in dorsolateral striatum is accompanied by increased reactivity of both microglia and astrocytes. Triple-antigen immunofluorescent staining was carried out on striatal sections obtained from sham-lesioned mice (A-A'') and mice sacrificed at 1 day (B-B''), 3 days (C-C'') as well as 5 days (D-D'') post 6-OHDA lesion, using antibodies against Tyrosine Hydroxylase (TH, green, A-D), ionized calcium binding adaptor 1 (Iba1, red, A'-D') and glial fibrillary acidic protein (GFAP, cyan, A''-D''). Scale bar: 50 μm.

## Time and cell-type specific interactions between microglia and SPN dendrites

As mentioned above, by 5 DPL, a residual amount of microglial activity is still evident in the DA-denervated striatum. Is it simply because microglia take time to die down? Could there be another possibility? We can't help to link it with the spine loss observed in iSPNs at 5 DPL (*Paper I*). In addition, microglia are renowned in mediating spine pruning during the brain development (Paolicelli et al., 2011; Schafer et al., 2012) and in some pathophysiological conditions (Geloso & D'Ambrosi, 2021). Thereby, we induced a viral expression of enhanced green fluorescent protein (eGFP) selectively in striatal iSPNs and dSPNs, under cell type-specific promoters. Striatal sections were stained against GFP and Iba1, in an attempt to visualize and quantify potential interactions (or proximity) between SPN spines/dendrites and microglia, with the help of confocal microscopy. As expected, the percentage of interaction (where signals from two channels overlapped) pixels over the total GFP pixels from iSPNs in 5-DPL striatal materials, was shown as 4-fold of that observed in sham-lesioned mice (Fig 11. G). Whereas when eGFP was expressed in dSPNs, barely a 2-fold change of 5-DPL over the sham values was obtained. On the other hand, the count of microglial cells at 5 DPL in both sets of striatal preparations (iSPN- and dSPN- expression of GFP) showed twice the number counted from the sham-lesioned mice (Fig 11. H).

What about the chronic stage after the lesion? First of all, quantification of microglial cell numbers showed no difference between sham and 28-DPL mice (Fig 11. H). Then to what extent do dendrites/spines of iSPNs or dSPNs interact with microglia? A 2-fold change of interaction points between iSPN dendrites and microglia at 28 DPL was noticed as comparison to that in the sham group (Fig 11. G). A similar trend was present in regard to the interactions between dSPN-expressing $GFP^+$ dendrites and microglia, however this was not statistically significant.

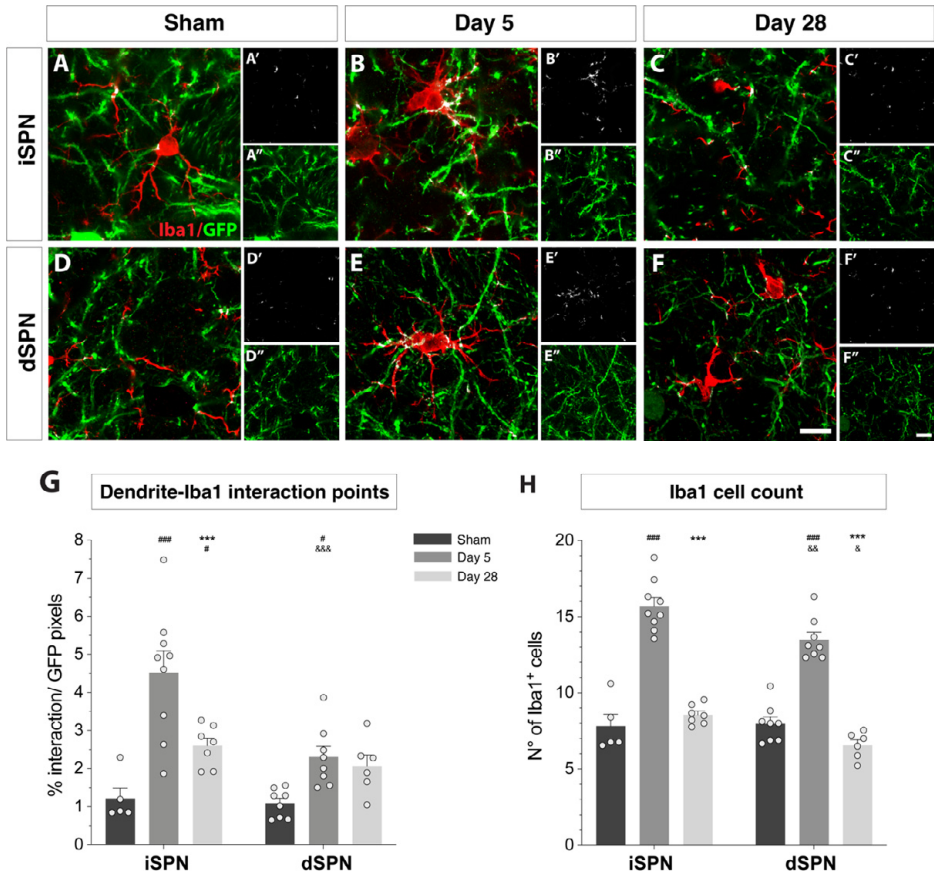


**Figure 11.** Physical contacts between microglia and dendrites of SPNs are increased at 5 DPL. Enhanced green fluorophore protein (eGFP) were expressed via viral vector transduction under iSPN- and dSPN- specific promoters (*A2a-R* and *Drd1a-R*, respectively). Double immunofluorescent staining of eGFP-filled neuronal dendrites (green) and Iba1 positive microglia (red) was carried out on striatal sections acquired from sham-lesioned mice (A-A'', D-D''), and mice from 5-DPL (B-B'', E-E'') and 28-DPL (C-C'', F-F'') experimental groups. Representative images of iSPN dendrites interacting with microglia are shown in A-A'' to C-C'', and those of dSPN dendrites with microglia seen in D-D'' to F-F''. Pixels co-occupied by both channels are highlighted in a separate set of microphotographs (A'-F'). Scale bar: 10 µm. (G) Quantification of dendrite-Iba1 interaction points for iSPNs and dSPNs respectively, at two intervals following 6-OHDA lesion is compared to that in sham-lesion condition. Counts of co-localized pixels were normalized to GFP-positive pixels. (H) Numbers of Iba1-positive microglia from two time points after 6-OHDA lesion as well as from sham-lesioned condition, are counted in both iSPN- and dSPN- GFP-expressing striatal materials. N = 5-9 mice. *Statistical comparison*: two-way ANOVA with Tukey's multiple comparison test. (G) Time: F (2, 37) 19.93 $p < 0.0001$; SPN subtype: F (1, 37) 10.38 $p = 0.0027$; Interaction: F (2,37) 5.033 $p = 0.0117$. (H) Time: F (2, 37) 136.4 $p < 0.0001$; SPN subtype: F (1, 37) 10.69 $p = 0.0023$; Interaction: F (2,37) 3.228 $p = 0.0510$. *** $p < 0.001$ vs. 5 DPL (within the same SPN population); $^{\#}$ $p < 0.05$, $^{\#\#\#}$ $p < 0.001$ vs. sham (within the same SPN population); $^{\&}$ $p < 0.05$, $^{\&\&}$ $p < 0.01$, $^{\&\&\&}$ $p < 0.001$ comparing the same experimental groups between two SPN subtypes.

## Upregulation of inflammatory markers with a bell-shape temporal profile

In order to evaluate the possibility that astrocytes were induced by microglia-derived cytokines, namely, TNF-α, C1q and IL-1α (Liddelow et al., 2017), in our context. We extracted total mRNA from the lesioned striata at different time points, and carried out RT-PCR to measure mRNA content of the above three molecules. In addition, IL-1β, a potent proinflammatory cytokine, and caspase-3, which was upregulated and activated in the striatum early after MFB lesion and involved in iSPN spine pruning (Fieblinger et al., 2022) were also measured. In brief, all five mediators displayed a "bell-shape" expression profile over 2-, 5- and 28- days post 6-OHDA lesion (Fig 12). TNF-α mRNA content peaked at 2 DPL, sustaining a high expression at 5 DPL over the control values. C1q and IL-1α both started to increase at 2 DPL, and peak at 5 DPL. Besides, IL-1β mRNA levels were significantly upregulated at 5 DPL, fitting the pro-inflammatory profile in the DA-denervated striatum. And caspase-3 mRNA was upregulated at both 2 DPL and 5 DPL, providing additive evidence on previously detected increase in caspase-3 proteins.

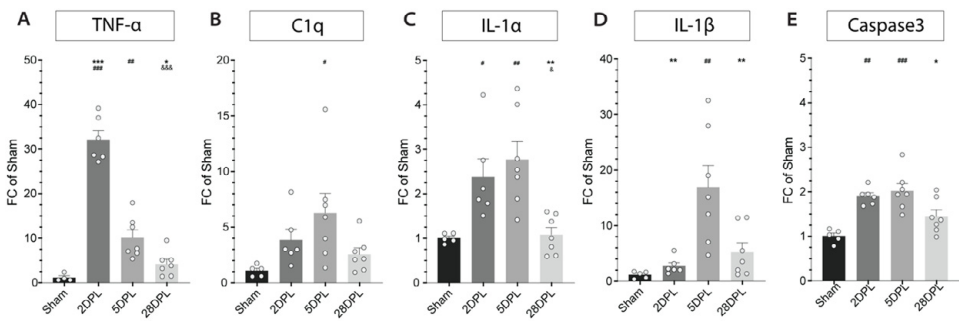


**Figure 12.** Gene transcription levels of inflammatory markers and caspase-3 in the DA-denervated striata over a 28-day time course. Using quantitative real time PCR technique, mRNA levels of TNF-α (A), C1qα (B), IL-1α (C), IL-1β (D) and caspase-3 (E) are determined at 2, 5 and 28 DPL after 6-OHDA lesion. Data are shown as fold change (mean ± SEM) over the average mRNA levels from the sham-lesioned mice. N = 5-7 mice. *Statistical comparison*: one-way ANOVA with Tukey's multiple comparison test. * $p < 0.05$, ** $p < 0.01$, *** $p < 0.001$ vs. 5 DPL; $^{\#}$ $p < 0.05$, $^{\#\#}$ $p < 0.01$, $^{\#\#\#}$ $p < 0.001$ vs. Sham; $^{\&}$ $p < 0.05$, $^{\&\&}$ $p < 0.01$, $^{\&\&\&}$ $p < 0.001$ vs. 2 DPL.

## Summary:

The results show the different temporal dynamics of microglial and astrocytic activation following acute DA denervation, where microglia are activated very early but transiently, and this is accompanied by a slower and more sustained astrocytic response. The microglial response is triggered by the loss of DA axon fibres, but can potentially contribute to a reorganization of SPN structure, and particularly to the early spine pruning of iSPNs. The observed glial responses are accompanied by an early upregulation of pro-inflammatory factors that may create a hostile environment for striatal neurons. Our results deepen the understanding of how

striatal cells cope with the degeneration of dopaminergic axons, and highlight a potential glial role in the structural reorganization of SPNs.

# Paper IV. Fluvoxamine induces functional neurorestoration via the Sigma-1 receptor in a mouse model of nigrostriatal dopaminergic degeneration

## Functional neurorestoration by fluvoxamine treatment in 6-OHDA lesioned mice

In the last study, we set out to investigate the neuroprotective function of fluvoxamine as a Sig-1R agonist. In this study, a mouse model of the intrastriatal 6-OHDA lesion is preferred in order to test the neuroprotective effects of the treatment since it allows for a less aggressive process of nigrostriatal DA degeneration (Francardo, 2018). The same model has been used to test selective Sig-1R agonists and has shown positive results (Francardo et al., 2014; Francardo et al., 2019). Now we use it to test fluvoxamine, which was not developed as a Sig-1R agonist in the first place, but later on discovered to have a high binding affinity to the Sig-1R (Albayrak & Hashimoto, 2017; Hashimoto, 2009).

The aim of the first experiment is to test two different daily doses of fluvoxamine starting right away on the day of 6-OHDA injection. The lower dose (0.3 mg/kg) corresponds to the effective dose of high-affinity Sig-1R agonists in the same mouse model (Francardo et al., 2014; Francardo et al., 2019), while the high dose (20 mg/kg) equals the therapeutic dose as a selective serotonin reuptake inhibitor (SSRI) used to treat depression, after a dose conversion from human to mouse.

We first assessed fluvoxamine's effects on behaviour impairment (Fig 13. A, B). Interestingly, both doses restored cylinder test performance in lesioned mice to a none-lesioned level at 4$^{th}$ and 5$^{th}$ week of the treatment (Fig 14. A), and also largely improved the unbiased forelimb use in stepping test, although the higher dose apparently exerted a larger effect magnitude than the low dose at 5$^{th}$ week of treatment (Fig 14. B). After harvest the brain materials at the end of the treatment, immunohistochemical staining against TH and CD68 was carried out on striatal and nigral sections in order to evaluate neuroprotective and anti-inflammatory effects at cellular and molecular level. We found that both 0.3 and 20 mg/kg doses of fluvoxamine helped to preserve approximately 25% nigral DA cells compared to the vehicle-treated group (Fig 14. C). Unexpectedly, high-resolution fibre density analysis in the lesioned striatum only revealed a significantly higher fibre content in the 20 mg/kg fluvoxamine-treated mice compared to the vehicle-treated ones, but this effect was absent in the low dose-treated mice (Fig 14. E, F). Lastly, CD68-

counting analysis in the whole SN indicated both doses are capable of bringing microglial activity to a basal level measured in the sham-control group (Fig 14. D).

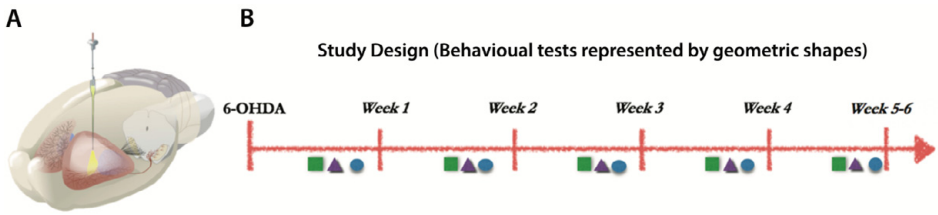


**Figure 13**. Experimental schematic illustration. (A) Intrastriatal 6-OHDA lesion in mice was performed via a glass capillary-attached Hamilton syringe. In total 2 µl of 6-OHDA solution was infused at two sites of the right-side striatum. (B) General study design. Once intrastriatal 6-OHDA lesion was carried out, two doses of fluvoxamine (0.3 and 20 mg/kg) were administrated to lesioned mice daily for 35 days. Behavioural tests were carried out once per week. Immediate-start treatment regimen (IS) was initiated on the day of lesion lasting from week 1 to 5, whereas delay-start treatment (DS) began on the 8$^{th}$ day following the lesion and last throughout week 2 to 6.

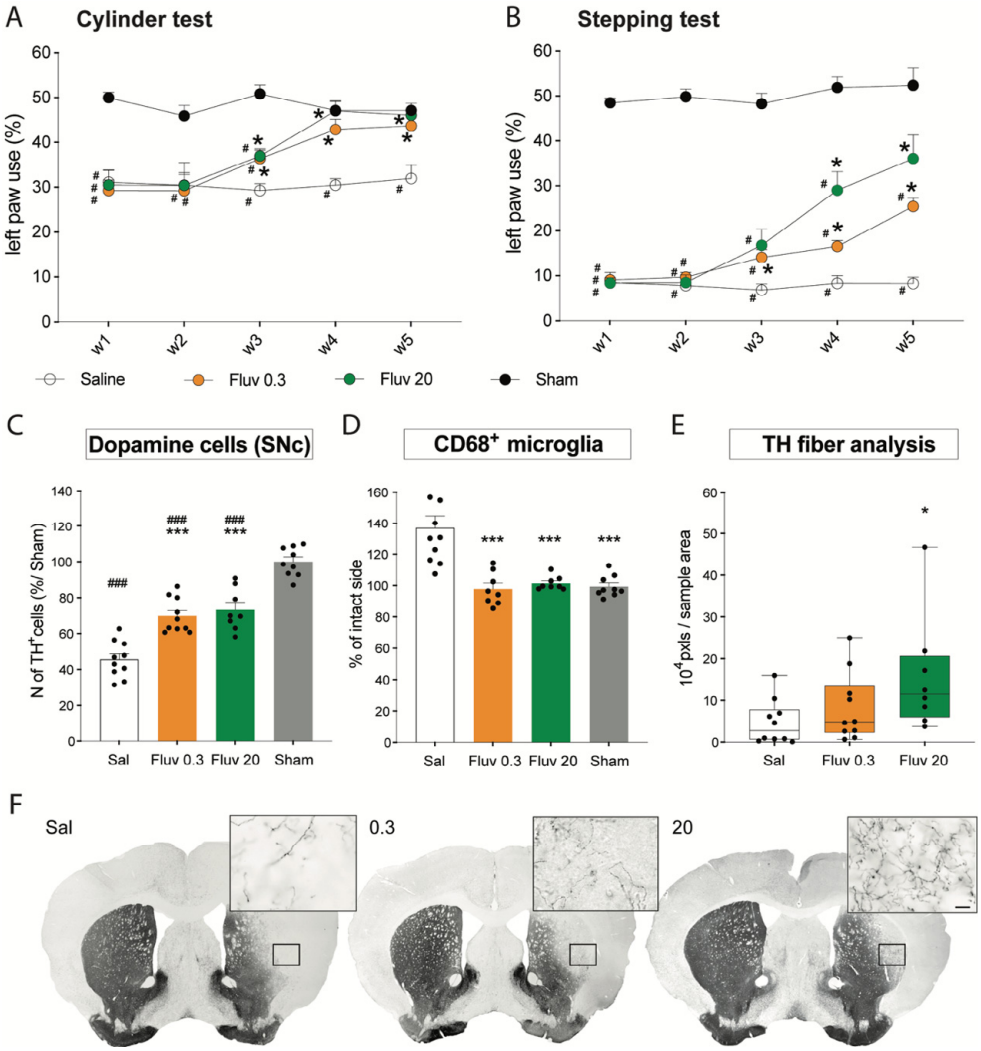


**Figure 14.** Chronic treatment with fluvoxamine in mice induces behaviour improvement, neurohistological restoration and dampens the microglial activation in the SN. Forelimb use asymmetry (cylinder test, A, and stepping test, B) were assessed once per week for 5 consecutive weeks, in mice treated with 0.3 mg/kg fluvoxamine (Fluv 0.3), 20 mg/kg fluvoxamine (Fluv 20) and vehicle (saline, Sal) in immediate-start (IS) treatment regimen. Results are expressed as percentage of supporting wall contacts (A) and adjusting steps (B) performed with the forelimb contralateral to the side of lesion (left paw). *Statistical comparison*: two-way ANOVA with Tukey's multiple comparison test. (A) Cylinder test- Time: $F_{(3.014, 99.48)}$ 11.09, $p < 0.0001$; Treatment: $F_{(3, 33)}$ 22.71, $p < 0.0001$; Interaction: $F_{(12, 132)}$ 4.170, $p < 0.0001$. (B) Stepping Test- Time: $F_{(2.704, 89.23)}$ 22.67, $p < 0.0001$; Treatment: $F_{(3, 33)}$ 277.5, $p < 0.0001$; Interaction: $F_{(12, 132)}$ 6.471, $p < 0.0001$. * $p < 0.05$ vs. Saline; # $p < 0.05$ vs. Sham. (C) Stereological counts of TH-positive cells in the SNc. Total numbers from 4 sections throughout the whole SNc from the lesioned side are summed up and expressed as percentage of the average in the Sham group. (D) Manual quantification of CD68-positive microglia in the SN. Data are shown as average cell counts from 3 levels of nigral sections on the lesioned side, each normalized to its own intact side of the same level of SN. (E) Image segmentation analysis of TH-positive fibres in the striatum. Total pixels are added up from 2 lesion-side striatal sections. Box and whiskers stand for the minimum and the maximum with the median. (F-F'') Representative images in low magnification of striatal sections that are stained against TH and presented from Sham (F), Fluv 0.3 (F') and Fluv 20 (F''), respectively. High-magnification insets on the same sections show conspicuous differences in fibre density and morphology. Scale bar: 10 µm. *Statistical comparison*: (C, D) one-way ANOVA with Tukey's multiple comparison test. *** $p < 0.001$ vs. Saline; ### $p < 0.001$ vs. Sham. (E) Kruskal-Wallis test with Dunn's multiple comparison. * $p < 0.05$ vs. Saline. N = 8-10 mice.

## Fluvoxamine treatment is effective even with a delayed-start treatment design

A following-up experiment was designed to test the treatment effect of 20 mg/kg fluvoxamine using a delayed start (DS) treatment protocol, namely initiating the treatment on the 8$^{th}$ day of the lesion, in comparison to the treatment effect observed with IS regimen (Fig 15). Cylinder test performances in both IS- and DS- treated mice were comparably improved at the end of treatment (5$^{th}$ week for IS, 6$^{th}$ week for DS, Fig 15. B). More prominently improved performances were found in the stepping test, where both treatment protocols managed to restore the unbiased forelimb use to an equivalent level of the sham-lesioned mice (Fig 15. C). Stereological counts of DA cells in the lesioned side of SNc and the fibre density analysis in the lesioned striatum showed no differences between IS- and DS-treatments regarding neuroprotective efficacies in the impaired nigrostriatal DA system (Fig 15. D, F). Besides, as observed in the previous experiment, both treatment regimen also reversed the number of nigral CD68-positive microglia to the non-lesioned status (Fig 15. E).

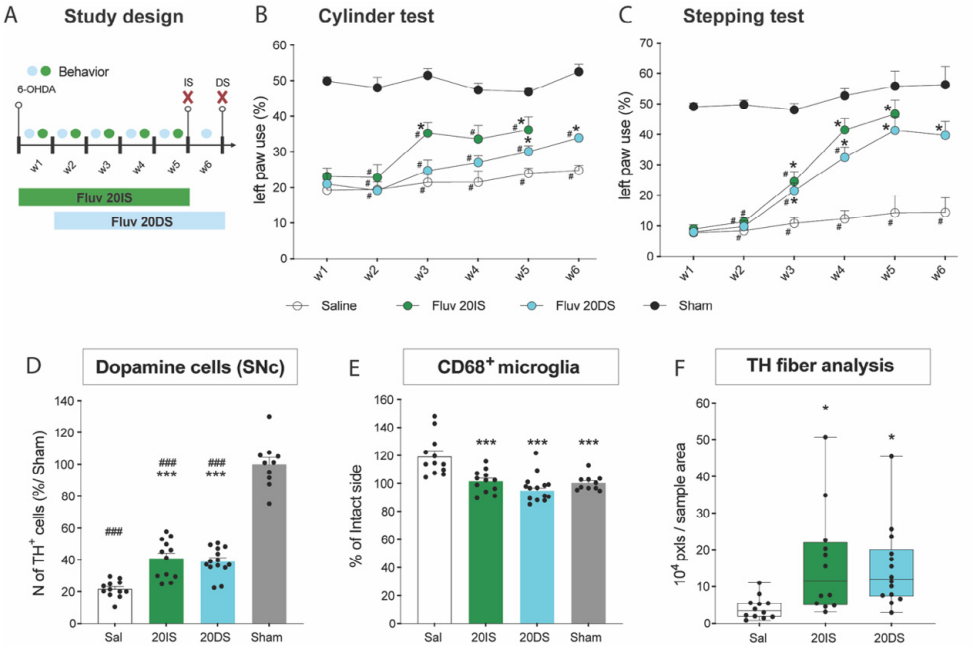


**Figure 15.** Both IS and DS treatments with the high dose of fluvoxamine induce comparable motor improvement and restoration of the nigrostriatal DA system while blunting the microglial activation in the SN. (A) Study design of the current experiment. Forelimb use asymmetry (cylinder test, B, and stepping test, C) were assessed once per week, in sham-lesioned mice and mice treated with IS- and DS- regimen of 20 mg/kg fluvoxamine (20IS and 20DS, respectively), as well as vehicle (Sal). (D) Stereological counts of TH-positive cells in the SN ipsilateral to the lesion. (E) Manual counting of CD68-positive microglial cells in the SN. (F) Image segmentation analysis of TH-positive fibres in the lesioned striatum. *Statistical comparison*: (B, C) two-way ANOVA (corresponding to 1st to 5th treatment weeks) with Tukey's multiple comparison test. (B) Cylinder test- Time: $F_{(3.025,\ 133.1)}$ 13.13, $p < 0.0001$; Treatment: $F_{(3,\ 44)}$ 35.01, $p < 0.0001$; Interaction: $F_{(12,\ 176)}$ 2.959, $p = 0.0009$. (C) Stepping Test- Time: $F_{(2.292,\ 100.8)}$ 41.80, $p < 0.0001$; Treatment: $F_{(3,\ 44)}$ 38.73, $p < 0.0001$; Interaction: $F_{(12,\ 176)}$ 7.395, $p < 0.0001$. * $p < 0.05$ vs. Saline; # $p < 0.05$ vs. Sham. (D, E) One-way ANOVA with Tukey's multiple comparison test. *** $p < 0.001$ vs. Saline; ### $p < 0.001$ vs. Sham. (F) Kruskal-Wallis test with Dunn's multiple comparison test. * $p < 0.05$ vs. Saline. N = 10-14 mice.

## Fluvoxamine treatment is ineffective in 6-OHDA-lesioned mice lacking Sig-1R

In order to verify whether the observed neurorestorative effect of fluvoxamine treatment was due to the activation of Sig-1R, we evaluated 20 mg/kg fluvoxamine with both IS and DS protocols, in Sig-1R-ablated genetic mice (Sig-1R KO). Both behaviour tests performed in lesion-sustaining Sig-1R KO mice showed no improvement with either IS or DS treating regimen (Fig 16. B, C). Accordingly, assessment in nigrostriatal dopaminergic impairment came out negative in terms of neurorestorative or neuroprotective effects (Fig 16. D, E). Neither did the microglial reactivity be dampened by fluvoxamine treatment starting either early or later (Fig 16. E, G). Taken together, all the benefits exerted by fluvoxamine were abolished by the blockade of Sig-1R signalling.

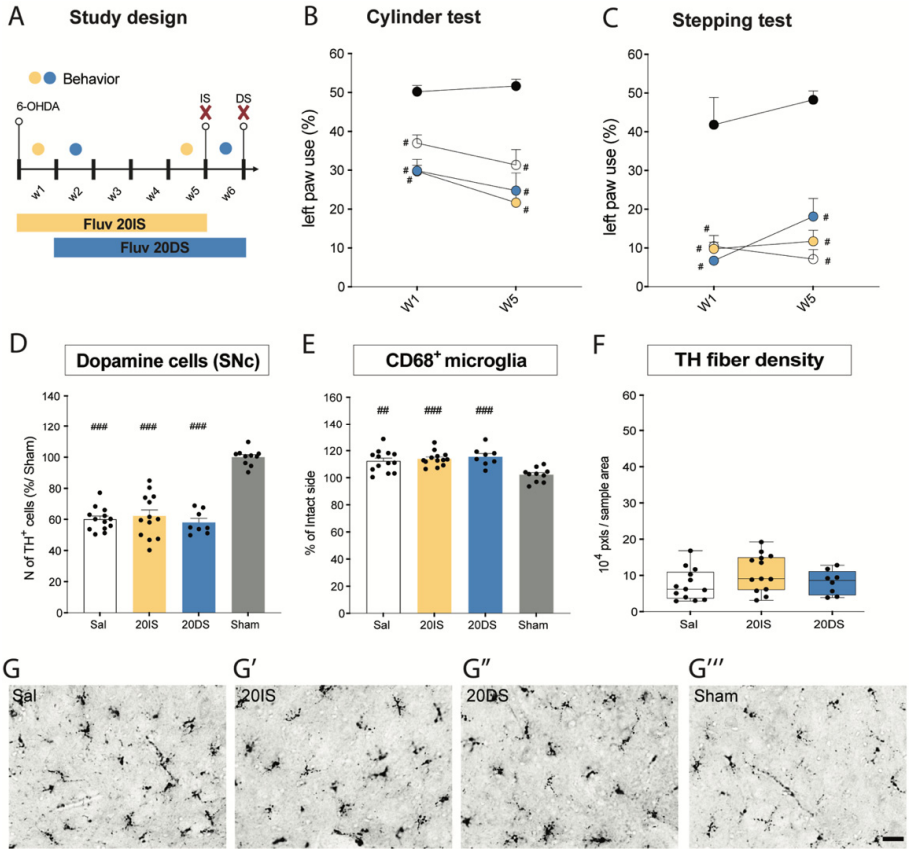


**Figure 16.** Fluvoxamine does not exert any improving or protective effects in 6-OHDA-lesioned mice lacking the Sig-1Rs. (A) Study design of the current experiment. Forelimb use asymmetry (cylinder test, B, and stepping test, C) were assessed at 1st and 5th weeks after the onset of 20 mg/kg fluvoxamine treatment in the Sig-1R-knockout mice (20IS: behaviour assessed 1st and 5th week; 20DS: behaviour assessed 2nd and 6th week). (D) Stereological counts of TH-positive cells on the lesioned side of SNc from the Sig-1R-knockout mice. (E) Manual counts of CD68-positive microglial cells in the SN from the Sig-1R-knockout mice. (F) TH-positive fibre analysis in the lesioned striatum from the lesion-sustaining Sig-1R-knockout mice. (G-G'') Representative images of CD68-stained dorsolateral striatum on the lesioned side of Sig-1R-knockout mice, from all four experimental groups. Scale bar: 20 µm. *Statistical comparisons*: (B, C) two-way ANOVA with Tukey's multiple comparison test. (B) Cylinder test- Time: $F_{(1, 40)}$ 5.662, $p = 0.0222$; Treatment: $F_{(3, 40)}$ 21.58, $p < 0.0001$; Interaction: $F_{(3, 40)}$ 1.285, $p = 0.2925$. (C) Stepping Test- Time: $F_{(1, 40)}$ 3.008, $p = 0.0906$; Treatment: $F_{(3, 40)}$ 46.86, $p < 0.0001$; Interaction: $F_{(3, 40)}$ 1.687, $p = 0.1851$. $^{\#}p < 0.05$ vs. Sham. (D, E) One-way ANOVA with Tukey's multiple comparison test. $^{\#\#\#}p < 0.001$ vs. Sham. (F) Kruskal-Wallis test with Dunn's multiple comparison test. N = 8-13 mice.

## Summary:

This study explored fluvoxamine as a potential neuroprotective treatment in a model of nigrostriatal dopaminergic degeneration. Our results show that fluvoxamine partially protected nigral DA neurons and improved the animals´ motor deficits, while also reducing microglial activation. These effects were seen using both a low dose sufficient to activate Sig-1R (0.3 mg/kg/day) and the therapeutic equivalent dose of selective serotonin reuptake inhibitor in mice (20 mg/kg/day). Fluvoxamine

was able to produce significant improvement even when the treatment was started one week later than the onset of dopaminergic degeneration. None of the above beneficial effects occurred when the nigrostriatal lesion and fluvoxamine treatment were given to Sig-1R knockout animals. The results indicate that fluvoxamine may be further pursued as a potential disease-modifying treatment for PD.

# Discussion

Dopamine is a key neuromodulator in the brain as it regulates movement, cognitive processes, and affective states. The principal target of dopaminergic projections is the striatum, which is also the largest component of the basal ganglia. The striatal complex comprises topographically and functionally distinct regions forming parallel neuronal circuits involving the cortex and the thalamus. It is the loss of dopaminergic projections to the motor part of the striatum (putamen in humans) that causes the motor deficits of PD. However, the functional and structural consequences of DA denervation on the cells of the striatum are poorly understood. In this thesis work, we set out to characterize dynamic responses of both neurons and glial cells in the dorsolateral striatum (the mouse equivalent of the putamen) following a loss of dopaminergic innervation.

The experimental subjects in our studies include wild-type mice and various transgenic mouse lines. In all studies, mice sustained 6-OHDA lesions of the nigrostriatal DA projections to mimic an advanced stage of PD with overt motor deficits. Any experimental model of a human disease presents both pros and cons. The advantage of 6-OHDA-based models is that they are highly reproducible across laboratories and mouse lines and moreover time-efficient. Indeed, mice sustaining 6-OHDA lesions of the nigrostriatal DA pathway rapidly develop phenotypic changes that are highly relevant to PD. In particular, these models exhibit structural alterations of striatal neurons similar to those found in post-mortem striatal tissue from PD patients. The disadvantage of these models is that they lack a formation of intraneuronal protein aggregates rich in alpha-synuclein, a pathological feature that occurs in human PD both within DA neurons and in many other neuronal types (although not in striatal SPNs). In addition, while the loss of striatal DA innervation in PD occurs over many years, the dopaminergic degeneration induced by 6-OHDA is very rapid. Indeed, the results obtained in the thesis´ papers I-III show that, following 6-OHDA injection into the MFB, the loss of DA fibres in the dorsolateral (motor) striatum is complete already within 5 days, even though the loss of DA cell bodies in the substantia nigra has a slower time course. The rapid course of striatal DA denervation in the MFB lesion model has offered us an opportunity to study both early and chronic adaptations of striatal cells to the loss of DA input, focusing on either SPNs (papers I-II) or glial cells (paper III). Taken together, our results reveal profound differences between the changes occurring early or late after the lesion, which will be discussed in the following sections. While investigating

structural and functional changes of striatal cells, we also evaluated a pharmacological treatment having the potential to help DA neurons and nigrostriatal projections to cope with partial damage. This treatment is fluvoxamine, an SSRI antidepressant previously demonstrated to act as a Sigma-1 receptor agonist in many experimental systems. Our study confirms that fluvoxamine stimulates Sigma-1 receptors, and moreover reveals that treatment with fluvoxamine produces a gradual recovery of motor functions, a dopaminergic neurorestoration, and a dampening of microglial activation in mice with intrastriatal 6-OHDA lesions (*Paper IV*).

## Neuronal responses

In studies I and II, the focus was put on structural and electrophysiological changes of SPNs, which are the principal neurons of the striatum. As already mentioned in the Introduction to this thesis, SPNs are divided in two major groups. The iSPNs ("i" for indirect pathway) project to the GPe and express DA receptor D2, which is coupled to an inhibitory G protein. The dSPNs ("d" for direct pathway) project to the basal ganglia output nuclei (GPi and SNr) and express DA receptor D1, which is coupled to a facilitatory G protein. Due to their expression of DA receptor types mediating opposite cellular responses, iSPNs and dSPNs respond in different ways to the loss of DA input. While iSPNs tend to become more active, the activity of dSPNs is reduced. Previous studies had indicated that DA-denervated iSPNs undergo a pruning of dendritic spines as an attempt to reduce their levels of synaptic excitation, thus bringing back their activity levels to the normal set point (a process referred to as homeostatic plasticity).

In Paper I, we investigated the temporal course and potential mediators of iSPN dendritic spine pruning focusing on the early stage of DA denervation. The results of this study shows that the loss of iSPN dendritic spines occurs already within 5 days post-lesion and that it coincides with a non-apoptotic activation of caspase-3. Using an immunohistochemical method, caspase-3 upregulation was observed in both glial cells and iSPNs dendrites. The loss of iSPN spines was accompanied by a loss of cortically-induced LTD in the same neurons. This finding indicates that, despite being attributed to a homeostatic response, the pruning of iSPN spines alters the synaptic connectivity of these neurons in a pathological manner, causing synaptic dysfunction. Importantly, the results of paper I show that both the loss of spines and the loss of LTD in iSPNs can be prevented by treating mice with a pan-caspase inhibitor over the few days after the lesion. These experiments were conducted using the potent pan-caspase inhibitor Q-VD-OPh as there are no selective caspase-3 inhibitors suitable for systemic administration. Since caspase-3 is the effector protein of both intrinsic and extrinsic apoptotic pathways, we think that the inhibition of the upstream caspases 7-9 by Q-VD-OPh does not invalidate the main conclusion of paper I, namely, that caspase-3 activation mediates loss of

spines and corticostriatal LTD in iSPNs following the loss of DA inputs. We were not able to address whether the prevention of iSPNs alterations by Q-VD-OPh might translate in a long-term benefit, such as, an attenuation of the lesion-induced motor deficits. In order to address this question, it would have been necessary to examine the animals with suitable behavioural tests at least 2-3 weeks after the lesion and caspase inhibition treatment. This type of experiment might be considered in future investigations on the subject.

In Paper II we compared structural and functional changes of dSPNs at acute and chronic stages following DA denervation, that is, at 5 vs. 28 days post lesion. At the late time point, dSPNs showed significant reductions in both dendritic complexity and spine density, which were not detectable at 5 days post-lesion. At the same late time point, dSPNs also exhibited a marked increase in intrinsic excitability (reduced rheobase current, increased input resistance, more evoked action potentials in response to depolarising currents), which was not present in the early stage of denervation. The increase in neuronal excitability was accompanied by a marked reduction in inward-rectifying potassium (Kir) currents. These currents are very important to SPNs as they are needed to dampen the effect of depolarising stimuli and maintain these neurons in their normal hyperpolarised state. The loss of dendritic complexity at 28 days post lesion had been seen also in a previous study by (Fieblinger, Graves, et al., 2014) and found to affect both iSPNs and dSPNs. It is not surprising that a major reorganization of the dendritic arbour takes some time to occur. However, spine loss can be a rapid process, and we have shown that iSPNs exhibit a reduction in spine density already at 5 days post lesion (paper I). Thus, the delayed spine loss of dSPNs can be interpreted as depending on mechanisms distinct from those causing iSPN spine loss in the same lesion model. As dSPNs become hypoactive after DA denervation, their spine pruning cannot be considered as a homeostatic response, but should rather be interpreted as a pathological change. This change is likely to depend on a loss of D1 receptor-mediated stimulation and possibly also on trophic signaling deprivation (Andreska et al., 2023). Our results showing dSPN spine loss at 28 days post lesion are a variance with those of previous publications based on direct visualization of SPN dendrites during electrophysiological recordings. These publications found no spine loss in dSPNs at 3-4 weeks after MFB lesion (Fieblinger, Graves, et al., 2014), or a really delayed loss, becoming significant only at 60 days after the same lesion (Graves & Surmeier, 2019). We believe that our results showing dSPN spine pruning at 28 days are more reliable as they are based on a more precise morphological methods where dSPNs dendrites were analyzed in fixated brain slices using confocal microscopy.

# Glial responses

In the recent decade, neuroinflammatory processes mediated by glial cells have gained more and more attention in the search for causes and mechanisms of neurodegenerative diseases, including PD (Kuter et al., 2020). As constitutive cellular populations that undertake the first line of immune defense in the central nervous system, microglia and astrocytes react to a variety of pathophysiological conditions with altered gene and protein expression, as well as release of chemical mediators that can affect nearby cells. In paper III, microglial and astrocytic markers were studied in the striatum in mice sustaining 6-OHDA lesion in the MFB, which were euthanised at different time points after the lesion (1-28 days). We found a peak of microglial activation and astrocytic reactivity between 3 and 5 days post lesion. Thereafter the microglial activation declined, reaching basal levels by 28 days. However, astrocytic reactivity remained clearly elevated above the baseline until the last time point. The increased glial reactivity was accompanied by an upregulation of the proinflammatory cytokines TNF-alpha, IL-1alpha, and IL-1beta, with peaks of upregulation observed between 2 and 5 days post-lesion.

What do these findings imply? One reason behind the prompt and strong glial response could be that the lesion-induced decomposition of DA axons activates microglia to clear the resulting debris. This explanation seems feasible for microglia, as we observed that indexes of microglia activation (i.e. enlarged Iba1-positive cell somata and CD68 positivity) reached their peak at 3 days post lesion, at the time point when dystrophic dopaminergic fibres were still visible in the dorsolateral striatum although the fine dopaminergic axonal mesh was gone. The expression of reactive microglial markers started to decline already at 5 days post lesion, a time when dopaminergic axon fibres were no longer visible in the dorsolateral striatum. This suggests that, once microglial cells have served their role in clearing the axonal debris, they rapidly return to their baseline state. However, factors released by the highly reactive microglia can trigger a more long-lived astrocytic response. In a seminal study, Liddelow and colleagues (Liddelow et al., 2017) showed that activated microglial cells induce a reactive state of astrocytes (defined as "A1") by secreting TNF-alpha, IL-1-alpha and C1q. It is noteworthy that we found a significant striatal upregulation of all these factors within the first 5 days post lesion, with a very strong TNF-alpha upregulation occurring already on the second day.

In paper III, we also asked the question whether reactive microglia may be involved in the process of iSPN spine pruning, which occurs within the first 5 days post lesion. We found close microglia-dendrites contact formation at 5 days post lesion on both iSPNs and dSPNs. However, the number of microglial contacts was 2-fold larger on iSPN compared to dSPN dendrites. Thereby it is reasonable to propose that microglia indeed contribute to the iSPN spine loss occurring within 5 days post lesion. This proposition should however be confirmed using high-resolution

techniques enabling to visualize an engulfment of iSPN spines (or spine components) by nearby microglia. Electron microscopy or STED microscopy may be suitable techniques for this purpose. Interestingly, it has recently been reported that, in addition to microglia, astrocytes contribute substantially to synapse elimination in a model of Alzheimer´s disease (Dejanovic et al., 2022). We can therefore hypothesize that the sustained astrocytic reactivity observed in our study contributes to the process of SPN remodeling during the first 3-4 weeks post DA denervation, a time frame when both iSPNs and dSPNs undergo dendritic regression and dSPN undergo a delayed spine loss (Fieblinger, Graves, et al., 2014; Li et al., 2024). Further studies addressing this important hypothesis are clearly warranted.

The upregulation of striatal C1q mRNA detected during the first 5 days post 6-OHDA lesion is particularly interesting because C1q is the initiating protein of the classic complement system. In turn, the complement system has been shown to modulate synaptic plasticity and spine remodelling (Berkowitz et al., 2021). For example, in a mouse model of Alzheimer´s disease, C1q was found to be upregulated and attached to plaque-associated synapses (Hong et al., 2016). Moreover, inhibiting C1q, C3, or the microglial complement receptor CR3 all reduced the extent of synapse loss in this disease model (Hong et al., 2016). Taken together, the above results are compatible with the hypothesis that C1q released by microglia both mediates the toxic transition of astrocytes and opsonizes SPN dendritic spines for glial-mediated phagocytotic activity, ultimately leading to loss of synapses and dysfunctions in corticostriatal synaptic transmission.

# Harnessing neuronal and glial responses for therapeutic purposes: focus on the Sigma-1 receptor

Similar to other neurodegenerative diseases, the clinical and pathological progression of PD is driven by complex and parallel pathways of cellular dysfunctions (Espay et al., 2019). Compounds stimulating the Sig-1R help both glia and neurons to cope with the consequences of such dysfunctions by enhancing several pathways of cellular defence and repair (reviewed in the introductory paragraph "*The sigma-1 receptor as a potential target for disease-modifying treatments")*

Studies evaluating effects of Sig-1R agonists in experimental models of PD have been pioneered by Francardo and colleagues, who provided the first evidence that a selective Sig-1R agonist (PRE-084) and a candidate drug with high binding affinity for Sig-1R (pridopidine) promote behavioural recovery and sprouting of dopaminergic fibres in the most denervated striatal regions in a 6-OHDA mouse model of PD (Francardo et al., 2014; Francardo et al., 2019). In addition, these treatments induced a striatal upregulation of GDNF and BDNF and reduced the

phagocytic activation of microglia (marked by CD68 immunopositivity) in both SN and the striatum (Francardo et al., 2014, 2019). These and other studies suggest that targeting Sig-1Rs is a promising target for disease-modifying therapies.

The selective serotonin reuptake inhibitor (SSRI) fluvoxamine binds to the Sig-1R with low nanomolar affinity (Narita et al., 1996), that is, with the same affinity of experimental compounds used in animal studies, such as PRE-084. In paper IV, we have examined the effects of chronic treatment with fluvoxamine in mice sustaining intrastriatal injection of 6-OHDA (a model of partial dopaminergic degeneration resembling the pattern seen in early stages of PD). Five weeks-treatment with fluvoxamine at the doses of 0.3 or 20 mg/kg/day produced a gradual and significant improvement of forelimb use. The behavioural recovery was paralleled by an increased number of DA neurons and a reduced number of CD68-positive microglial cells in the substantia nigra. An increased density of dopaminergic fibres in the striatum was detected only with the 20 mg/kg dose. The same protocol of 6-OHDA lesion and fluvoxamine treatment was then applied to Sig-1R knockout mice. In these animals, the treatment did not produce any motor improvement and had no effect on either the expression levels of dopaminergic cell markers or the number of CD68-positive microglial cells. These results verify the hypothesis that fluvoxamine acts as a Sig-1R agonist to achieve neurorestorative effects in this model of PD. The results moreover encourage further research on the effects of fluvoxamine on pathogenic pathways of relevance to PD. Finally, the results confirm that the Sig-1R is a promising therapeutic target to achieve disease-modifying effects in PD.

# Summary and conclusions

This thesis work presents a vast set of new findings that shed light on dynamic changes of the main cell categories present in the striatum following the loss of dopaminergic axon fibres. The main contributions of the work can be summarised as follows:

- Caspase-3 is a key mediator of the spine loss and synaptic dysfunction affecting iSPNs (striatal neurons forming the indirect pathway) early after the loss of their DA input. Treating animals with a systemically active pan-caspase inhibitor during the first 5 days post lesion prevented these changes.
- dSPNs (striatal neurons forming the direct pathway) undergo delayed spine loss simultaneously with a dendritic regression and an elevation of intrinsic excitability (caused by reduced Kir currents). These maladaptive effects are bound to alter the synaptic connectivity and responsiveness to excitatory inputs in the affected neurons.
- The loss of dopaminergic innervation goes hand in hand with a strong but transient activation of microglia peaking at 3 days post lesion and slightly preceding the activation of astrocytes. While microglial activation quickly declines to basal levels, the astrocytic reactivity clearly remains above baseline at all examined time points (i.e. until 28 days post lesion). This pattern of glial reactivity is accompanied by upregulation of pro-inflammatory molecules in the DA-denervated striata. Interestingly, we show for the first time that activated microglial cells at 5 days post lesion form close contacts with SPN dendrites, and that these contacts are significantly more abundant on iSPNs compared to dSPNs. These data suggest that microglia are an active player in the spine pruning of iSPNs, which indeed takes place within the first few days post lesion.
- This thesis work also contributes to the evaluation of fluvoxamine as a potential treatment to milden the course or the consequences of nigrostriatal dopaminergic degeneration. Our data prove that chronic treatment with fluvoxamine can partially protect nigral DA neurons and their axonal terminations in the striatum, while reducing CD68-positive microglial reactivity and improving the recovery of motor function. By applying the experimental procedures to Sig-1R knockout mice, we verified that all above beneficial responses of fluvoxamine were dependent on the presence of Sig-1R.

# Future perspectives

Many of the interesting results of this thesis warrant further investigations that can improve our pathophysiological understanding of PD and lead to optimized treatment options. Some examples are given below:

Regarding the neuronal response to DA denervation, Paper I and Paper II did not address the mechanisms underlying the dendritic regression that affect both iSPNs and dSPNs during the 4 weeks following a loss of dopaminergic innervation (Fieblinger, Graves, et al., 2014). This dendritic regression is an important phenomenon to be studied further because (i) a similar phenomenon occurs in the human disease, and (ii) such a dramatic structural rearrangement is predicted to have profound consequences on the pattern of SPN synaptic connectivity and function. Since the dendritic regression occurs in both of the SPN populations despite their segregated expression of very different DA receptor types, it means that the mechanisms mediating the regression of SPN dendrites do not simply stem from a deficit in DA receptor stimulation but may be due to a secondary mechanism associated with the loss of DA inputs. In paper III we show that astrocytes display a prolonged hyper-reactive profile until 28 days post lesion, and studies in other disease models have reported that astrocytes can prune synapses through phagocytosis (Konishi et al., 2022; Lee et al., 2021). Therefore, the next pressing question is to understand whether the sustained astrocytic reactivity observed in paper III plays a role in mediating dendritic pruning of both SPN categories in this PD model. A possible approach to address this question would be to investigate physical contacts between astroglia and SPN dendrites using high-resolution morphological methods. Secondly, we could characterize activities of phagocytic receptors in astrocytes (such as MEGF10 and MERTK (Lee et al., 2021)). Alongside, it would be interesting to study the expression of typical phagocytic receptors in microglia (such as CR3 and TREM2 (Filipello et al., 2018; Scott-Hewitt et al., 2020) in the same time frame.

Regarding the glial response, a phenotypic characterization of microglia and astrocytes in our experimental models would be very important and timely. The classic model of pro- and anti- inflammatory microglia (M1- versus M2) has been briefly mentioned in the Introduction. These two phenotypes can be identified based on the expression of pro- and anti-inflammatory cytokines (Guo et al., 2022). However, the binary concept of two polarized microglial types has been strongly debated, and more differentiated phenotypic microglial classes were gradually

promoted based on their location, functions, and physiological conditions (Paolicelli et al., 2022). Based on these considerations, we have undertaken studies using single-nuclei RNA sequencing of both glial and neuronal cells in mice euthanized at 5 and 28 days post lesion, and the data analysis is now in progress. Studying how different cell categories respond to the loss of dopaminergic innervation will not only improve our pathophysiological understanding of PD, but also provide indications about new potential therapeutic targets with both symptomatic and disease modifying efficacy.

The results of paper IV provide an example of translational efforts and show that a clinically used drug (fluvoxamine) has a neurorestorative action on the damaged nigrostriatal DA system via the Sig-1R. These results call for further investigations of fluvoxamine as a potential disease-modifying treatment for PD. To this end, the efficacy of fluvoxamine should be examined in additional disease models and on a larger number of molecular and functional endpoints.

# Acknowledgement

I would like to take this opportunity to thank everyone who has contributed to the studies in my PhD education. First of all, I have to thank my supervisor, Prof. Angela Cenci Nilsson. Thank you for taking me in as a PhD student so promptly, which I understand is an unusual case in the Swedish system. You led me into the field of Parkinson's Disease, helping me to realize the meaning and importance of our work to PD patients. Everyone looks up to you in this group, as you are always the lighthouse for all us sailing boats in the ocean of science. Under your coaching, I turned from a naïve and ignorant student into a professional scientist with humble attitude, more mature mind and infinite passion of new discoveries in the field. Thank you again for not giving me up in the most difficult times. There are now and then bumps and detours on the journey, but in the end, I am only grateful to all the things happened along the way, even those bad ones, because I learned even more seriously from failures and criticisms. Looking into the future, I really hope there will be more time for me work by your side, since there is still so much more that I could learn from you and so much more that we can do together.

As my co-supervisor, I need to thank Tim Fieblinger, the best electrophysiologist I personally got to know. You have a special charming personality, and versatile strong professional skills. When I was just enrolled in this PhD program, it was my goal to live up to your high skills in electrophysiology… (too bad you left for Germany too early). I also have to thank Daniella Ottosson, as my co-supervisor. Thank you for the presence and your kindness. To Praveen, one of my most important collaborators. Thank you for providing prompt technical support and help me with the result analysis. You are very approachable and knowledgeable! Lastly, I want to thank the Multipark platform for providing a stimulating research environment.

Next big thanks go to my present and former colleagues of the Basal Ganglia Pathophysiology group: Anki, Veronica, Irene, Laura, Erik, Silvia, Elena, Katrine, Osama, Valentina, Ana, Teodor, Markus. Thank you for being there for me when I was in desperate moments. Thank you for lending me a hand when I reached out for help in the lab. Thank you for giving both the verbal and spiritual support any time and any occasion I needed it. I won't forget any of those precious time we spent together, talking and laughing. You all deeply touched my heart, and this feeling will last forever as fresh whenever I recall those memories.

Some of the familiar happy faces that easily cheer me up when seeing in the corridors of BMC: Roberta, Sam, Iben, Na, Marios, Tekla, Nagesh, Jessica, Claire, Isak, Megg, Lisette, Lavania. Just by smiling at me and small casual talks easily light up my heart buried in the darkness. Thank you all for the care and encouraging words!

我要感谢我的父母，养育我，教育我，支持我出国留学，支持我追求远在异国他乡的梦想。儿行千里母担忧。我知道你们很想我，我不在你们身边的每一天你们都在担心我，担心我熬不住读书的苦和压力。当我为学业苦恼和煎熬的时候，你们内心承受的煎熬分毫不比我少。即便如此，感谢爸爸妈妈从不曾以爱为名捆绑我的自由，限制我自由飞翔的翅膀。你们是最优秀的父母。

我所有圈内圈外的中国朋友, BMC 和生态楼的小伙伴们，那些年咱们吃的火锅，爬过的山，斗过的嘴你还记得吗？说的就你们：白亦光，张涛，王琦，刘娜，樊智猛，黄金田，好多次被你们这些怨种气到无语啊。

B11 楼的奕奕姐，BMC 神经病这行里的大姐，给了我很多便利。那些年我抄过你的 portfolio, presentation slides, report, kappa，我都记着呢。很多次我想我要是和你一个组就好了，应该会少受很多罪吧。这么说好像也不太合适，毕竟我们组对我也很好了。不过如果有的选，我还是想和你一组工作。

陪我去巴黎看铁塔的璐姐，在老板这遇到你真的是缘分，我很遗憾因为疫情咱们的西班牙之旅没有成行，但是你在组里陪我这一年给了我很多安慰。你成熟，睿智，勤奋上进，事业有成，家庭美满，我是真的羡慕你。等我回国路过上海一定要去找你。只怕我到时候胖得你认不出来。

最后感谢我在隆德最重要的家人：王蕊霖，黄园园，王雨浓，虽然你们都比我小很多，但是我心里从来不曾感觉到有代沟。我们在一起喷过的人，吐过的槽，扒过的卦，喝过的酒 （包括吐出来的），断过的片，发过的疯，唱过的歌，满满的全都是回忆。很感谢在博士快结束的时候认识了你们，也很遗憾没有更早一点拥有这段缘分。以后即使天各一方，各奔东西，在我心里，你们永远是我的弟弟妹妹。

# References


Albayrak, Y., & Hashimoto, K. (2017). Sigma-1 Receptor Agonists and Their Clinical Implications in Neuropsychiatric Disorders. *Adv Exp Med Biol*, *964*, 153-161. https://doi.org/10.1007/978-3-319-50174-1_11

Albin, R. L., Young, A. B., & Penney, J. B. (1989). The functional anatomy of basal ganglia disorders. *Trends Neurosci*, *12*(10), 366-375. https://doi.org/10.1016/0166-2236(89)90074-x

Alcacer, C., Andreoli, L., Sebastianutto, I., Jakobsson, J., Fieblinger, T., & Cenci, M. A. (2017). Chemogenetic stimulation of striatal projection neurons modulates responses to Parkinson's disease therapy. *J Clin Invest*, *127*(2), 720-734. https://doi.org/10.1172/JCI90132

Allahtavakoli, M., & Jarrott, B. (2011). Sigma-1 receptor ligand PRE-084 reduced infarct volume, neurological deficits, pro-inflammatory cytokines and enhanced anti-inflammatory cytokines after embolic stroke in rats. *Brain Res Bull*, *85*(3-4), 219-224. https://doi.org/10.1016/j.brainresbull.2011.03.019

André, V. M., Cepeda, C., Cummings, D. M., Jocoy, E. L., Fisher, Y. E., Yang, X. W., & Levine, M. S. (2010). Dopamine modulation of excitatory currents in the striatum is dictated by the expression of D1 or D2 receptors and modified by endocannabinoids. *European Journal of Neuroscience*, *31*(1), 14-28. https://doi.org/10.1111/j.1460-9568.2009.07047.x

Andreska, T., Luningschror, P., Wolf, D., McFleder, R. L., Ayon-Olivas, M., Rattka, M., Drechsler, C., Perschin, V., Blum, R., Aufmkolk, S., Granado, N., Moratalla, R., Sauer, M., Monoranu, C., Volkmann, J., Ip, C. W., Stigloher, C., & Sendtner, M. (2023). DRD1 signaling modulates TrkB turnover and BDNF sensitivity in direct pathway striatal medium spiny neurons. *Cell Rep*, *42*(6), 112575. https://doi.org/10.1016/j.celrep.2023.112575

Bagetta, V., Picconi, B., Marinucci, S., Sgobio, C., Pendolino, V., Ghiglieri, V., Fusco, F. R., Giampa, C., & Calabresi, P. (2011). Dopamine-dependent long-term depression is expressed in striatal spiny neurons of both direct and indirect pathways: implications for Parkinson's disease. *J Neurosci*, *31*(35), 12513-12522. https://doi.org/10.1523/JNEUROSCI.2236-11.2011

Bamford, N. S., Zhang, H., Schmitz, Y., Wu, N. P., Cepeda, C., Levine, M. S., Schmauss, C., Zakharenko, S. S., Zablow, L., & Sulzer, D. (2004). Heterosynaptic dopamine neurotransmission selects sets of corticostriatal terminals. *Neuron*, *42*(4), 653-663. https://doi.org/Doi 10.1016/S0896-6273(04)00265-X

Banati, R. B., Daniel, S. E., & Blunt, S. B. (1998). Glial pathology but absence of apoptotic nigral neurons in long-standing Parkinson's disease. *Mov Disord*, *13*(2), 221-227. https://doi.org/10.1002/mds.870130205

Behensky, A. A., Yasny, I. E., Shuster, A. M., Seredenin, S. B., Petrov, A. V., & Cuevas, J. (2013). Afobazole activation of sigma-1 receptors modulates neuronal responses to amyloid-beta25-35. *J Pharmacol Exp Ther*, *347*(2), 468-477. https://doi.org/10.1124/jpet.113.208330

Berkowitz, S., Chapman, J., Dori, A., Gofrit, S. G., Maggio, N., & Shavit-Stein, E. (2021). Complement and Coagulation System Crosstalk in Synaptic and Neural Conduction in the Central and Peripheral Nervous Systems. *Biomedicines*, *9*(12). https://doi.org/10.3390/biomedicines9121950

Bernheimer, H., Birkmayer, W., Hornykiewicz, O., Jellinger, K., & Seitelberger, F. (1973). Brain dopamine and the syndromes of Parkinson and Huntington. Clinical, morphological and neurochemical correlations. *J Neurol Sci*, *20*(4), 415-455. https://doi.org/10.1016/0022-510x(73)90175-5

Blank, T., Nijholt, I., Teichert, U., Kugler, H., Behrsing, H., Fienberg, A., Greengard, P., & Spiess, J. (1997). The phosphoprotein DARPP-32 mediates cAMP-dependent potentiation of striatal N-methyl-D-aspartate responses. *Proc Natl Acad Sci U S A*, *94*(26), 14859-14864. https://doi.org/10.1073/pnas.94.26.14859

Blume, S. R., Cass, D. K., & Tseng, K. Y. (2009). Stepping test in mice: a reliable approach in determining forelimb akinesia in MPTP-induced Parkinsonism. *Exp Neurol*, *219*(1), 208-211. https://doi.org/10.1016/j.expneurol.2009.05.017

Bove, J., & Perier, C. (2012). Neurotoxin-based models of Parkinson's disease. *Neuroscience*, *211*, 51-76. https://doi.org/10.1016/j.neuroscience.2011.10.057

Braak, H., Del Tredici, K., Rub, U., de Vos, R. A., Jansen Steur, E. N., & Braak, E. (2003). Staging of brain pathology related to sporadic Parkinson's disease. *Neurobiol Aging*, *24*(2), 197-211. https://doi.org/10.1016/s0197-4580(02)00065-9

Burke, D. A., Rotstein, H. G., & Alvarez, V. A. (2017). Striatal Local Circuitry: A New Framework for Lateral Inhibition. *Neuron*, *96*(2), 267-284. https://doi.org/10.1016/j.neuron.2017.09.019

Calabresi, P., Maj, R., Pisani, A., Mercuri, N. B., & Bernardi, G. (1992). Long-term synaptic depression in the striatum: physiological and pharmacological characterization. *J Neurosci*, *12*(11), 4224-4233. https://doi.org/10.1523/JNEUROSCI.12-11-04224.1992

Cardoso, F., Goetz, C. G., Mestre, T. A., Sampaio, C., Adler, C. H., Berg, D., Bloem, B. R., Burn, D. J., Fitts, M. S., Gasser, T., Klein, C., de Tijssen, M. A. J., Lang, A. E., Lim, S. Y., Litvan, I., Meissner, W. G., Mollenhauer, B., Okubadejo, N., Okun, M. S., . . . Trenkwalder, C. (2023). A Statement of the MDS on Biological Definition, Staging, and Classification of Parkinson's Disease. *Mov Disord*. https://doi.org/10.1002/mds.29683

Castle, M., Aymerich, M. S., Sanchez-Escobar, C., Gonzalo, N., Obeso, J. A., & Lanciego, J. L. (2005). Thalamic innervation of the direct and indirect basal ganglia pathways in the rat: Ipsi- and contralateral projections. *J Comp Neurol*, *483*(2), 143-153. https://doi.org/10.1002/cne.20421

Cazorla, M., Shegda, M., Ramesh, B., Harrison, N. L., & Kellendonk, C. (2012). Striatal D2 receptors regulate dendritic morphology of medium spiny neurons via Kir2 channels. *J Neurosci*, *32*(7), 2398-2409. https://doi.org/10.1523/JNEUROSCI.6056-11.2012

Cenci, M. A., & Kumar, A. (2024). Cells, pathways, and models in dyskinesia research. *Curr Opin Neurobiol*, *84*, 102833. https://doi.org/10.1016/j.conb.2023.102833

Cenci, M. A., & Lundblad, M. (2007). Ratings of L-DOPA-induced dyskinesia in the unilateral 6-OHDA lesion model of Parkinson's disease in rats and mice. *Curr Protoc Neurosci*, *Chapter 9*, Unit 9 25. https://doi.org/10.1002/0471142301.ns0925s41

Cenci, M. A., Skovgard, K., & Odin, P. (2022). Non-dopaminergic approaches to the treatment of motor complications in Parkinson's disease. *Neuropharmacology*, *210*, 109027. https://doi.org/10.1016/j.neuropharm.2022.109027

Cepeda, C., Buchwald, N. A., & Levine, M. S. (1993). Neuromodulatory Actions of Dopamine in the Neostriatum Are Dependent Upon the Excitatory Amino-Acid Receptor Subtypes Activated. *Proceedings of the National Academy of Sciences of the United States of America*, *90*(20), 9576-9580. https://doi.org/DOI 10.1073/pnas.90.20.9576

Cepeda, C., & Levine, M. S. (1998). Dopamine and N-methyl-D-aspartate receptor interactions in the neostriatum. *Dev Neurosci*, *20*(1), 1-18. https://doi.org/10.1159/000017294

Chen, L., Cummings, K. A., Mau, W., Zaki, Y., Dong, Z., Rabinowitz, S., Clem, R. L., Shuman, T., & Cai, D. J. (2020). The role of intrinsic excitability in the evolution of memory: Significance in memory allocation, consolidation, and updating. *Neurobiol Learn Mem*, *173*, 107266. https://doi.org/10.1016/j.nlm.2020.107266

Chen, Z., Li, G., & Liu, J. (2020). Autonomic dysfunction in Parkinson's disease: Implications for pathophysiology, diagnosis, and treatment. *Neurobiol Dis*, *134*, 104700. https://doi.org/10.1016/j.nbd.2019.104700

Chevallier, N., Keller, E., & Maurice, T. (2011). Behavioural phenotyping of knockout mice for the sigma-1 (sigma(1)) chaperone protein revealed gender-related anxiety, depressive-like and memory alterations. *J Psychopharmacol*, *25*(7), 960-975. https://doi.org/10.1177/0269881111400648

Choi, S., & Lovinger, D. M. (1997). Decreased probability of neurotransmitter release underlies striatal long-term depression and postnatal development of corticostriatal synapses. *Proc Natl Acad Sci U S A*, *94*(6), 2665-2670. https://doi.org/10.1073/pnas.94.6.2665

Croisier, E., Moran, L. B., Dexter, D. T., Pearce, R. K., & Graeber, M. B. (2005). Microglial inflammation in the parkinsonian substantia nigra: relationship to alpha-synuclein deposition. *J Neuroinflammation*, *2*, 14. https://doi.org/10.1186/1742-2094-2-14

Cui, G., Jun, S. B., Jin, X., Pham, M. D., Vogel, S. S., Lovinger, D. M., & Costa, R. M. (2013). Concurrent activation of striatal direct and indirect pathways during action initiation. *Nature*, *494*(7436), 238-242. https://doi.org/10.1038/nature11846

Dalle, E., Daniels, W. M., & Mabandla, M. V. (2017a). Fluvoxamine maleate normalizes striatal neuronal inflammatory cytokine activity in a Parkinsonian rat model associated with depression. *Behav Brain Res*, *316*, 189-196. https://doi.org/10.1016/j.bbr.2016.08.005

Dalle, E., Daniels, W. M. U., & Mabandla, M. V. (2017b). Fluvoxamine maleate effects on dopamine signaling in the prefrontal cortex of stressed Parkinsonian rats: Implications for learning and memory. *Brain Res Bull*, *132*, 75-81. https://doi.org/10.1016/j.brainresbull.2017.05.014

Day, M., Wang, Z., Ding, J., An, X., Ingham, C. A., Shering, A. F., Wokosin, D., Ilijic, E., Sun, Z., Sampson, A. R., Mugnaini, E., Deutch, A. Y., Sesack, S. R., Arbuthnott, G. W., & Surmeier, D. J. (2006). Selective elimination of glutamatergic synapses on striatopallidal neurons in Parkinson disease models. *Nat Neurosci*, *9*(2), 251-259. https://doi.org/10.1038/nn1632

DeCoster, M. A., Klette, K. L., Knight, E. S., & Tortella, F. C. (1995). Sigma receptor-mediated neuroprotection against glutamate toxicity in primary rat neuronal cultures. *Brain Res*, *671*(1), 45-53. https://doi.org/10.1016/0006-8993(94)01294-r

Dehkordi, M. H., Munn, R. G. K., & Fearnhead, H. O. (2022). Non-Canonical Roles of Apoptotic Caspases in the Nervous System. *Front Cell Dev Biol*, *10*, 840023. https://doi.org/10.3389/fcell.2022.840023

Dejanovic, B., Wu, T., Tsai, M. C., Graykowski, D., Gandham, V. D., Rose, C. M., Bakalarski, C. E., Ngu, H., Wang, Y., Pandey, S., Rezzonico, M. G., Friedman, B. A., Edmonds, R., De Maziere, A., Rakosi-Schmidt, R., Singh, T., Klumperman, J., Foreman, O., Chang, M. C., . . . Hanson, J. E. (2022). Complement C1q-dependent excitatory and inhibitory synapse elimination by astrocytes and microglia in Alzheimer's disease mouse models. *Nat Aging*, *2*(9), 837-850. https://doi.org/10.1038/s43587-022-00281-1

Ding, Z. B., Song, L. J., Wang, Q., Kumar, G., Yan, Y. Q., & Ma, C. G. (2021). Astrocytes: a double-edged sword in neurodegenerative diseases. *Neural Regen Res*, *16*(9), 1702-1710. https://doi.org/10.4103/1673-5374.306064

Dong, H., Ma, Y., Ren, Z., Xu, B., Zhang, Y., Chen, J., & Yang, B. (2016). Sigma-1 Receptor Modulates Neuroinflammation After Traumatic Brain Injury. *Cell Mol Neurobiol*, *36*(5), 639-645. https://doi.org/10.1007/s10571-015-0244-0

Donoghue, J. P., & Herkenham, M. (1986). Neostriatal projections from individual cortical fields conform to histochemically distinct striatal compartments in the rat. *Brain Res*, *365*(2), 397-403. https://doi.org/10.1016/0006-8993(86)91658-6

Dube, L., Smith, A. D., & Bolam, J. P. (1988). Identification of synaptic terminals of thalamic or cortical origin in contact with distinct medium-size spiny neurons in the rat neostriatum. *J Comp Neurol*, *267*(4), 455-471. https://doi.org/10.1002/cne.902670402

Dunah, A. W., Sirianni, A. C., Fienberg, A. A., Bastia, E., Schwarzschild, M. A., & Standaert, D. G. (2004). Dopamine D1-dependent trafficking of striatal N-methyl-D-aspartate glutamate receptors requires Fyn protein tyrosine kinase but not DARPP-32. *Mol Pharmacol*, *65*(1), 121-129. https://doi.org/10.1124/mol.65.1.121

Durieux, P. F., Bearzatto, B., Guiducci, S., Buch, T., Waisman, A., Zoli, M., Schiffmann, S. N., & d'Exaerde, A. D. K. (2009). D

R striatopallidal neurons inhibit both locomotor and drug reward processes. *Nature Neuroscience*, *12*(4), 393-395. https://doi.org/10.1038/nn.2286

Espay, A. J., Vizcarra, J. A., Marsili, L., Lang, A. E., Simon, D. K., Merola, A., Josephs, K. A., Fasano, A., Morgante, F., Savica, R., Greenamyre, J. T., Cambi, F., Yamasaki, T. R., Tanner, C. M., Gan-Or, Z., Litvan, I., Mata, I. F., Zabetian, C. P., Brundin, P., . . . Leverenz, J. B. (2019). Revisiting protein aggregation as pathogenic in sporadic Parkinson and Alzheimer diseases. *Neurology*, *92*(7), 329-337. https://doi.org/10.1212/WNL.0000000000006926

Fearnley, J. M., & Lees, A. J. (1991). Ageing and Parkinson's disease: substantia nigra regional selectivity. *Brain*, *114 ( Pt 5)*, 2283-2301. https://doi.org/10.1093/brain/114.5.2283

Fieblinger, T., Graves, S. M., Sebel, L. E., Alcacer, C., Plotkin, J. L., Gertler, T. S., Chan, C. S., Heiman, M., Greengard, P., Cenci, M. A., & Surmeier, D. J. (2014). Cell type-specific plasticity of striatal projection neurons in parkinsonism and L-DOPA-induced dyskinesia. *Nat Commun*, *5*, 5316. https://doi.org/10.1038/ncomms6316

Fieblinger, T., Li, C., Espa, E., & Cenci, M. A. (2022). Non-Apoptotic Caspase-3 Activation Mediates Early Synaptic Dysfunction of Indirect Pathway Neurons in the Parkinsonian Striatum. *Int J Mol Sci*, *23*(10). https://doi.org/10.3390/ijms23105470

Fieblinger, T., Sebastianutto, I., Alcacer, C., Bimpisidis, Z., Maslava, N., Sandberg, S., Engblom, D., & Cenci, M. A. (2014). Mechanisms of dopamine D1 receptor-mediated ERK1/2 activation in the parkinsonian striatum and their modulation by metabotropic glutamate receptor type 5. *J Neurosci*, *34*(13), 4728-4740. https://doi.org/10.1523/JNEUROSCI.2702-13.2014

Fieblinger, T., Zanetti, L., Sebastianutto, I., Breger, L. S., Quintino, L., Lockowandt, M., Lundberg, C., & Cenci, M. A. (2018). Striatonigral neurons divide into two distinct morphological-physiological phenotypes after chronic L-DOPA treatment in parkinsonian rats. *Sci Rep*, *8*(1), 10068. https://doi.org/10.1038/s41598-018-28273-5

Filipello, F., Morini, R., Corradini, I., Zerbi, V., Canzi, A., Michalski, B., Erreni, M., Markicevic, M., Starvaggi-Cucuzza, C., Otero, K., Piccio, L., Cignarella, F., Perrucci, F., Tamborini, M., Genua, M., Rajendran, L., Menna, E., Vetrano, S., Fahnestock, M., . . . Matteoli, M. (2018). The Microglial Innate Immune Receptor TREM2 Is Required for Synapse Elimination and Normal Brain Connectivity. *Immunity*, *48*(5), 979-991 e978. https://doi.org/10.1016/j.immuni.2018.04.016

Francardo, V. (2018). Modeling Parkinson's disease and treatment complications in rodents: Potentials and pitfalls of the current options. *Behav Brain Res*, *352*, 142-150. https://doi.org/10.1016/j.bbr.2017.12.014

Francardo, V., Bez, F., Wieloch, T., Nissbrandt, H., Ruscher, K., & Cenci, M. A. (2014). Pharmacological stimulation of sigma-1 receptors has neurorestorative effects in experimental parkinsonism. *Brain*, *137*(Pt 7), 1998-2014. https://doi.org/10.1093/brain/awu107

Francardo, V., Geva, M., Bez, F., Denis, Q., Steiner, L., Hayden, M. R., & Cenci, M. A. (2019). Pridopidine Induces Functional Neurorestoration Via the Sigma-1 Receptor in a Mouse Model of Parkinson's Disease. *Neurotherapeutics*, *16*(2), 465-479. https://doi.org/10.1007/s13311-018-00699-9

Francardo, V., Recchia, A., Popovic, N., Andersson, D., Nissbrandt, H., & Cenci, M. A. (2011). Impact of the lesion procedure on the profiles of motor impairment and molecular responsiveness to L-DOPA in the 6-hydroxydopamine mouse model of Parkinson's disease. *Neurobiol Dis*, *42*(3), 327-340. https://doi.org/10.1016/j.nbd.2011.01.024

Fusi, S., Drew, P. J., & Abbott, L. F. (2005). Cascade models of synaptically stored memories. *Neuron*, *45*(4), 599-611. https://doi.org/10.1016/j.neuron.2005.02.001

Gagnon, D., Petryszyn, S., Sanchez, M. G., Bories, C., Beaulieu, J. M., De Koninck, Y., Parent, A., & Parent, M. (2017). Striatal Neurons Expressing D1 and D2 Receptors are Morphologically Distinct and Differently Affected by Dopamine Denervation in Mice. *Sci Rep*, *7*, 41432. https://doi.org/10.1038/srep41432

Gardoni, F., & Bellone, C. (2015). Modulation of the glutamatergic transmission by Dopamine: a focus on Parkinson, Huntington and Addiction diseases. *Front Cell Neurosci*, *9*, 25. https://doi.org/10.3389/fncel.2015.00025

Gaspar, P., Duyckaerts, C., Alvarez, C., Javoy-Agid, F., & Berger, B. (1991). Alterations of dopaminergic and noradrenergic innervations in motor cortex in Parkinson's disease. *Ann Neurol*, *30*(3), 365-374. https://doi.org/10.1002/ana.410300308

Geloso, M. C., & D'Ambrosi, N. (2021). Microglial Pruning: Relevance for Synaptic Dysfunction in Multiple Sclerosis and Related Experimental Models. *Cells*, *10*(3). https://doi.org/10.3390/cells10030686

Gerdeman, G. L., Ronesi, J., & Lovinger, D. M. (2002). Postsynaptic endocannabinoid release is critical to long-term depression in the striatum. *Nat Neurosci*, *5*(5), 446-451. https://doi.org/10.1038/nn832

Gerfen, C. R. (1984). The neostriatal mosaic: compartmentalization of corticostriatal input and striatonigral output systems. *Nature*, *311*(5985), 461-464. https://doi.org/10.1038/311461a0

Gerfen, C. R., Engber, T. M., Mahan, L. C., Susel, Z., Chase, T. N., Monsma, F. J., Jr., & Sibley, D. R. (1990). D1 and D2 dopamine receptor-regulated gene expression of striatonigral and striatopallidal neurons. *Science*, *250*(4986), 1429-1432. https://doi.org/10.1126/science.2147780

Gerfen, C. R., & Surmeier, D. J. (2011). Modulation of striatal projection systems by dopamine. *Annu Rev Neurosci*, *34*, 441-466. https://doi.org/10.1146/annurev-neuro-061010-113641

Gertler, T. S., Chan, C. S., & Surmeier, D. J. (2008). Dichotomous anatomical properties of adult striatal medium spiny neurons. *J Neurosci*, *28*(43), 10814-10824. https://doi.org/10.1523/JNEUROSCI.2660-08.2008

Gong, S., Zheng, C., Doughty, M. L., Losos, K., Didkovsky, N., Schambra, U. B., Nowak, N. J., Joyner, A., Leblanc, G., Hatten, M. E., & Heintz, N. (2003). A gene expression atlas of the central nervous system based on bacterial artificial chromosomes. *Nature*, *425*(6961), 917-925. https://doi.org/10.1038/nature02033

Graves, S. M., & Surmeier, D. J. (2019). Delayed Spine Pruning of Direct Pathway Spiny Projection Neurons in a Mouse Model of Parkinson's Disease. *Front Cell Neurosci*, *13*, 32. https://doi.org/10.3389/fncel.2019.00032

Greif, G. J., Lin, Y. J., Liu, J. C., & Freedman, J. E. (1995). Dopamine-modulated potassium channels on rat striatal neurons: specific activation and cellular expression. *J Neurosci*, *15*(6), 4533-4544. https://doi.org/10.1523/JNEUROSCI.15-06-04533.1995

Griesmaier, E., Posod, A., Gross, M., Neubauer, V., Wegleiter, K., Hermann, M., Urbanek, M., Keller, M., & Kiechl-Kohlendorfer, U. (2012). Neuroprotective effects of the sigma-1 receptor ligand PRE-084 against excitotoxic perinatal brain injury in newborn mice. *Exp Neurol*, *237*(2), 388-395. https://doi.org/10.1016/j.expneurol.2012.06.030

Guo, S., Wang, H., & Yin, Y. (2022). Microglia Polarization From M1 to M2 in Neurodegenerative Diseases. *Front Aging Neurosci*, *14*, 815347. https://doi.org/10.3389/fnagi.2022.815347

Haas, S. J., Zhou, X., Machado, V., Wree, A., Krieglstein, K., & Spittau, B. (2016). Expression of Tgfbeta1 and Inflammatory Markers in the 6-hydroxydopamine Mouse Model of Parkinson's Disease. *Front Mol Neurosci*, *9*, 7. https://doi.org/10.3389/fnmol.2016.00007

Haber, S. N., Fudge, J. L., & McFarland, N. R. (2000). Striatonigrostriatal pathways in primates form an ascending spiral from the shell to the dorsolateral striatum. *J Neurosci*, *20*(6), 2369-2382. https://doi.org/10.1523/JNEUROSCI.20-06-02369.2000

Halassa, M. M., Fellin, T., & Haydon, P. G. (2007). The tripartite synapse: roles for gliotransmission in health and disease. *Trends Mol Med*, *13*(2), 54-63. https://doi.org/10.1016/j.molmed.2006.12.005

Halassa, M. M., & Haydon, P. G. (2010). Integrated brain circuits: astrocytic networks modulate neuronal activity and behavior. *Annu Rev Physiol*, *72*, 335-355. https://doi.org/10.1146/annurev-physiol-021909-135843

Hallett, P. J., Spoelgen, R., Hyman, B. T., Standaert, D. G., & Dunah, A. W. (2006). Dopamine D1 activation potentiates striatal NMDA receptors by tyrosine phosphorylation-dependent subunit trafficking. *J Neurosci*, *26*(17), 4690-4700. https://doi.org/10.1523/JNEUROSCI.0792-06.2006

Hanisch, U. K., & Kettenmann, H. (2007). Microglia: active sensor and versatile effector cells in the normal and pathologic brain. *Nat Neurosci*, *10*(11), 1387-1394. https://doi.org/10.1038/nn1997

Hashimoto, K. (2009). Sigma-1 receptors and selective serotonin reuptake inhibitors: clinical implications of their relationship. *Cent Nerv Syst Agents Med Chem*, *9*(3), 197-204. https://doi.org/10.2174/1871524910909030197

Hayashi, T., & Su, T. P. (2003). Sigma-1 receptors (sigma(1) binding sites) form raft-like microdomains and target lipid droplets on the endoplasmic reticulum: roles in endoplasmic reticulum lipid compartmentalization and export. *J Pharmacol Exp Ther*, *306*(2), 718-725. https://doi.org/10.1124/jpet.103.051284

Hayashi, T., & Su, T. P. (2007). Sigma-1 receptor chaperones at the ER-mitochondrion interface regulate Ca(2+) signaling and cell survival. *Cell*, *131*(3), 596-610. https://doi.org/10.1016/j.cell.2007.08.036

Haydon, P. G., & Carmignoto, G. (2006). Astrocyte control of synaptic transmission and neurovascular coupling. *Physiol Rev*, *86*(3), 1009-1031. https://doi.org/10.1152/physrev.00049.2005

Hernández-Echeagaray, E., Starling, A. J., Cepeda, C., & Levine, M. S. (2004). Modulation of AMPA currents by D2 dopamine receptors in striatal medium-sized spiny neurons:: are dendrites necessary? *European Journal of Neuroscience*, *19*(9), 2455-2463. https://doi.org/10.1111/j.0953-816X.2004.03344.x

Hernandez-Lopez, S., Tkatch, T., Perez-Garci, E., Galarraga, E., Bargas, J., Hamm, H., & Surmeier, D. J. (2000). D2 dopamine receptors in striatal medium spiny neurons reduce L-type Ca2+ currents and excitability via a novel PLC[beta]1-IP3-calcineurin-signaling cascade. *J Neurosci*, *20*(24), 8987-8995. https://doi.org/10.1523/JNEUROSCI.20-24-08987.2000

Herve, D., Rogard, M., & Levi-Strauss, M. (1995). Molecular analysis of the multiple Golf alpha subunit mRNAs in the rat brain. *Brain Res Mol Brain Res*, *32*(1), 125-134. https://doi.org/10.1016/0169-328x(95)00070-9

Higley, M. J., & Sabatini, B. L. (2010). Competitive regulation of synaptic Ca2+ influx by D2 dopamine and A2A adenosine receptors. *Nat Neurosci*, *13*(8), 958-966. https://doi.org/10.1038/nn.2592

Holtman, I. R., Skola, D., & Glass, C. K. (2017). Transcriptional control of microglia phenotypes in health and disease. *J Clin Invest*, *127*(9), 3220-3229. https://doi.org/10.1172/JCI90604

Hong, S., Beja-Glasser, V. F., Nfonoyim, B. M., Frouin, A., Li, S., Ramakrishnan, S., Merry, K. M., Shi, Q., Rosenthal, A., Barres, B. A., Lemere, C. A., Selkoe, D. J., & Stevens, B. (2016). Complement and microglia mediate early synapse loss in Alzheimer mouse models. *Science*, *352*(6286), 712-716. https://doi.org/10.1126/science.aad8373

Hurst, C. G. (1965). Brain Mechanisms and Intelligence, a Quantitative Study of Injuries to the Brain - Lashley,Ks. *Journal of Speech and Hearing Disorders*, *30*(2), 194-196. <Go to ISI>://WOS:A1965CAY3500013

Hyrskyluoto, A., Pulli, I., Tornqvist, K., Ho, T. H., Korhonen, L., & Lindholm, D. (2013). Sigma-1 receptor agonist PRE084 is protective against mutant huntingtin-induced cell degeneration: involvement of calpastatin and the NF-kappaB pathway. *Cell Death Dis*, *4*(5), e646. https://doi.org/10.1038/cddis.2013.170

Imamura, K., Hishikawa, N., Sawada, M., Nagatsu, T., Yoshida, M., & Hashizume, Y. (2003). Distribution of major histocompatibility complex class II-positive microglia and cytokine profile of Parkinson's disease brains. *Acta Neuropathol*, *106*(6), 518-526. https://doi.org/10.1007/s00401-003-0766-2

Jahanshahi, M., Obeso, I., Baunez, C., Alegre, M., & Krack, P. (2015). Parkinson's disease, the subthalamic nucleus, inhibition, and impulsivity. *Mov Disord*, *30*(2), 128-140. https://doi.org/10.1002/mds.26049

Jocoy, E. L., Andre, V. M., Cummings, D. M., Rao, S. P., Wu, N., Ramsey, A. J., Caron, M. G., Cepeda, C., & Levine, M. S. (2011). Dissecting the contribution of individual receptor subunits to the enhancement of N-methyl-d-aspartate currents by dopamine D1 receptor activation in striatum. *Front Syst Neurosci*, *5*, 28. https://doi.org/10.3389/fnsys.2011.00028

Johnston, M. V., Ishida, A., Ishida, W. N., Matsushita, H. B., Nishimura, A., & Tsuji, M. (2009). Plasticity and injury in the developing brain. *Brain Dev*, *31*(1), 1-10. https://doi.org/10.1016/j.braindev.2008.03.014

Kandel, E. R. (2001). The molecular biology of memory storage: a dialogue between genes and synapses. *Science*, *294*(5544), 1030-1038. https://doi.org/10.1126/science.1067020

Karschin, C., Dissmann, E., Stuhmer, W., & Karschin, A. (1996). IRK(1-3) and GIRK(1-4) inwardly rectifying K+ channel mRNAs are differentially expressed in the adult rat brain. *J Neurosci*, *16*(11), 3559-3570. https://doi.org/10.1523/JNEUROSCI.16-11-03559.1996

Kawaguchi, Y. (1997). Neostriatal cell subtypes and their functional roles. *Neuroscience Research*, *27*(1), 1-8. https://doi.org/Doi 10.1016/S0168-0102(96)01134-0

Kisilevsky, A. E., Mulligan, S. J., Altier, C., Iftinca, M. C., Varela, D., Tai, C., Chen, L., Hameed, S., Hamid, J., Macvicar, B. A., & Zamponi, G. W. (2008). D1 receptors physically interact with N-type calcium channels to regulate channel distribution and dendritic calcium entry. *Neuron*, *58*(4), 557-570. https://doi.org/10.1016/j.neuron.2008.03.002

Konishi, H., Koizumi, S., & Kiyama, H. (2022). Phagocytic astrocytes: Emerging from the shadows of microglia. *Glia*, *70*(6), 1009-1026. https://doi.org/10.1002/glia.24145

Kravitz, A. V., Freeze, B. S., Parker, P. R. L., Kay, K., Thwin, M. T., Deisseroth, K., & Kreitzer, A. C. (2010). Regulation of parkinsonian motor behaviours by optogenetic control of basal ganglia circuitry. *Nature*, *466*(7306), 622-U627. https://doi.org/10.1038/nature09159

Kravitz, A. V., & Kreitzer, A. C. (2012). Striatal mechanisms underlying movement, reinforcement, and punishment. *Physiology (Bethesda)*, *27*(3), 167-177. https://doi.org/10.1152/physiol.00004.2012

Kreitzer, A. C., & Malenka, R. C. (2007). Endocannabinoid-mediated rescue of striatal LTD and motor deficits in Parkinson's disease models. *Nature*, *445*(7128), 643-647. https://doi.org/10.1038/nature05506

Kreutzberg, G. W. (1996). Microglia: a sensor for pathological events in the CNS. *Trends Neurosci*, *19*(8), 312-318. https://doi.org/10.1016/0166-2236(96)10049-7

Kuter, K. Z., Cenci, M. A., & Carta, A. R. (2020). The role of glia in Parkinson's disease: Emerging concepts and therapeutic applications. *Prog Brain Res*, *252*, 131-168. https://doi.org/10.1016/bs.pbr.2020.02.004

Kyrylkova, K., Kyryachenko, S., Leid, M., & Kioussi, C. (2012). Detection of apoptosis by TUNEL assay. *Methods Mol Biol*, *887*, 41-47. https://doi.org/10.1007/978-1-61779-860-3_5

Lahmy, V., Meunier, J., Malmstrom, S., Naert, G., Givalois, L., Kim, S. H., Villard, V., Vamvakides, A., & Maurice, T. (2013). Blockade of Tau hyperphosphorylation and Abeta(1)(-)(4)(2) generation by the aminotetrahydrofuran derivative ANAVEX2-73, a mixed muscarinic and sigma(1) receptor agonist, in a nontransgenic mouse model of Alzheimer's disease. *Neuropsychopharmacology*, *38*(9), 1706-1723. https://doi.org/10.1038/npp.2013.70

Lanciego, J. L., Luquin, N., & Obeso, J. A. (2012). Functional neuroanatomy of the basal ganglia. *Cold Spring Harb Perspect Med*, *2*(12), a009621. https://doi.org/10.1101/cshperspect.a009621

Lee, J. H., Kim, J. Y., Noh, S., Lee, H., Lee, S. Y., Mun, J. Y., Park, H., & Chung, W. S. (2021). Astrocytes phagocytose adult hippocampal synapses for circuit homeostasis. *Nature*, *590*(7847), 612-617. https://doi.org/10.1038/s41586-020-03060-3

Lerner, T. N., & Kreitzer, A. C. (2012). RGS4 is required for dopaminergic control of striatal LTD and susceptibility to parkinsonian motor deficits. *Neuron*, *73*(2), 347-359. https://doi.org/10.1016/j.neuron.2011.11.015

Levine, M. S., Li, Z., Cepeda, C., Cromwell, H. C., & Altemus, K. L. (1996). Neuromodulatory actions of dopamine on synaptically-evoked neostriatal responses in slices. *Synapse*, *24*(1), 65-78. https://doi.org/10.1002/syn.890240102

Li, C., Elabi, O. F., Fieblinger, T., & Cenci, M. A. (2024). Structural-functional properties of direct-pathway striatal neurons at early and chronic stages of dopamine denervation. *Eur J Neurosci*, *59*(6), 1227-1241. https://doi.org/10.1111/ejn.16166

Liddelow, S. A., & Barres, B. A. (2017). Reactive Astrocytes: Production, Function, and Therapeutic Potential. *Immunity*, *46*(6), 957-967. https://doi.org/10.1016/j.immuni.2017.06.006

Liddelow, S. A., Guttenplan, K. A., Clarke, L. E., Bennett, F. C., Bohlen, C. J., Schirmer, L., Bennett, M. L., Munch, A. E., Chung, W. S., Peterson, T. C., Wilton, D. K., Frouin, A., Napier, B. A., Panicker, N., Kumar, M., Buckwalter, M. S., Rowitch, D. H., Dawson, V. L., Dawson, T. M., . . . Barres, B. A. (2017). Neurotoxic reactive astrocytes are induced by activated microglia. *Nature*, *541*(7638), 481-487. https://doi.org/10.1038/nature21029

Liu, J. C., DeFazio, R. A., Espinosa-Jeffrey, A., Cepeda, C., de Vellis, J., & Levine, M. S. (2004). Calcium modulates dopamine potentiation of N-methyl-D-aspartate responses: electrophysiological and imaging evidence. *J Neurosci Res*, *76*(3), 315-322. https://doi.org/10.1002/jnr.20079

Lofrumento, D. D., Saponaro, C., Cianciulli, A., De Nuccio, F., Mitolo, V., Nicolardi, G., & Panaro, M. A. (2011). MPTP-induced neuroinflammation increases the expression of pro-inflammatory cytokines and their receptors in mouse brain. *Neuroimmunomodulation*, *18*(2), 79-88. https://doi.org/10.1159/000320027

Lovinger, D. M., Tyler, E. C., & Merritt, A. (1993). Short- and long-term synaptic depression in rat neostriatum. *J Neurophysiol*, *70*(5), 1937-1949. https://doi.org/10.1152/jn.1993.70.5.1937

Lundblad, M., Andersson, M., Winkler, C., Kirik, D., Wierup, N., & Cenci, M. A. (2002). Pharmacological validation of behavioural measures of akinesia and dyskinesia in a rat model of Parkinson's disease. *Eur J Neurosci*, *15*(1), 120-132. https://doi.org/10.1046/j.0953-816x.2001.01843.x

Lundblad, M., Picconi, B., Lindgren, H., & Cenci, M. A. (2004). A model of L-DOPA-induced dyskinesia in 6-hydroxydopamine lesioned mice: relation to motor and cellular parameters of nigrostriatal function. *Neurobiol Dis*, *16*(1), 110-123. https://doi.org/10.1016/j.nbd.2004.01.007

Lundblad, M., Usiello, A., Carta, M., Hakansson, K., Fisone, G., & Cenci, M. A. (2005). Pharmacological validation of a mouse model of l-DOPA-induced dyskinesia. *Exp Neurol*, *194*(1), 66-75. https://doi.org/10.1016/j.expneurol.2005.02.002

Luty, A. A., Kwok, J. B., Dobson-Stone, C., Loy, C. T., Coupland, K. G., Karlstrom, H., Sobow, T., Tchorzewska, J., Maruszak, A., Barcikowska, M., Panegyres, P. K., Zekanowski, C., Brooks, W. S., Williams, K. L., Blair, I. P., Mather, K. A., Sachdev, P. S., Halliday, G. M., & Schofield, P. R. (2010). Sigma nonopioid intracellular receptor 1 mutations cause frontotemporal lobar degeneration-motor neuron disease. *Ann Neurol*, *68*(5), 639-649. https://doi.org/10.1002/ana.22274

Lynd-Balta, E., & Haber, S. N. (1994a). The organization of midbrain projections to the striatum in the primate: sensorimotor-related striatum versus ventral striatum. *Neuroscience*, *59*(3), 625-640. https://doi.org/10.1016/0306-4522(94)90182-1

Lynd-Balta, E., & Haber, S. N. (1994b). The organization of midbrain projections to the ventral striatum in the primate. *Neuroscience*, *59*(3), 609-623. https://doi.org/10.1016/0306-4522(94)90181-3

Mallet, N., Ballion, B., Le Moine, C., & Gonon, F. (2006). Cortical inputs and GABA interneurons imbalance projection neurons in the striatum of parkinsonian rats. *J Neurosci*, *26*(14), 3875-3884. https://doi.org/10.1523/JNEUROSCI.4439-05.2006

Martin, J. P. (1966). The caudate nuclei and locomotion. *Ann R Coll Surg Engl*, *38*(3), 166-175. https://www.ncbi.nlm.nih.gov/pubmed/4951630

Martinez, F. O., & Gordon, S. (2014). The M1 and M2 paradigm of macrophage activation: time for reassessment. *F1000Prime Rep*, *6*, 13. https://doi.org/10.12703/P6-13

Mathur, B. N., & Lovinger, D. M. (2012). Endocannabinoid-dopamine interactions in striatal synaptic plasticity. *Front Pharmacol*, *3*, 66. https://doi.org/10.3389/fphar.2012.00066

Matsuda, W., Furuta, T., Nakamura, K. C., Hioki, H., Fujiyama, F., Arai, R., & Kaneko, T. (2009). Single nigrostriatal dopaminergic neurons form widely spread and highly dense axonal arborizations in the neostriatum. *J Neurosci*, *29*(2), 444-453. https://doi.org/10.1523/JNEUROSCI.4029-08.2009

Mavlyutov, T. A., Epstein, M. L., Andersen, K. A., Ziskind-Conhaim, L., & Ruoho, A. E. (2010). The sigma-1 receptor is enriched in postsynaptic sites of C-terminals in mouse motoneurons. An anatomical and behavioral study. *Neuroscience*, *167*(2), 247-255. https://doi.org/10.1016/j.neuroscience.2010.02.022

McGeer, P. L., Itagaki, S., Boyes, B. E., & McGeer, E. G. (1988). Reactive microglia are positive for HLA-DR in the substantia nigra of Parkinson's and Alzheimer's disease brains. *Neurology*, *38*(8), 1285-1291. https://doi.org/10.1212/wnl.38.8.1285

McNeill, T. H., Brown, S. A., Rafols, J. A., & Shoulson, I. (1988). Atrophy of medium spiny I striatal dendrites in advanced Parkinson's disease. *Brain Res*, *455*(1), 148-152. https://doi.org/10.1016/0006-8993(88)90124-2

Mettler, F. A. (1945). Effects of Bilateral Simultaneous Subcortical Lesions in the Primate. *Journal of Neuropathology and Experimental Neurology*, *4*(2), 99-122. https://doi.org/Doi 10.1097/00005072-194504000-00001

Mettler, F. A., & Mettler, C. C. (1940). Labyrinthine disregard after removal of the caudate. *Proceedings of the Society for Experimental Biology and Medicine*, *45*, 473-475. <Go to ISI>://WOS:000202406400159

Mettler, F. A., & Mettler, C. C. (1942). The effects of striatal injury. *Brain*, *65*, 242-255. https://doi.org/DOI 10.1093/brain/65.3.242

Miki, Y., Mori, F., Kon, T., Tanji, K., Toyoshima, Y., Yoshida, M., Sasaki, H., Kakita, A., Takahashi, H., & Wakabayashi, K. (2014). Accumulation of the sigma-1 receptor is common to neuronal nuclear inclusions in various neurodegenerative diseases. *Neuropathology*, *34*(2), 148-158. https://doi.org/10.1111/neup.12080

Morales, I., Sanchez, A., Rodriguez-Sabate, C., & Rodriguez, M. (2015). The degeneration of dopaminergic synapses in Parkinson's disease: A selective animal model. *Behav Brain Res*, *289*, 19-28. https://doi.org/10.1016/j.bbr.2015.04.019

Mori, T., Hayashi, T., Hayashi, E., & Su, T. P. (2013). Sigma-1 receptor chaperone at the ER-mitochondrion interface mediates the mitochondrion-ER-nucleus signaling for cellular survival. *PLoS One*, *8*(10), e76941. https://doi.org/10.1371/journal.pone.0076941

Mori, T., Hayashi, T., & Su, T. P. (2012). Compromising sigma-1 receptors at the endoplasmic reticulum render cytotoxicity to physiologically relevant concentrations of dopamine in a nuclear factor-kappaB/Bcl-2-dependent mechanism: potential relevance to Parkinson's disease. *J Pharmacol Exp Ther*, *341*(3), 663-671. https://doi.org/10.1124/jpet.111.190868

Murphy, J. A., Stein, I. S., Lau, C. G., Peixoto, R. T., Aman, T. K., Kaneko, N., Aromolaran, K., Saulnier, J. L., Popescu, G. K., Sabatini, B. L., Hell, J. W., & Zukin, R. S. (2014). Phosphorylation of Ser1166 on GluN2B by PKA is critical to synaptic NMDA receptor function and Ca2+ signaling in spines. *J Neurosci*, *34*(3), 869-879. https://doi.org/10.1523/JNEUROSCI.4538-13.2014

Nagatsu, T., Mogi, M., Ichinose, H., & Togari, A. (2000). Cytokines in Parkinson's disease. *J Neural Transm Suppl*(58), 143-151. https://www.ncbi.nlm.nih.gov/pubmed/11128604

Narita, N., Hashimoto, K., Tomitaka, S., & Minabe, Y. (1996). Interactions of selective serotonin reuptake inhibitors with subtypes of sigma receptors in rat brain. *Eur J Pharmacol*, *307*(1), 117-119. https://doi.org/10.1016/0014-2999(96)00254-3

Nelson, A. B., & Kreitzer, A. C. (2014). Reassessing models of basal ganglia function and dysfunction. *Annu Rev Neurosci*, *37*, 117-135. https://doi.org/10.1146/annurev-neuro-071013-013916

Nguyen, L., Lucke-Wold, B. P., Mookerjee, S., Kaushal, N., & Matsumoto, R. R. (2017). Sigma-1 Receptors and Neurodegenerative Diseases: Towards a Hypothesis of Sigma-1 Receptors as Amplifiers of Neurodegeneration and Neuroprotection. *Adv Exp Med Biol*, *964*, 133-152. https://doi.org/10.1007/978-3-319-50174-1_10

Nguyen, L., Lucke-Wold, B. P., Mookerjee, S. A., Cavendish, J. Z., Robson, M. J., Scandinaro, A. L., & Matsumoto, R. R. (2015). Role of sigma-1 receptors in neurodegenerative diseases. *J Pharmacol Sci*, *127*(1), 17-29. https://doi.org/10.1016/j.jphs.2014.12.005

Nimmerjahn, A., Kirchhoff, F., & Helmchen, F. (2005). Resting microglial cells are highly dynamic surveillants of brain parenchyma in vivo. *Science*, *308*(5726), 1314-1318. https://doi.org/10.1126/science.1110647

Nisenbaum, E. S., & Wilson, C. J. (1995). Potassium currents responsible for inward and outward rectification in rat neostriatal spiny projection neurons. *J Neurosci*, *15*(6), 4449-4463. https://doi.org/10.1523/JNEUROSCI.15-06-04449.1995

Nishijima, H., Suzuki, S., Kon, T., Funamizu, Y., Ueno, T., Haga, R., Suzuki, C., Arai, A., Kimura, T., Suzuki, C., Meguro, R., Miki, Y., Yamada, J., Migita, K., Ichinohe, N., Ueno, S., Baba, M., & Tomiyama, M. (2014). Morphologic changes of dendritic spines of striatal neurons in the levodopa-induced dyskinesia model. *Mov Disord*, *29*(3), 336-343. https://doi.org/10.1002/mds.25826

Paolicelli, R. C., Bolasco, G., Pagani, F., Maggi, L., Scianni, M., Panzanelli, P., Giustetto, M., Ferreira, T. A., Guiducci, E., Dumas, L., Ragozzino, D., & Gross, C. T. (2011). Synaptic pruning by microglia is necessary for normal brain development. *Science*, *333*(6048), 1456-1458. https://doi.org/10.1126/science.1202529

Paolicelli, R. C., Sierra, A., Stevens, B., Tremblay, M. E., Aguzzi, A., Ajami, B., Amit, I., Audinat, E., Bechmann, I., Bennett, M., Bennett, F., Bessis, A., Biber, K., Bilbo, S., Blurton-Jones, M., Boddeke, E., Brites, D., Brone, B., Brown, G. C., . . . Wyss-Coray, T. (2022). Microglia states and nomenclature: A field at its crossroads. *Neuron*, *110*(21), 3458-3483. https://doi.org/10.1016/j.neuron.2022.10.020

Parkinson, J. (2002). An essay on the shaking palsy. 1817. *J Neuropsychiatry Clin Neurosci*, *14*(2), 223-236; discussion 222. https://doi.org/10.1176/jnp.14.2.223

Pavese, N., Rivero-Bosch, M., Lewis, S. J., Whone, A. L., & Brooks, D. J. (2011). Progression of monoaminergic dysfunction in Parkinson's disease: a longitudinal 18F-dopa PET study. *Neuroimage*, *56*(3), 1463-1468. https://doi.org/10.1016/j.neuroimage.2011.03.012

Peviani, M., Salvaneschi, E., Bontempi, L., Petese, A., Manzo, A., Rossi, D., Salmona, M., Collina, S., Bigini, P., & Curti, D. (2014). Neuroprotective effects of the Sigma-1 receptor (S1R) agonist PRE-084, in a mouse model of motor neuron disease not linked to SOD1 mutation. *Neurobiol Dis*, *62*, 218-232. https://doi.org/10.1016/j.nbd.2013.10.010

Pisanu, A., Lecca, D., Mulas, G., Wardas, J., Simbula, G., Spiga, S., & Carta, A. R. (2014). Dynamic changes in pro- and anti-inflammatory cytokines in microglia after PPAR-gamma agonist neuroprotective treatment in the MPTPp mouse model of progressive Parkinson's disease. *Neurobiol Dis*, *71*, 280-291. https://doi.org/10.1016/j.nbd.2014.08.011

Prensa, L., & Parent, A. (2001). The nigrostriatal pathway in the rat: A single-axon study of the relationship between dorsal and ventral tier nigral neurons and the striosome/matrix striatal compartments. *J Neurosci*, *21*(18), 7247-7260. https://doi.org/10.1523/JNEUROSCI.21-18-07247.2001

Ransohoff, R. M., & Perry, V. H. (2009). Microglial physiology: unique stimuli, specialized responses. *Annu Rev Immunol*, *27*, 119-145. https://doi.org/10.1146/annurev.immunol.021908.132528

Redgrave, P., Prescott, T. J., & Gurney, K. (1999). The basal ganglia: a vertebrate solution to the selection problem? *Neuroscience*, *89*(4), 1009-1023. https://doi.org/10.1016/s0306-4522(98)00319-4

Redgrave, P., Rodriguez, M., Smith, Y., Rodriguez-Oroz, M. C., Lehericy, S., Bergman, H., Agid, Y., DeLong, M. R., & Obeso, J. A. (2010). Goal-directed and habitual control in the basal ganglia: implications for Parkinson's disease. *Nat Rev Neurosci*, *11*(11), 760-772. https://doi.org/10.1038/nrn2915

Robson, M. J., Turner, R. C., Naser, Z. J., McCurdy, C. R., Huber, J. D., & Matsumoto, R. R. (2013). SN79, a sigma receptor ligand, blocks methamphetamine-induced microglial activation and cytokine upregulation. *Exp Neurol*, *247*, 134-142. https://doi.org/10.1016/j.expneurol.2013.04.009

Robson, M. J., Turner, R. C., Naser, Z. J., McCurdy, C. R., O'Callaghan, J. P., Huber, J. D., & Matsumoto, R. R. (2014). SN79, a sigma receptor antagonist, attenuates methamphetamine-induced astrogliosis through a blockade of OSMR/gp130 signaling and STAT3 phosphorylation. *Exp Neurol*, *254*, 180-189. https://doi.org/10.1016/j.expneurol.2014.01.020

Sabino, V., Cottone, P., Parylak, S. L., Steardo, L., & Zorrilla, E. P. (2009). Sigma-1 receptor knockout mice display a depressive-like phenotype. *Behav Brain Res*, *198*(2), 472-476. https://doi.org/10.1016/j.bbr.2008.11.036

Sano, H., Yasoshima, Y., Matsushita, N., Kaneko, T., Kohno, K., Pastan, I., & Kobayashi, K. (2003). Conditional ablation of striatal neuronal types containing dopamine D2 receptor disturbs coordination of basal ganglia function. *Journal of Neuroscience*, *23*(27), 9078-9088. <Go to ISI>://WOS:000185822200008

Sato, S., Kawamata, T., Kobayashi, T., & Okada, Y. (2014). Antidepressant fluvoxamine reduces cerebral infarct volume and ameliorates sensorimotor dysfunction in experimental stroke. *Neuroreport*, *25*(10), 731-736. https://doi.org/10.1097/WNR.0000000000000162

Schafer, D. P., Lehrman, E. K., Kautzman, A. G., Koyama, R., Mardinly, A. R., Yamasaki, R., Ransohoff, R. M., Greenberg, M. E., Barres, B. A., & Stevens, B. (2012). Microglia sculpt postnatal neural circuits in an activity and complement-dependent manner. *Neuron*, *74*(4), 691-705. https://doi.org/10.1016/j.neuron.2012.03.026

Scheuer, T., & Catterall, W. A. (2006). Control of neuronal excitability by phosphorylation and dephosphorylation of sodium channels. *Biochem Soc Trans*, *34*(Pt 6), 1299-1302. https://doi.org/10.1042/BST0341299

Scott-Hewitt, N., Perrucci, F., Morini, R., Erreni, M., Mahoney, M., Witkowska, A., Carey, A., Faggiani, E., Schuetz, L. T., Mason, S., Tamborini, M., Bizzotto, M., Passoni, L., Filipello, F., Jahn, R., Stevens, B., & Matteoli, M. (2020). Local externalization of phosphatidylserine mediates developmental synaptic pruning by microglia. *EMBO J*, *39*(16), e105380. https://doi.org/10.15252/embj.2020105380

Sebastianutto, I., Cenci, M. A., & Fieblinger, T. (2017). Alterations of striatal indirect pathway neurons precede motor deficits in two mouse models of Huntington's disease. *Neurobiol Dis*, *105*, 117-131. https://doi.org/10.1016/j.nbd.2017.05.011

Sedelis, M., Schwarting, R. K., & Huston, J. P. (2001). Behavioral phenotyping of the MPTP mouse model of Parkinson's disease. *Behav Brain Res*, *125*(1-2), 109-125. https://doi.org/10.1016/s0166-4328(01)00309-6

Selemon, L. D., & Goldman-Rakic, P. S. (1985). Longitudinal topography and interdigitation of corticostriatal projections in the rhesus monkey. *J Neurosci*, *5*(3), 776-794. https://doi.org/10.1523/JNEUROSCI.05-03-00776.1985

Seth, P., & Koul, N. (2008). Astrocyte, the star avatar: redefined. *J Biosci*, *33*(3), 405-421. https://doi.org/10.1007/s12038-008-0060-5

Shen, W., Flajolet, M., Greengard, P., & Surmeier, D. J. (2008). Dichotomous dopaminergic control of striatal synaptic plasticity. *Science*, *321*(5890), 848-851. https://doi.org/10.1126/science.1160575

Shen, Y. C., Wang, Y. H., Chou, Y. C., Liou, K. T., Yen, J. C., Wang, W. Y., & Liao, J. F. (2008). Dimemorfan protects rats against ischemic stroke through activation of sigma-1 receptor-mediated mechanisms by decreasing glutamate accumulation. *J Neurochem*, *104*(2), 558-572. https://doi.org/10.1111/j.1471-4159.2007.05058.x

Shimazawa, M., Sugitani, S., Inoue, Y., Tsuruma, K., & Hara, H. (2015). Effect of a sigma-1 receptor agonist, cutamesine dihydrochloride (SA4503), on photoreceptor cell death against light-induced damage. *Exp Eye Res*, *132*, 64-72. https://doi.org/10.1016/j.exer.2015.01.017

Shimazu, S., Katsuki, H., Takenaka, C., Tomita, M., Kume, T., Kaneko, S., & Akaike, A. (2000). sigma receptor ligands attenuate N-methyl-D-aspartate cytotoxicity in dopaminergic neurons of mesencephalic slice cultures. *Eur J Pharmacol*, *388*(2), 139-146. https://doi.org/10.1016/s0014-2999(99)00852-3

Smith, Y., Raju, D. V., Pare, J. F., & Sidibe, M. (2004). The thalamostriatal system: a highly specific network of the basal ganglia circuitry. *Trends Neurosci*, *27*(9), 520-527. https://doi.org/10.1016/j.tins.2004.07.004

Stephens, B., Mueller, A. J., Shering, A. F., Hood, S. H., Taggart, P., Arbuthnott, G. W., Bell, J. E., Kilford, L., Kingsbury, A. E., Daniel, S. E., & Ingham, C. A. (2005). Evidence of a breakdown of corticostriatal connections in Parkinson's disease. *Neuroscience*, *132*(3), 741-754. https://doi.org/10.1016/j.neuroscience.2005.01.007

Stoof, J. C., & Kebabian, J. W. (1984). Two dopamine receptors: biochemistry, physiology and pharmacology. *Life Sci*, *35*(23), 2281-2296. https://doi.org/10.1016/0024-3205(84)90519-8

Streit, W. J. (2002). Microglia as neuroprotective, immunocompetent cells of the CNS. *Glia*, *40*(2), 133-139. https://doi.org/10.1002/glia.10154

Su, T. P., Hayashi, T., Maurice, T., Buch, S., & Ruoho, A. E. (2010). The sigma-1 receptor chaperone as an inter-organelle signaling modulator. *Trends Pharmacol Sci*, *31*(12), 557-566. https://doi.org/10.1016/j.tips.2010.08.007

Suarez, L. M., Alberquilla, S., Garcia-Montes, J. R., & Moratalla, R. (2018). Differential Synaptic Remodeling by Dopamine in Direct and Indirect Striatal Projection Neurons in Pitx3(-/-) Mice, a Genetic Model of Parkinson's Disease. *J Neurosci*, *38*(15), 3619-3630. https://doi.org/10.1523/JNEUROSCI.3184-17.2018

Suarez, L. M., Solis, O., Carames, J. M., Taravini, I. R., Solis, J. M., Murer, M. G., & Moratalla, R. (2014). L-DOPA treatment selectively restores spine density in dopamine receptor D2-expressing projection neurons in dyskinetic mice. *Biol Psychiatry*, *75*(9), 711-722. https://doi.org/10.1016/j.biopsych.2013.05.006

Surmeier, D. J., Ding, J., Day, M., Wang, Z., & Shen, W. (2007). D1 and D2 dopamine-receptor modulation of striatal glutamatergic signaling in striatal medium spiny neurons. *Trends Neurosci*, *30*(5), 228-235. https://doi.org/10.1016/j.tins.2007.03.008

Surmeier, D. J., Graves, S. M., & Shen, W. (2014). Dopaminergic modulation of striatal networks in health and Parkinson's disease. *Curr Opin Neurobiol*, *29*, 109-117. https://doi.org/10.1016/j.conb.2014.07.008

Surmeier, D. J., & Kitai, S. T. (1993). D1 and D2 dopamine receptor modulation of sodium and potassium currents in rat neostriatal neurons. *Prog Brain Res*, *99*, 309-324. https://doi.org/10.1016/s0079-6123(08)61354-0

Surmeier, D. J., Shen, W., Day, M., Gertler, T., Chan, S., Tian, X., & Plotkin, J. L. (2010). The role of dopamine in modulating the structure and function of striatal circuits. *Prog Brain Res*, *183*, 149-167. https://doi.org/10.1016/S0079-6123(10)83008-0

Tagliaferro, P., & Burke, R. E. (2016). Retrograde Axonal Degeneration in Parkinson Disease. *J Parkinsons Dis*, *6*(1), 1-15. https://doi.org/10.3233/JPD-150769

Tang, Y., & Le, W. (2016). Differential Roles of M1 and M2 Microglia in Neurodegenerative Diseases. *Mol Neurobiol*, *53*(2), 1181-1194. https://doi.org/10.1007/s12035-014-9070-5

Tchedre, K. T., Huang, R. Q., Dibas, A., Krishnamoorthy, R. R., Dillon, G. H., & Yorio, T. (2008). Sigma-1 receptor regulation of voltage-gated calcium channels involves a direct interaction. *Invest Ophthalmol Vis Sci*, *49*(11), 4993-5002. https://doi.org/10.1167/iovs.08-1867

Tchedre, K. T., & Yorio, T. (2008). sigma-1 receptors protect RGC-5 cells from apoptosis by regulating intracellular calcium, Bax levels, and caspase-3 activation. *Invest Ophthalmol Vis Sci*, *49*(6), 2577-2588. https://doi.org/10.1167/iovs.07-1101

Tome, D., Fonseca, C. P., Campos, F. L., & Baltazar, G. (2017). Role of Neurotrophic Factors in Parkinson's Disease. *Curr Pharm Des*, *23*(5), 809-838. https://doi.org/10.2174/1381612822666161208120422

Vergara, R., Rick, C., Hernandez-Lopez, S., Laville, J. A., Guzman, J. N., Galarraga, E., Surmeier, D. J., & Bargas, J. (2003). Spontaneous voltage oscillations in striatal projection neurons in a rat corticostriatal slice. *J Physiol*, *553*(Pt 1), 169-182. https://doi.org/10.1113/jphysiol.2003.050799

Vidal-Itriago, A., Radford, R. A. W., Aramideh, J. A., Maurel, C., Scherer, N. M., Don, E. K., Lee, A., Chung, R. S., Graeber, M. B., & Morsch, M. (2022). Microglia morphophysiological diversity and its implications for the CNS. *Front Immunol*, *13*, 997786. https://doi.org/10.3389/fimmu.2022.997786

Villalba, R. M., Lee, H., & Smith, Y. (2009). Dopaminergic denervation and spine loss in the striatum of MPTP-treated monkeys. *Exp Neurol*, *215*(2), 220-227. https://doi.org/10.1016/j.expneurol.2008.09.025

Villard, V., Espallergues, J., Keller, E., Alkam, T., Nitta, A., Yamada, K., Nabeshima, T., Vamvakides, A., & Maurice, T. (2009). Antiamnesic and neuroprotective effects of the aminotetrahydrofuran derivative ANAVEX1-41 against amyloid beta(25-35)-induced toxicity in mice. *Neuropsychopharmacology*, *34*(6), 1552-1566. https://doi.org/10.1038/npp.2008.212

Walsh, J. P. (1993). Depression of excitatory synaptic input in rat striatal neurons. *Brain Res*, *608*(1), 123-128. https://doi.org/10.1016/0006-8993(93)90782-i

Wang, Q., Wang, Y., Liao, F. F., & Zhou, F. M. (2024). Dopaminergic inhibition of the inwardly rectifying potassium current in direct pathway medium spiny neurons in normal and parkinsonian striatum. *bioRxiv*. https://doi.org/10.1101/2024.04.29.590632

Wegleiter, K., Hermann, M., Posod, A., Wechselberger, K., Stanika, R. I., Obermair, G. J., Kiechl-Kohlendorfer, U., Urbanek, M., & Griesmaier, E. (2014). The sigma-1 receptor agonist 4-phenyl-1-(4-phenylbutyl) piperidine (PPBP) protects against newborn excitotoxic brain injury by stabilizing the mitochondrial membrane potential in vitro and inhibiting microglial activation in vivo. *Exp Neurol*, *261*, 501-509. https://doi.org/10.1016/j.expneurol.2014.07.022

Weintraub, D., Aarsland, D., Chaudhuri, K. R., Dobkin, R. D., Leentjens, A. F., Rodriguez-Violante, M., & Schrag, A. (2022). The neuropsychiatry of Parkinson's disease: advances and challenges. *Lancet Neurol*, *21*(1), 89-102. https://doi.org/10.1016/S1474-4422(21)00330-6

Weintraub, D., David, A. S., Evans, A. H., Grant, J. E., & Stacy, M. (2015). Clinical spectrum of impulse control disorders in Parkinson's disease. *Mov Disord*, *30*(2), 121-127. https://doi.org/10.1002/mds.26016

West, M. J. (1999). Stereological methods for estimating the total number of neurons and synapses: issues of precision and bias. *Trends Neurosci*, *22*(2), 51-61. https://doi.org/10.1016/s0166-2236(98)01362-9

Westin, J. E., Lindgren, H. S., Gardi, J., Nyengaard, J. R., Brundin, P., Mohapel, P., & Cenci, M. A. (2006). Endothelial proliferation and increased blood-brain barrier permeability in the basal ganglia in a rat model of 3,4-dihydroxyphenyl-L-alanine-induced dyskinesia. *J Neurosci*, *26*(37), 9448-9461. https://doi.org/10.1523/JNEUROSCI.0944-06.2006

Wolf, S. A., Boddeke, H. W., & Kettenmann, H. (2017). Microglia in Physiology and Disease. *Annu Rev Physiol*, *79*, 619-643. https://doi.org/10.1146/annurev-physiol-022516-034406

Wu, Z., Li, L., Zheng, L. T., Xu, Z., Guo, L., & Zhen, X. (2015). Allosteric modulation of sigma-1 receptors by SKF83959 inhibits microglia-mediated inflammation. *J Neurochem*, *134*(5), 904-914. https://doi.org/10.1111/jnc.13182

Yamada, T., Kawamata, T., Walker, D. G., & McGeer, P. L. (1992). Vimentin immunoreactivity in normal and pathological human brain tissue. *Acta Neuropathol*, *84*(2), 157-162. https://doi.org/10.1007/BF00311389

Young, C. B., Reddy, V., & Sonne, J. (2024). Neuroanatomy, Basal Ganglia. In *StatPearls*. https://www.ncbi.nlm.nih.gov/pubmed/30725826

Yun, S. P., Kam, T. I., Panicker, N., Kim, S., Oh, Y., Park, J. S., Kwon, S. H., Park, Y. J., Karuppagounder, S. S., Park, H., Kim, S., Oh, N., Kim, N. A., Lee, S., Brahmachari, S., Mao, X., Lee, J. H., Kumar, M., An, D., . . . Ko, H. S. (2018). Block of A1 astrocyte conversion by microglia is neuroprotective in models of Parkinson's disease. *Nat Med*, *24*(7), 931-938. https://doi.org/10.1038/s41591-018-0051-5

Zaja-Milatovic, S., Milatovic, D., Schantz, A. M., Zhang, J., Montine, K. S., Samii, A., Deutch, A. Y., & Montine, T. J. (2005). Dendritic degeneration in neostriatal medium spiny neurons in Parkinson disease. *Neurology*, *64*(3), 545-547. https://doi.org/10.1212/01.WNL.0000150591.33787.A4

Zhai, S., Shen, W., Graves, S. M., & Surmeier, D. J. (2019). Dopaminergic modulation of striatal function and Parkinson's disease. *J Neural Transm (Vienna)*, *126*(4), 411-422. https://doi.org/10.1007/s00702-019-01997-y